R. & M. No. 3426

MINISTRY OF AVIATION

AERONAUTICAL RESEARCH COUNCIL
REPORTS AND MEMORANDA

Effects of Longitudinal Elastic Camber on Slender Aircraft in Steady Symmetrical Flight

Parts I and II

By A. S. Taylor, M.Sc., A.F.R.Ae.S. and W. F. W. Urich, B.Sc.

LONDON: HER MAJESTY'S STATIONERY OFFICE
1966

PRICE £1 17s. 0d. NET

Effects of Longitudinal Elastic Camber on Slender Aircraft in Steady Symmetrical Flight

Parts I and II

By A. S. Taylor, M.Sc., A.F.R.Ae.S. and W. F. W. Urich, B.Sc.

Communicated by the Deputy Controller Aircraft (Research and Development), Ministry of Aviation

*Reports and Memoranda No. 3426**

June, 1964

Foreword (1965).

The work described in this R. & M. originated in a suggestion made to the first author, in 1959, by Professor B. Etkin of Toronto University. In 1957 the slender-delta type of configuration had been adopted in the U.K. as the most promising for a supersonic transport aircraft designed to cruise at about $M = 2{\cdot}0$, and by 1959 one or two exploratory studies of the aeroelastic behaviour of such layouts had been made. Professor Etkin now suggested a mode of attack on the steady and quasi-steady aeroelastic problems, whereby such an aircraft would be regarded as a 'free-free' beam subject only to longitudinal bending, while aerodynamic loadings would be calculated in accordance with slender-wing theory. Under such conditions the mode of deformation corresponding to a particular steady or quasi-steady state is directly calculable by numerical solution of the appropriate differential equation, and the effects of aeroelasticity on the various trim, stability and manoeuvrability criteria are then readily computed.

Following this suggestion, the first of the present authors developed the relevant mathematical theory in a general form, which permits some freedom of choice as to the method of calculating the aerodynamic loadings. Then, in collaboration with the second author, he embarked on a comprehensive programme of numerical applications (using a 'Mercury' digital computer) in which the influence of various parameters (planform, stiffness and mass distributions, etc.) on the aeroelastic characteristics was to be studied. The sensitivity of results to changes in the aerodynamic assumptions was also to be considered. By the end of 1962 a considerable volume of computations had been completed for one particular planform. Slender-wing theory had been used throughout for the calculation of aerodynamic loading due to elastic camber and the effects of varying stiffness and mass distributions had been investigated. At this stage, however, the impending transfer of the authors to other duties cast doubt upon the possibility of extending the work any further. Accordingly, the report which forms Part I of this R. & M. was written. This describes the method and presents the results of the calculations performed up to that time.

Subsequently, the first author was able to carry the investigation a stage further by repeating the earlier calculations, using piston-theory aerodynamics instead of slender-wing theory for the computation of loading due to elastic camber. An extension to the theory of Part I, and appropriate modifications to computer programmes, made it possible also to calculate the effects of elastic camber on the longitudinal distributions of

* Replaces R.A.E. Reports Nos. Aero. 2684 and Structures 296—A.R.C. 25 763 and 26 192.

shear force and bending moment. This stage of the work was described in a report which forms Part II of this R. & M. This includes a recapitulation of the essential steps of the mathematical analysis given in Part I, so that although it is complementary to the first Part, it is also sufficiently self-contained to be read independently if, for instance, the reader's main interest is in the effects on shear forces and bending moments.

The method of these reports was originally conceived at a time when attention was focussed on the 'completely integrated' slender-wing configuration, rather than on configurations involving a discrete fuselage plus a thin slender wing, such as that adopted for the Anglo-French 'Concord' aircraft. Although the assumption of 'beam-like' behaviour might have been reasonably valid for the former type of layout, BAC-Sud calculations for the 'Concord' have shown that for such an aircraft account must be taken of spanwise deformations.

PART I

Estimation of the Effect of Longitudinal Elastic Camber on Trim and Manoeuvrability of Slender Aircraft

By A. S. TAYLOR, M.Sc., A.F.R.Ae.S. and W. F. W. URICH, B.Sc.

Summary.

An approximate method of estimating the effect of aeroelasticity on the longitudinal trim and quasi-steady manoeuvrability of slender aircraft has been developed. It is assumed that, structurally, the aircraft behaves as a 'free-free' beam, subject only to longitudinal bending, and that the total chordwise aerodynamic loading (including that due to elastic camber) varies linearly with local angle of attack, and is thus calculable by superposition of a number of 'elementary' distributions. It is then possible to set up the differential equation for the deflected beam, and by solving it on a digital computer, in conjunction with the equations of overall equilibrium, obtain the distributions of elastic camber, the angles of attack of the centreline chord and the elevon angles appropriate to the aircraft in trimmed level flight and in the steady pull-up manoeuvre.

The theory is developed in detail for the cases where the loading due to elastic camber is assumed to be in accordance with slender-wing theory and piston theory respectively. The practicability of the method has been demonstrated by application (using slender-wing theory) to a possible design for a supersonic ($M = 2{\cdot}2$) transport aircraft, and from the calculations, some tentative conclusions have been drawn regarding the likely order of the effects for such an aircraft.

LIST OF CONTENTS

LIST OF CONTENTS—*continued*

LIST OF APPENDICES

LIST OF ILLUSTRATIONS

LIST OF ILLUSTRATIONS—*continued*

Figure

1. *Introduction.*

1.1. *General Background to the Investigation.*

This report describes the derivation of an approximate method for estimating the effect of aeroelasticity on the longitudinal trim and manoeuvrability of slender aircraft. It also presents the results obtained from the numerical application of the method to a possible supersonic transport aircraft, designed to cruise at $M = 2{\cdot}2$.

Since 1957, when the slender-delta type of configuration was adopted in this country as the most promising for such an aircraft, intensive research has been concentrated on various aspects of the design problem which it was thought might be strongly influenced by the novelty of this layout. One such focus of attention has been in the domain of aeroelasticity, for at the outset, little or nothing was known of the potential aeroelastic characteristics of slender configurations.

At the Royal Aircraft Establishment, several workers, including E. G. Broadbent, W. G. Molyneux, A. D. N. Smith and Ll. T. Niblett made exploratory studies of the aeroelastic behaviour of such configurations. This work included the examination of dynamic stability characteristics, using the assumed-mode type of flutter analysis, and also the estimation of the effect of aeroelasticity on longitudinal and lateral control effectiveness. At the same time, Zbrozek investigated the effect of aeroelasticity on the longitudinal short-period response of a slender aircraft, obtaining both a quasi-static solution, and a 'dynamic' solution involving the assumption of a single structural mode, namely the first normal mode of longitudinal bending, which he calculated by a method of successive approximation. He also made estimates of elevator effectiveness.

Aeroelastic studies on more specific designs were made by J. C. A. Baldock of Handley Page Ltd. and by R. E. Hodges of Bristol Aircraft Ltd.

Among the tentative conclusions to be drawn from this unpublished work are the following:

(i) Classical (coupled-mode type) flutter is unlikely to occur on a strength-designed slender supersonic transport aircraft, but flexibility will exert a destabilizing influence on its longitudinal short-period mode at cruising Mach numbers.

(ii) Elevator power* is reduced by flexibility.

(iii) The reductions in short-period stability and elevator power, noted under (i) and (ii) respectively, exert opposing influences on elevator effectiveness, as measured by the incremental normal acceleration per unit deflection. With practical configurations, the net effect of flexibility at supersonic speeds is likely to be a reduction in elevator effectiveness (i.e. an increase in elevator angle per g).

(iv) Although longitudinal structural modes exert the predominant effects on longitudinal stability and control effectiveness, the effect of spanwise structural modes is not entirely negligible.

(v) The magnitude, if not the nature, of the aeroelastic effects under consideration may depend rather critically on the delicate balance between the opposing distributions of aerodynamic and inertia loading considered in relation to the stiffness distribution. Consequently, the results of calculations may vary considerably according to the aerodynamic theory employed. Thus, when using slender-body theory, Hodges obtained results quite different from the mutually compatible ones obtained with a lifting-surface theory and piston theory.

---

* Defined as the pitching moment about the c.g. per unit elevator deflection, with the aircraft restrained at the c.g.

The early work of R.A.E. investigators had necessarily to be based on somewhat crude assumptions as to mass and stiffness distributions. The active interest of the present authors in these problems began, however, at a time when aircraft firms were beginning to make fairly detailed design studies in connection with the supersonic transport project, so that there was opened up the possibility {welcome, in view of (v) above} of making an aeroelastic investigation based on stiffness and mass distributions rather more realistic than those assumed in the earlier studies.

Meanwhile, Professor B. Etkin of Toronto University had, while working at the R.A.E., suggested a mode of attack on the steady and quasi-steady aeroelastic problems, whereby the aircraft would be regarded as a 'free-free' beam subject only to longitudinal bending, while aerodynamic loadings would be calculated in accordance with slender-wing theory. Under such conditions the mode of deformation corresponding to a particular steady or quasi-steady state is directly calculable by numerical solution of the appropriate differential equation, and the effects of aeroelasticity on the various trim, stability and manoeuvrability criteria are then readily computed. A. S. Taylor, the first of the present authors, pursued this suggestion and by the end of 1960 had elaborated the mathematical theory described in Section 2 of this report.

All the investigations so far mentioned were based on the assumption of attached flow, which is implicit in the linear formulae for lift which have been used. In practice, of course, the flow will be detached in 'off-design' conditions and the variation of lift with incidence is likely to be appreciably non-linear.

Dr. Hancock of Queen Mary College, London, made somewhat restricted use of non-linear aerodynamics, in applying independently a method basically similar to the authors', to the problem of trim for uniform flat-plate wings of various planforms[1]. His results suggested that the aeroelastic characteristics of non-linearly loaded, slender aircraft might differ radically from those of similar, linearly loaded aircraft. However, it appears probable that the non-linear formula for lift used by Hancock, in common with most of those suggested by other theoretical investigators, tends to exaggerate the non-linear effect considerably at the moderate angles of attack which are primarily concerned in this kind of investigation. Thus, while the possible importance of non-linear effects should certainly be borne in mind in future aeroelastic investigations, it would be premature to suggest that the broad conclusions of previous investigations are seriously invalidated by their assumption of linear aerodynamics.

Subsequent studies of the static stability and manoeuvrability of slender aircraft[2, 3, 4, 5] led Hancock and Milne to question the validity and applicability of the classical Gates and Lyon theory (which uses the concept of 'modified derivatives' to deal with flexible aircraft), in relation to flexible aircraft of this configuration. Their findings, coupled with the observations of Zbrozek and the present authors, concerning the lack of physical significance attaching to 'modified' derivatives for a flexible slender aircraft, prompted a reappraisal of the classical theory as applied to flexible aircraft in general.

The difficulties of aeroelastic calculation which are peculiar to the slender integrated configuration, stem from the fact that the whole of the structure is concerned in the deformations, whereas in dealing with the conventional configurations of the past, it has usually been possible to consider only individual components to deform, the remainder of the structure being assumed rigid. Milne[6] has made an important contribution to the resolution of these difficulties in a report which presents an integrated analytical treatment of the equilibrium and stability of the flexible aeroplane in flight. The equations of motion for such an aeroplane are developed in as general a manner as possible and

the analysis is then applied to a detailed study of the equilibrium and stability of the slender, integrated aeroplane configuration.

1.2. *Scope of the Present Investigation.*

In relation to some of the work referred to above, the aims of the present investigation were modest and the underlying assumptions somewhat restrictive. Thus the method described ignores spanwise deformations and seeks only to determine the effect of longitudinal bending on the trimmed shape of the aircraft (including elevon deflection) in steady rectilinear flight and in the quasi-steady pull-up manoeuvre. The technique is essentially that of the 'method of modified derivatives', the relevant principles of which are, for the benefit of readers unfamiliar with it, outlined in Section 1.3.1.

As developed herein, our method assumes linear aerodynamics and, as regards the loading due to elastic camber, is restricted to either slender-body theory or piston theory. Subject to the linearity assumption, however, other contributions to the total aerodynamic loading may be specified in accordance with the best available experimental or theoretical data.

Section 2 of this report gives the mathematical outline of the method, some of the more detailed aspects of which are described in Appendix I. Section 3 summarizes the computations required for the trim and manoeuvrability analysis of a specific design, while Section 4 gives an account of the numerical applications. The practicability of the method and the significance of the numerical results are discussed in Section 5, and the overall conclusions, with suggestions for possible future work, are given in Section 6.

1.2.1. *Note on the application of the method of modified derivatives.*—As already postulated, we assume linear aerodynamics. Then, in the general case of the quasi-steady pull-up manoeuvre at specified Mach number and altitude, with incremental normal acceleration ng, (which includes steady rectilinear flight as the special case with $n = 0$) the resultant loading (aerodynamic and inertial) on the *rigid* aircraft would be a linear function of n, q (pitching velocity), η (elevon deflection), α_0 (the angle of attack of the centre-section chord) and $\alpha_b(\xi)$, the chordwise distribution of built-in camber relative to the centre-section chord. Of these five parameters, n and q are kinematically related; hence, if we assume $\alpha_b(\xi)$ is known, then for a specified value of n, only the parameters α_0, η remain to be determined in order that the aircraft configuration and the resultant loading shall be completely defined. The two parameters in question may be evaluated by simultaneous solution of the two equations of overall equilibrium for the aircraft (equations of normal forces and of pitching moments about the c.g.). In coefficient form, these equations may be expressed as

$$\bar{C}_L = \bar{C}_{L0} + \frac{\partial \bar{C}_L}{\partial \alpha_0}\alpha_0 + \frac{\partial \bar{C}_L}{\partial \eta}\eta + \frac{\partial \bar{C}_L}{\partial q}q + \frac{\partial \bar{C}_L}{\partial n}(n+1) = \frac{(n+1)\bar{W}}{\frac{1}{2}\rho V^2 S}$$

and

$$\bar{C}_m = \bar{C}_{m0} + \frac{\partial \bar{C}_m}{\partial \alpha_0}\alpha_0 + \frac{\partial \bar{C}_m}{\partial \eta}\eta + \frac{\partial \bar{C}_m}{\partial q}q + \frac{\partial \bar{C}_m}{\partial n}(n+1) = 0$$

where $\bar{C}_{L0}$ and $\bar{C}_{m0}$ correspond to the angle of attack distribution $\alpha_b(\xi)$* and where, for the rigid aircraft, $\partial \bar{C}_L/\partial n = \partial \bar{C}_m/\partial n = 0$.

* In the detailed mathematical development (Section 2) it will be found convenient to replace $\{\alpha_b(\xi) + \alpha_0\}$ by $\{\alpha_d(\xi) + \alpha'_0\}$, where the distribution $\alpha_d(\xi)$ corresponds to the 'design C_L' and α'_0 is the *additional* angle of attack. C_{L0}, C_{m0} will then correspond to $\alpha_d(\xi)$ rather than $\alpha_b(\xi)$, but the general argument is unaffected.

When we consider the flexible aircraft, we find that the resultant loading depends on an additional parameter, namely the distribution of elastic camber $\alpha_e(\xi)$, which introduces additional terms into the equations of overall equilibrium, which now effectively contain three unknowns α_0, η and $\alpha_e(\xi)$. However, the (differential) equation of aeroelastic equilibrium provides the third simultaneous equation necessary for the solution of the problem. By virtue of the linearity assumptions, the solution of the differential equation for $\alpha_e(\xi)$ is expressible as a sum of terms proportional to α_0, η, q and $(n+1)$ respectively, together with a term independent of those parameters, which results from loading due to $\alpha_b(\xi)$. Thus $\alpha_e(\xi)$ may be eliminated from the equations of overall equilibrium at the expense of introducing additional terms in each equation, proportional to α_0, η, q and $(n+1)$ respectively, together with a fifth term in each case, independent of those parameters. It is thus possible to rewrite the equations of overall equilibrium for the flexible aircraft in forms identical with those set out above for the rigid aircraft, but the coefficients $\bar{C}_{L0}$, $\bar{C}_{m0}$, and the derivatives $\partial\bar{C}_L/\partial\alpha_0$, $\partial\bar{C}_m/\partial\alpha_0$, etc., will have values modified, in comparison with those for the rigid aircraft, to take account of the effects of flexibility. In particular, $\partial\bar{C}_L/\partial n$ and $\partial\bar{C}_m/\partial n$ will not be zero for the flexible aircraft.

In application to a 'conventional' (wing+fuselage+tail) aircraft, the method of modified derivatives yields modified derivatives which have some physical significance, but as will be discussed later (Section 2.6.1), those calculated for an integrated configuration have no true physical significance of their own, and their calculation must be regarded purely as a convenient mathematical device for arriving at the solutions for the equilibrium states.

2. *Mathematical Outline of Proposed Method of Estimation.*

2.1. *Basic Assumptions.*

We consider the configuration illustrated in Fig. 1, with chordwise distributions of weight and bending rigidity denoted by $W(\xi)$ and $B(\xi) = EI(\xi)$ respectively. (*See* Figs. 2 and 3.)

All incidences are assumed small, so that $\xi \approx \xi'$ and in assessing deformations $z_e'(\xi') = l\zeta_e'(\xi')$ relative to $O(\xi', \zeta')$ we approximate to the normal forces by the corresponding lift forces ($\cos\alpha \approx 1$, drag forces neglected). The neutral axis of the beam representing the aircraft, and the mean camber line of the centre section are assumed to coincide.

We consider the aircraft in steady, manoeuvring flight, (initiated from trimmed level flight at speed V and lift coefficient $\bar{C}_{Lt}$) with incremental normal acceleration ng.

The distribution of effective local angle of attack may be expressed as

$$\alpha(\xi) = \alpha_b(\xi) + \alpha_0 + \alpha_q(\xi) + \alpha_e(\xi) \tag{1}$$

where

$\alpha_b(\xi)$ is the distribution of built-in camber relative to the centre-section chord ($\equiv$ line joining nose of aircraft to mid-point of trailing edge),

α_0 is the angle of attack of the centre-section chord,

$\alpha_q(\xi)$ is the effective camber distribution due to the pitching velocity q,

$\alpha_e(\xi)$ is the distribution of elastic camber.

We have

$$\alpha_q(\xi) = \hat{q}(\xi - \bar{\xi}), \tag{2}$$

where $\hat{q} = ql/V$ is the non-dimensionalised pitching velocity, related to n by

$$\frac{\hat{q}}{n} = \frac{\bar{C}_{Lt}}{2\mu} \text{ with } \mu = \frac{\bar{W}}{g\rho Sl}, \tag{3}$$

$\overline{W} = l\int_0^1 W(\xi)d\xi$ is the total weight of the aircraft, S its gross plan area and ρ is the air density.

Since the basic aerodynamic design of an aircraft of the type under consideration is usually realised in terms of a 'design C_L lift distribution' and a 'lift distribution due to additional angle of attack', it is desirable to rewrite (1) in the form

$$\alpha(\xi) = \alpha_d(\xi) + \alpha_0' + \alpha_q(\xi) + \alpha_e(\xi) \tag{4}$$

where $\alpha_d(\xi) = \alpha_b(\xi) + \alpha_{0d}$ is the angle of attack distribution corresponding to the design C_L, and

$$\alpha_0' = \alpha_0 - \alpha_{0d},$$

α_{0d} being the angle of attack of the centreline at the design C_L.

If η is the control deflection, we assume that the aerodynamic lift per unit length at station ξ may be expressed as

$$L(\xi) = L_\alpha(\xi) + L_\eta(\xi) \tag{5}$$

where the respective contributions are due to the $\alpha(\xi)$ distribution and η. On the assumption that the local lift varies linearly with local angle of attack, we may express $L_\alpha(\xi)$ for $0 \leqslant \xi \leqslant 1$ as

$$L_\alpha(\xi) = L_{\alpha_d}(\xi) + L_{\alpha_0'}(\xi) + L_{\alpha_q}(\xi) + L_{\alpha_e}(\xi). \tag{6}$$

Now $L_{\alpha_0'}(\xi)$, $L_{\alpha_q}(\xi)$ and $L_\eta(\xi)$ will be proportional to α_0', $\hat{q}$ and η respectively so that from (5) and (6) we may write

$$L(\xi) = Ql\{\phi_d(\xi) + \alpha_0'\phi_0(\xi) + \hat{q}\phi_q(\xi) + \phi_e(\xi) + \eta\phi_\eta(\xi)\} \tag{7}$$

where $Q = \frac{1}{2}\rho V^2$ is the kinetic pressure and the $\phi(\xi)$ are all non-dimensional functions, which may in general depend on Mach number. Within the limits of the linearity assumption we are free to prescribe each of the $\phi(\xi)$ by any convenient method, without necessarily restricting ourselves to the same method for all functions in a particular instance. Thus $\phi_d(\xi)$, $\phi_0(\xi)$ and $\phi_\eta(\xi)$ may be determined from the most accurate combination of experimental and theoretical data that is available, while in general we shall have to fall back on a simple (linearised) theory, such as slender-wing or piston theory, for the specification of $\phi_q(\xi)$ and $\phi_e(\xi)$. We may assume that in accordance with such a theory we may write

$$\phi_e(\xi) = \phi\{\alpha_e(\xi), \xi\} \tag{8}$$

where ϕ is linear in $\alpha_e(\xi)$ and its derivatives with respect to ξ.

2.2. *The Conditions of Overall Equilibrium.*

The total lift $\bar{L}$ and the total moment about the c.g. $\overline{M}$ are given by

$$\bar{L} = l\int_0^1 L(\xi)d\xi \tag{9}$$

$$\overline{M} = l^2\int_0^1 L(\xi)(\bar{\xi} - \xi)d\xi = \bar{L}\bar{\xi}l - l^2\int_0^1 L(\xi)\xi\, d\xi \tag{10}$$

and for overall equilibrium these must be equated to $(n+1)\overline{W}$ and 0 respectively, where $\overline{W} = l\int_0^1 W(\xi)d\xi$ is the total weight of the aircraft. Using (7) and expressing in coefficient form, we have, if S denotes gross plan area,

$$\overline{C}_L = \frac{\overline{L}}{QS} = \frac{l^2}{S}\left\{\int_0^1 \phi_d(\xi)\,d\xi + \alpha_0' \int_0^1 \phi_0(\xi)d\xi + \hat{q}\int_0^1 \phi_q(\xi)d\xi + \right.$$
$$\left. + \int_0^1 \phi_e(\xi)d\xi + \eta\int_0^1 \phi_\eta(\xi)d\xi\right\} = \frac{(n+1)\overline{W}}{QS} \tag{11}$$

$$\overline{C}_m = \frac{\overline{M}}{QSl} = \overline{C}_L\bar{\xi} - \frac{l^2}{S}\left\{\int_0^1 \phi_d(\xi)\xi\,d\xi + \alpha_0' \int_0^1 \phi_0(\xi)\xi\,d\xi + \hat{q}\int_0^1 \phi_q(\xi)\xi\,d\xi + \right.$$
$$\left. + \int_0^1 \phi_e(\xi)\xi\,d\xi + \eta\int_0^1 \phi_\eta(\xi)\xi\,d\xi\right\} = 0 \tag{12}$$

2.3. *The Equation of Aeroelastic Equilibrium.*

The distribution of total chordwise loading per unit length which produces the elastic camber $\alpha_e(\xi)$ is

$$\mathscr{L}(\xi) = L(\xi) - (n+1)W(\xi). \tag{13}$$

It should be noted that this distributed loading $(0 \leqslant \xi \leqslant 1)$ must be self-equilibrating for the aircraft as a whole. Employing standard beam theory, we obtain as the differential equation defining the deflected shape of the beam:

$$\frac{d^2}{d\xi^2}\left\{B(\xi)\frac{d\alpha_e}{d\xi}\right\} = -l^3\mathscr{L}(\xi) \tag{14}$$

or substituting for $\mathscr{L}(\xi)$ from (13) and (7) and using (8)

$$\frac{d^2}{d\xi^2}\left\{B(\xi)\frac{d\alpha_e}{d\xi}\right\} + Ql^4\phi\{\alpha_e(\xi),\,\xi\}$$
$$= (n+1)l^3W(\xi) - Ql^4\{\phi_d(\xi) + \alpha_0'\phi_0(\xi) + \hat{q}\phi_q(\xi) + \eta\phi_\eta(\xi)\}. \tag{15}$$

2.4. *Control Setting and Wing Angle of Attack Distribution for Steady Flight.*

To define completely the aircraft configuration, in a given steady-flight condition, we have to determine the three unknown quantities α_0, η and $\alpha_e(\xi)$ from the two equations of overall equilibrium (11) and (12), and the differential equation (15), for which we must specify three boundary conditions, namely, that the bending moment and shear at the nose should be zero and that there should be no relative ζ' displacement between the nose and trailing edge.* Mathematically, this requires

$$\left[\frac{d\alpha_e}{d\xi}\right]_{\xi=0} = 0; \tag{16}$$

$$\left[\frac{d}{d\xi}\left\{B(\xi)\frac{d\alpha_e}{d\xi}\right\}\right]_{\xi=0} = 0; \tag{17a}$$

and

$$\int_0^1 \alpha_e(\xi)d\xi = 0. \tag{18}$$

* The last requirement follows from the fact that we are considering the distribution of local angle of attack to be essentially compounded of an angle of attack α_0 of the centreline chord plus a distribution of camber relative to that chord.

In view of (16), (17a) reduces to

$$\left[\frac{d^2\alpha_e}{d\xi^2}\right]_{\xi=0} = 0. \tag{17b}$$

It is readily shown that, if the conditions of overall equilibrium (11) and (12) are satisfied, then the additionally necessary conditions, that the bending moment and shear at the trailing edge should vanish, are automatically satisfied.

2.5. *Solution of the Differential Equation.*

2.5.1. *General.*—The precise manner in which we tackle the solution of (15) will depend on the specific form of the function $\phi\{\alpha_e(\xi), \xi\}$. We may at once observe, however, that with our underlying assumptions of linearity, the equation (15) will be linear, so that we may solve it by superposition of five elementary solutions corresponding to the five terms on the right-hand side. Thus the solution may be expressed as

$$\alpha_e(\xi) = (n+1)\frac{\partial\alpha_e(\xi)}{\partial n} + \alpha_{ed}(\xi) + \alpha_0'\frac{\partial\alpha_e(\xi)}{\partial\alpha_0'} + \hat{q}\frac{\partial\alpha_e(\xi)}{\partial\hat{q}} + \eta\frac{\partial\alpha_e(\xi)}{\partial\eta} \tag{19}$$

where $\partial\alpha_e(\xi)/\partial n$, $\alpha_{ed}(\xi)$, $\partial\alpha_e(\xi)/\partial\alpha_0'$, $\partial\alpha_e(\xi)/\partial\hat{q}$ and $\partial\alpha_e(\xi)/\partial\eta$ are the solutions of (15) with the right-hand side put equal to $l^3W(\xi)$, $-Ql^4\phi_d(\xi)$, $-Ql^4\phi_0(\xi)$, $-Ql^4\phi_q(\xi)$ and $-Ql^4\phi_\eta(\xi)$ respectively; the assumed boundary conditions in each case are (16), (17b) and (18).*

We are also able to write

$$\phi_e(\xi) = (n+1)\frac{\partial\phi_e(\xi)}{\partial n} + \phi_{ed}(\xi) + \alpha_0'\frac{\partial\phi_e(\xi)}{\partial\alpha_0'} + \hat{q}\frac{\partial\phi_e(\xi)}{\partial\hat{q}} + \eta\frac{\partial\phi_e(\xi)}{\partial\eta}. \tag{20}$$

In the following section we give the detailed mathematical development for the case where the function $\phi\{\alpha_e(\xi), \xi\}$ is assumed, as it was for the numerical work of the present investigation, to be appropriate to slender-wing theory. The corresponding development using piston theory is given in Appendix I.

2.5.2. *Solution using slender-wing theory.*—If the loading due to elastic camber is assumed to be in accordance with slender-wing theory, we have

$$L_{\alpha_e}(\xi) = Ql2\pi\left(\frac{s_T}{l}\right)^2\frac{d}{d\xi}\left[\alpha_e(\xi)\left\{\frac{s(\xi)}{s_T}\right\}^2\right] \tag{21a}$$

or

$$\phi_e(\xi) = 2\pi\left(\frac{s_T}{l}\right)^2\frac{d}{d\xi}\left[\alpha_e(\xi)\left\{\frac{s(\xi)}{s_T}\right\}^2\right]. \tag{21b}$$

For convenience and consistency we will assume the loading due to $\alpha_q(\xi)$ also to be in accordance with slender-wing theory, writing

$$L_{\alpha_q}(\xi) = Ql2\pi\left(\frac{s_T}{l}\right)^2\frac{d}{d\xi}\left[\alpha_q(\xi)\left\{\frac{s(\xi)}{s_T}\right\}^2\right] \tag{22a}$$

or, by virtue of equations (2) and (7)

$$\phi_q(\xi) = 2\pi\left(\frac{s_T}{l}\right)^2\frac{d}{d\xi}\left[(\xi-\bar{\xi})\left\{\frac{s(\xi)}{s_T}\right\}^2\right]. \tag{22b}$$

Equation (15) has to be solved for $0 \leqslant \xi \leqslant 1$ subject to the boundary conditions (16), (17b) and (18).

* For remarks concerning conditions at the trailing edge, *see* Section 2.6.1.

Now if we integrate (15) from the nose ($\xi = 0$) to station ξ, using equations (21b) and (22b) and the boundary condition (17a) we obtain {provided $s(0) = 0$}

$$\frac{d}{d\xi}\left\{B(\xi)\frac{d\alpha_e}{d\xi}\right\} + Ql^4 2\pi\left(\frac{s_T}{l}\right)^2\left\{\frac{s(\xi)}{s_T}\right\}^2\alpha_e(\xi)$$
$$= (n+1)l^2\bar{W}(\xi) - Ql^4\bar{\phi}_d(\xi) - Ql^4\alpha_0'\bar{\phi}_0(\xi) -$$
$$- Ql^4 2\pi\left(\frac{s_T}{l}\right)^2\left\{\frac{s(\xi)}{s_T}\right\}^2(\xi-\bar{\xi})\hat{q} - Ql^4\eta\bar{\phi}_\eta(\xi) \tag{23}$$

where

$$\bar{W}(\xi) = l\int_0^\xi W(\xi)d\xi \tag{24}$$

and

$$\bar{\phi}_d(\xi) = \int_0^\xi \phi_d(\xi)d\xi\,;\ \bar{\phi}_0(\xi) = \int_0^\xi \phi_0(\xi)d\xi\,;\ \bar{\phi}_\eta(\xi) = \int_0^\xi \phi_\eta(\xi)d\xi\,. \tag{25}$$

If we divide equation (23) through by $B(\xi)$, and write

$$\bar{B}(\xi) = \frac{B(\xi)}{Q_c l^4} \tag{26}$$

(where Q_c is the kinetic pressure in the design cruising condition) so that $\bar{B}(\xi)$ is a non-dimensional stiffness parameter, the equation may be expressed as

$$\{D^2 + f_1(\xi)D + f_2(\xi, Q)\}\alpha_e(\xi) = (n+1)F_1(\xi) + F_2(\xi, Q) + \alpha_0'F_3(\xi, Q) + \hat{q}F_4(\xi, Q) + \eta F_5(\xi, Q) \tag{27}$$

where

$$D \equiv \frac{d}{d\xi},$$

and

$$f_1(\xi) = \frac{1}{\bar{B}(\xi)}\frac{d\bar{B}(\xi)}{d\xi};\ f_2(\xi, Q) = \frac{2\pi}{\bar{B}(\xi)}\frac{Q}{Q_c}\left(\frac{s_T}{l}\right)^2\left\{\frac{s(\xi)}{s_T}\right\}^2 \tag{28}$$

$$\left.\begin{aligned} F_1(\xi) &= \frac{\bar{W}(\xi)}{\bar{B}(\xi)Q_c l^2},\\ F_2(\xi, Q) &= -\frac{Q}{Q_c}\frac{\bar{\phi}_d(\xi)}{\bar{B}(\xi)};\\ F_3(\xi, Q) &= -\frac{Q}{Q_c}\frac{\bar{\phi}_0(\xi)}{\bar{B}(\xi)};\\ F_4(\xi, Q) &= -f_2(\xi, Q)(\xi-\bar{\xi});\\ F_5(\xi, Q) &= -\frac{Q}{Q_c}\frac{\bar{\phi}_\eta(\xi)}{\bar{B}(\xi)}. \end{aligned}\right\} \tag{29}$$

Since equation (27) is linear, we may, as already indicated in the previous section, solve it by superposition of elementary solutions corresponding to the five terms on the right-hand side, writing

$$\alpha_e(\xi) = \sum_{r=1}^{5}\alpha_{er}(\xi)$$
$$= (n+1)\frac{\partial\alpha_e(\xi)}{\partial n} + \alpha_{ed}(\xi) + \alpha_0'\frac{\partial\alpha_e(\xi)}{\partial\alpha_0'} + \hat{q}\frac{\partial\alpha_e(\xi)}{\partial\hat{q}} + \eta\frac{\partial\alpha_e(\xi)}{\partial\eta} \tag{19bis}$$

where $\frac{\partial \alpha_e(\xi)}{\partial n}$, $\alpha_{ed}(\xi)$, $\frac{\partial \alpha_e(\xi)}{\partial \alpha_0'}$, $\frac{\partial \alpha_e(\xi)}{\partial \hat{q}}$, $\frac{\partial \alpha_e(\xi)}{\partial \eta}$ are the respective solutions of the equations

$$\{D^2 + f_1(\xi)D + f_2(\xi, Q)\}\alpha_e(\xi) = F_r(\xi, Q), \tag{30.r}$$

$$r = 1, \ldots\ldots 5.$$

with the forcing functions $F_r(\xi, Q)$ defined in equations (29). The equations should be solved with boundary conditions (16) and (18). The first of these, in conjunction with the boundary condition (17a), which has already been used in reducing the third-order equation (15) to the second-order equation (23), expresses the fact that the forward end of the beam is free. As discussed in Section 2.6.1, however, the solutions when evaluated for $\xi = 1$ will not correspond to a free rear end.

2.5.3. *A note on the technique of solving the differential equation by digital computer.*—In our numerical applications, the differential equations (30.r) have been solved on the 'Mercury' digital computer, using the special facilities provided for step-by-step integration. Application of this procedure depends on the knowledge of the starting values (at $\xi = 0$) of both $\alpha_e(\xi)$ and $d\alpha_e(\xi)/d\xi$, whereas the boundary conditions (16) and (18) provide us directly with only the second of these. {It may be noted that, in general, $\alpha_e(0) \neq 0$.} This difficulty may be overcome in the following way.

Suppose $\alpha_{e0}(\xi)$ is the solution of (30.r) which satisfies boundary condition (16) and also the condition

$$\alpha_{e0}(0) = \alpha_1 \tag{31}$$

where α_1 may be assigned any convenient value. Let $\alpha_e'(\xi)$ be the solution of the 'complementary' equation

$$\{D^2 + f_1(\xi)D + f_2(\xi, Q)\}\alpha_e(\xi) = 0 \tag{32}$$

which satisfies (16) and also the condition

$$\alpha_0'(0) = \alpha_2, \tag{33}$$

where α_2 is non-zero but otherwise arbitrary. Then the function

$$\alpha_e(\xi) = \alpha_{e0}(\xi) + k\alpha_e'(\xi) \tag{34}$$

where k is an undetermined constant, is a solution of (30.r) which satisfies boundary condition (16) and is such that

$$\alpha_e(0) = \alpha_1 + k\alpha_2. \tag{35}$$

We require a solution of (30.r) that satisfies (16) and (18). The function $\alpha_e(\xi)$ given by equation (34) will be such a solution provided that the constant k is chosen to satisfy the condition

$$\int_0^1 \{\alpha_{e0}(\xi) + k\alpha_e'(\xi)\}d\xi = 0, \tag{36}$$

i.e.

$$k = -\int_0^1 \alpha_{e0}(\xi)d\xi \Big/ \int_0^1 \alpha_e'(\xi)d\xi. \tag{37}$$

Thus we have to solve (30.r) with boundary conditions $\alpha_e(0) = \alpha_1$ and $[d\alpha_e/d\xi]_{\xi=0} = 0$, and (32) with boundary conditions $\alpha_e(0) = \alpha_2$, $[d\alpha_e/d\xi]_{\xi=0} = 0$, where α_1, α_2 may be assigned any convenient values ($\alpha_2 \neq 0$). If k is then evaluated from (37), the required solution of (30.r), which satisfies boundary conditions (16) and (18), will be given by equation (34). In the present application, α_1, α_2 have been taken to be 0 and 1°(0·01745 radian) respectively.

The solutions for α_{e0} and α_e' are readily obtained by the 'Mercury' integration routine since, in each case, the initial values of the dependent variable and its first differential coefficient are known.

2.6. *Restatement of the Conditions of Overall Equilibrium in Terms of 'Modified' Lift and Pitching-Moment Derivatives.*

We may express $\bar{C}_L$ and $\bar{C}_m$ in the forms

$$\left.\begin{aligned} \bar{C}_L &= \bar{C}_{L0} + \frac{\partial \bar{C}_L}{\partial \alpha_0'}\alpha_0' + \frac{\partial \bar{C}_L}{\partial \eta}\eta + \frac{\partial \bar{C}_L}{\partial \hat{q}}\hat{q} + \frac{\partial \bar{C}_L}{\partial n}(n+1) \\ \bar{C}_m &= \bar{C}_{m0} + \frac{\partial \bar{C}_m}{\partial \alpha_0'}\alpha_0' + \frac{\partial \bar{C}_m}{\partial \eta}\eta + \frac{\partial \bar{C}_m}{\partial \hat{q}}\hat{q} + \frac{\partial \bar{C}_m}{\partial n}(n+1) \end{aligned}\right\} \tag{38}$$

where $\bar{C}_{L0}$, $\bar{C}_{m0}$, $\partial \bar{C}_L/\partial \alpha_0'$, $\partial \bar{C}_m/\partial \alpha_0'$, etc. are 'modified' coefficients and partial derivatives incorporating the effects of elasticity.

Using (20) and noting that $\bar{W}/QS = \bar{C}_{Lt}$, we may rewrite (11) and (12) as

$$\left.\begin{aligned} \bar{C}_L &= \frac{l^2}{S}\left[\int_0^1 \{\phi_d(\xi) + \phi_{ed}(\xi)\}d\xi + \alpha_0'\left\{\int_0^1 \left\{\phi_0(\xi) + \frac{\partial \phi_e(\xi)}{\partial \alpha_0'}\right\} d\xi\right\} + \right. \\ &\quad + \hat{q}\left\{\int_0^1 \left\{\phi_q(\xi) + \frac{\partial \phi_e(\xi)}{\partial \hat{q}}\right\} d\xi\right\} + \eta\left\{\int_0^1 \left\{\phi_\eta(\xi) + \frac{\partial \phi_e(\xi)}{\partial \eta}\right\} d\xi\right\} + \\ &\quad \left. + (n+1)\int_0^1 \frac{\partial \phi_e(\xi)}{\partial n} d\xi\right] = (n+1)\bar{C}_{Lt} \\ \bar{C}_m &= \bar{C}_L\bar{\xi} - \frac{l^2}{S}\left[\int_0^1 \{\phi_d(\xi) + \phi_{ed}(\xi)\}\xi\, d\xi + \alpha_0'\left\{\int_0^1 \left\{\phi_0(\xi) + \frac{\partial \phi_e(\xi)}{\partial \alpha_0'}\right\} \xi\, d\xi\right\} + \right. \\ &\quad + \hat{q}\left\{\int_0^1 \left\{\phi_q(\xi) + \frac{\partial \phi_e(\xi)}{\partial \hat{q}}\right\} \xi\, d\xi\right\} + \eta\left\{\int_0^1 \left\{\phi_\eta(\xi) + \frac{\partial \phi_e(\xi)}{\partial \eta}\right\} \xi\, d\xi\right\} + \\ &\quad \left. + (n+1)\int_0^1 \frac{\partial \phi_e(\xi)}{\partial n} \xi\, d\xi\right] = 0. \end{aligned}\right\} \tag{39}$$

From (38) and (39) we obtain the following equations for determining α_0' and η:

$$\left.\begin{aligned} \frac{\partial \bar{C}_L}{\partial \alpha_0'}\alpha_0' + \frac{\partial \bar{C}_L}{\partial \eta}\eta &= (n+1)\bar{C}_{Lt} - \bar{C}_{L0} - \frac{\partial \bar{C}_L}{\partial \hat{q}}\hat{q} - \frac{\partial \bar{C}_L}{\partial n}(n+1) \\ \text{and} \quad \frac{\partial \bar{C}_m}{\partial \alpha_0'}\alpha_0' + \frac{\partial \bar{C}_m}{\partial \eta}\eta &= -\bar{C}_{m0} - \frac{\partial \bar{C}_m}{\partial \hat{q}}\hat{q} - \frac{\partial \bar{C}_m}{\partial n}(n+1) \end{aligned}\right\} \tag{40}$$

where the 'modified' coefficients and partial derivatives are given by

$$\left.\begin{aligned} \bar{C}_{L0} &= \frac{l^2}{S}\left[\int_0^1 \{\phi_a(\xi) + \phi_{ea}(\xi)\}d\xi\right] \\ \bar{C}_{m0} &= \bar{C}_{L0}\bar{\xi} - \frac{l^2}{S}\left[\int_0^1 \{\phi_a(\xi) + \phi_{ea}(\xi)\}\xi\, d\xi\right] \end{aligned}\right\} \tag{41}$$

$$\left.\begin{aligned} \frac{\partial \bar{C}_L}{\partial \alpha_0'} &= \frac{l^2}{S}\left[\int_0^1 \left\{\phi_0(\xi) + \frac{\partial \phi_e(\xi)}{\partial \alpha_0'}\right\} d\xi\right] \\ \frac{\partial \bar{C}_L}{\partial \eta} &= \frac{l^2}{S}\left[\int_0^1 \left\{\phi_\eta(\xi) + \frac{\partial \phi_e(\xi)}{\partial \eta}\right\} d\xi\right] \\ \frac{\partial \bar{C}_L}{\partial \hat{q}} &= \frac{l^2}{S}\left[\int_0^1 \left\{\phi_q(\xi) + \frac{\partial \phi_e(\xi)}{\partial \hat{q}}\right\} d\xi\right] \\ \frac{\partial \bar{C}_L}{\partial n} &= \frac{l^2}{S}\int_0^1 \frac{\partial \phi_e(\xi)}{\partial n}\, d\xi \end{aligned}\right\} \tag{42}$$

$$\left.\begin{aligned} \frac{\partial \bar{C}_m}{\partial \alpha_0'} &= \frac{\partial \bar{C}_L}{\partial \alpha_0'}\bar{\xi} - \frac{l^2}{S}\left[\int_0^1 \left\{\phi_0(\xi) + \frac{\partial \phi_e(\xi)}{\partial \alpha_0'}\right\} \xi\, d\xi\right] \\ \frac{\partial \bar{C}_m}{\partial \eta} &= \frac{\partial \bar{C}_L}{\partial \eta}\bar{\xi} - \frac{l^2}{S}\left[\int_0^1 \left\{\phi_\eta(\xi) + \frac{\partial \phi_e(\xi)}{\partial \eta}\right\} \xi\, d\xi\right] \\ \frac{\partial \bar{C}_m}{\partial \hat{q}} &= \frac{\partial \bar{C}_L}{\partial \hat{q}}\bar{\xi} - \frac{l^2}{S}\left[\int_0^1 \left\{\phi_q(\xi) + \frac{\partial \phi_e(\xi)}{\partial \hat{q}}\right\} \xi\, d\xi\right] \\ \frac{\partial \bar{C}_m}{\partial n} &= \frac{\partial \bar{C}_L}{\partial n}\bar{\xi} - \frac{l^2}{S}\int_0^1 \frac{\partial \phi_e(\xi)}{\partial n}\, \xi\, d\xi\,. \end{aligned}\right\} \tag{43}$$

For any condition of steady manoeuvring flight, with incremental normal acceleration ng, initiated from trimmed level flight at lift coefficient $\bar{C}_{Lt}$, we may deduce the additional angle of attack α_0' and the control deflection η by solution of equations (40), (remembering that $\hat{q} = n\bar{C}_{Lt}/2\mu$).

The particular forms assumed by equations (41) to (43) when $\phi_q(\xi)$ and $\phi_e(\xi)$ are taken to be in accordance with (*a*) slender-wing theory and (*b*) piston theory are given in Appendix I {equations (64) to (66) and (79) to (81) respectively}.

2.6.1. *A note on the significance of the 'modified' derivatives.*—To evaluate $\bar{C}_{L0}$, $\bar{C}_{m0}$ {equations (41)} and the pairs of partial derivatives {equations (42) and (43)} we have first to determine $\alpha_{ea}(\xi)$, $\partial\alpha_e(\xi)/\partial\alpha_0'$, etc. by solving the equation (15) with the right-hand side replaced in turn by quantities $-Ql^4\phi_a(\xi)$, $-Ql^4\phi_0(\xi)$, etc. proportional to its individual terms. In so doing, we are effectively considering the deflection of the beam under various distributed loadings which are not self-equilibrating. Thus if, in a particular case, we solve the differential equation using the leading-edge boundary conditions (16) and (17b) (corresponding to a free end), we shall not have zero shear and bending moment at the trailing edge and must, in fact, postulate that a force and moment be applied there to hold the beam in equilibrium. Now we could equally well (though less conveniently for computational purposes) assume the beam to be restrained at any arbitrarily chosen point along its length, and thus obtain an infinity of different deflected shapes. It is evident, therefore, that $\bar{C}_{L0}$ and $\bar{C}_{m0}$ and the partial derivatives with respect to the various parameters

α_0', n, etc. are not uniquely definable and that they have no real physical significance in relation to the freely flying aircraft. In particular, singularities of behaviour in the partial derivatives will not necessarily (or indeed usually) be reflected in singular behaviour of the aircraft.

These facts do not, however, invalidate the 'modified derivative' approach to the solution for the steady equilibrium states of the aircraft, *provided* that we evaluate all the modified derivatives under the *same* (arbitrary) conditions of constraint. For when we combine the elementary solutions of the differential equation in accordance with equation (19), having set $\hat{q} = n\bar{C}_{Lt}/2\mu$, and chosen α_0' and η to satisfy equations (40), we shall once again have the beam subject to a self-equilibrating distributed loading, so that the various constraining forces and moments introduced at the trailing edge (or other chosen point of restraint) must constitute a null system. Accordingly the final solution for $\alpha_e(\xi)$ will be (uniquely) appropriate to the 'free-free' condition of the beam.

2.7. *Particular Cases.*

2.7.1. *Trimmed level flight.*—In trimmed level flight $n = \hat{q} = 0$. The distribution of elastic camber is given by

$$\alpha_{et}(\xi) = \alpha_{ed}(\xi) + \frac{\partial\alpha_e(\xi)}{\partial n} + \alpha_{0t}'\frac{\partial\alpha_e(\xi)}{\partial\alpha_0'} + \eta_t\frac{\partial\alpha_e(\xi)}{\partial\eta} \tag{44}$$

where the additional angle of attack α_{0t}', and the control deflection η_t to trim, are the solutions of the equations

$$\left.\begin{aligned} \frac{\partial\bar{C}_L}{\partial\alpha_0'}\alpha_{0t}' + \frac{\partial\bar{C}_L}{\partial\eta}\eta_t &= \bar{C}_{Lt} - \bar{C}_{L0} - \frac{\partial\bar{C}_L}{\partial n} \\ \frac{\partial\bar{C}_m}{\partial\alpha_0'}\alpha_{0t}' + \frac{\partial\bar{C}_m}{\partial\eta}\eta_t &= -\bar{C}_{m0} - \frac{\partial\bar{C}_m}{\partial n}. \end{aligned}\right\} \tag{45}$$

The solutions may be expressed in the form

$$\alpha_{0t}' = \frac{\bar{C}_{Lt}H_{t\eta}}{\dfrac{\partial\bar{C}_m}{\partial\alpha_0'}\left(1 - \dfrac{K_{m\eta}}{K_m}\right)}; \qquad \eta_t = \frac{\bar{C}_{Lt}H_t}{\dfrac{\partial\bar{C}_m}{\partial\eta}\left(1 - \dfrac{K_m}{K_{m\eta}}\right)}; \tag{46}$$

where

$$K_m = -\frac{\partial\bar{C}_m}{\partial\alpha_0'}\Big/\frac{\partial\bar{C}_L}{\partial\alpha_0'}; \qquad K_{m\eta} = -\frac{\partial\bar{C}_m}{\partial\eta}\Big/\frac{\partial\bar{C}_L}{\partial\eta}; \tag{47}$$

and

$$\left.\begin{aligned} H_t &= K_m\left\{1 - \frac{1}{\bar{C}_{Lt}}\left(\bar{C}_{L0} + \frac{\partial\bar{C}_L}{\partial n}\right)\right\} - \frac{1}{\bar{C}_{Lt}}\left(\bar{C}_{m0} + \frac{\partial\bar{C}_m}{\partial n}\right) \\ H_{t\eta} &= K_{m\eta}\left\{1 - \frac{1}{\bar{C}_{Lt}}\left(\bar{C}_{L0} + \frac{\partial\bar{C}_L}{\partial n}\right)\right\} - \frac{1}{\bar{C}_{Lt}}\left(\bar{C}_{m0} + \frac{\partial\bar{C}_m}{\partial n}\right). \end{aligned}\right\} \tag{48}$$

2.7.2. *Control angle per g in the steady pull-up.*—The incremental elastic camber per g in the pull-up is given by

$$\frac{d\alpha_e(\xi)}{dn} = \frac{\partial\alpha_e(\xi)}{\partial n} + \frac{d\alpha_0'}{dn}\frac{\partial\alpha_e(\xi)}{\partial\alpha_0'} + \frac{\bar{C}_{Lt}}{2\mu}\frac{\partial\alpha_e(\xi)}{\partial\hat{q}} + \frac{d\eta}{dn}\frac{\partial\alpha_e(\xi)}{\partial\eta} \tag{49}$$

where the increments of root angle of attack and control deflection, $d\alpha_0'/dn$ and $d\eta/dn$ respectively, are the solutions of the equations

$$\left.\begin{aligned} \frac{\partial \bar{C}_L}{\partial \alpha_0'}\frac{d\alpha_0'}{dn} + \frac{\partial \bar{C}_L}{\partial \eta}\frac{d\eta}{dn} &= \bar{C}_{Lt} - \frac{\bar{C}_{Lt}}{2\mu}\frac{\partial \bar{C}_L}{\partial \hat{q}} - \frac{\partial \bar{C}_L}{\partial n} \\ \frac{\partial \bar{C}_m}{\partial \alpha_0'}\frac{d\alpha_0'}{dn} + \frac{\partial \bar{C}_m}{\partial \eta}\frac{d\eta}{dn} &= -\frac{\bar{C}_{Lt}}{2\mu}\frac{\partial \bar{C}_m}{\partial \hat{q}} - \frac{\partial \bar{C}_m}{\partial n}. \end{aligned}\right\} \tag{50}$$

The solutions may be expressed in the form

$$\frac{d\alpha_0'}{dn} = \frac{\bar{C}_{Lt}H_{m\eta}}{\dfrac{\partial \bar{C}_m}{\partial \alpha_0'}\left(1 - \dfrac{K_{m\eta}}{K_m}\right)}; \qquad \frac{d\eta}{dn} = \frac{\bar{C}_{Lt}H_m}{\dfrac{\partial \bar{C}_m}{\partial \eta}\left(1 - \dfrac{K_m}{K_{m\eta}}\right)}; \tag{51}$$

where K_m, $K_{m\eta}$ have been defined in equations (47) and where

$$\left.\begin{aligned} H_m &= K_m\left\{1 - \frac{1}{2\mu}\frac{\partial \bar{C}_L}{\partial \hat{q}} - \frac{1}{\bar{C}_{Lt}}\frac{\partial \bar{C}_L}{\partial n}\right\} - \frac{1}{2\mu}\frac{\partial \bar{C}_m}{\partial \hat{q}} - \frac{1}{\bar{C}_{Lt}}\frac{\partial \bar{C}_m}{\partial n} \\ H_{m\eta} &= K_{m\eta}\left\{1 - \frac{1}{2\mu}\frac{\partial \bar{C}_L}{\partial \hat{q}} - \frac{1}{\bar{C}_{Lt}}\frac{\partial \bar{C}_L}{\partial n}\right\} - \frac{1}{2\mu}\frac{\partial \bar{C}_m}{\partial \hat{q}} - \frac{1}{\bar{C}_{Lt}}\frac{\partial \bar{C}_m}{\partial n}. \end{aligned}\right\} \tag{52}$$

It may be noted that in the manoeuvrability theory for conventional aircraft, K_m and H_m would be identified as the restoring margin and manoeuvre margin respectively, with well-defined physical meanings. Here, since they represent partial derivatives relating to unbalanced states of the aircraft, these quantities are lacking in precise physical significance; in particular, the behaviour of H_m will not, in itself, tell us anything about the stability of the aircraft.

The second of equations (51) may be compared with the formula obtained by Gates and Lyon, in R. & M. 2027, for the manoeuvre discriminant $d\eta/dn$ of a conventional tailed aircraft. Their equation (82) effectively gives

$$\frac{d\eta}{dn} = -\frac{\bar{C}_{Lt}H_m}{V_T A_2} \tag{53}$$

where $V_T = \bar{V}/(1+F)$ is a 'modified' tail volume ratio and A_2 the 'modified' slope of the tailplane lift curve with respect to elevator angle. It can be shown that $-V_T A_2 = (\partial \bar{C}_m/\partial \eta)(1 - K_m/K_{m\eta})$ so that (51) and (53) are consistent.

2.8. *Determination of the Built-in Camber Distribution for a Particular Design.*

The aerodynamic design of a slender-wing aircraft will normally proceed from the specification of the load distribution required for optimum performance in the design cruising condition with undeflected elevons. From this the aerodynamicist will seek to deduce the required distribution of built-in camber, proceeding in the first instance, on the assumption that the aircraft is rigid. Strictly, however, the design load distribution should be realised by the *deformed* (flexible) wing in the design cruising condition and it is therefore desirable to check whether the inclusion of aeroelastic effects significantly influences the required distribution of camber.

We use suffix c to denote quantities appropriate to the design cruising condition, for which $n = \hat{q} = 0$, and for which we assume $\eta_t = 0$. The angle of attack distribution of the deformed wing in this condition is given by

$$\alpha_c(\xi) = \alpha_d(\xi) + \alpha_{0c}' + \alpha_{ec}(\xi). \tag{54}$$

The lift distribution $\{L_{\alpha c}(\xi)\}_{Q=Q_c}$ corresponding to $\alpha_c(\xi)$ at $Q = Q_c$ must be that specified to give optimum performance.

Now the distribution of total chordwise loading per unit length which produces the elastic camber $\alpha_{ec}(\xi)$ is

$$\mathscr{L}_c(\xi) = \{L_{\alpha c}(\xi)\}_{Q=Q_c} - W_c(\xi) \tag{55}$$

and the differential equation defining the deflected shape in accordance with standard beam theory is

$$\frac{d^2}{d\xi^2}\left\{B(\xi)\frac{d\alpha_{ec}}{d\xi}\right\} = -l^3\mathscr{L}_c(\xi) \tag{56}$$

where $\mathscr{L}_c(\xi)$ {unlike $\mathscr{L}(\xi)$ in the general deflection equation (14)} is a completely known function. Consequently, using the boundary conditions:

$$\left[\frac{d}{d\xi}\left\{B(\xi)\frac{d\alpha_{ec}}{d\xi}\right\}\right]_{\xi=0} = \left[\frac{d\alpha_{ec}}{d\xi}\right]_{\xi=0} = \int_0^1 \alpha_{ec}(\xi)d\xi = 0 \tag{57}$$

we may integrate (56) directly to obtain

$$\alpha_{ec}(\xi) = \int_0^1 d\xi \int_0^\xi d\xi_1 \left\{\frac{\int_0^{\xi_1} d\xi_2 \int_0^{\xi_2} \mathscr{L}_c{}^*(\xi_3)d\xi_3}{\bar{B}(\xi_1)}\right\} - \int_0^\xi d\xi_1 \left\{\frac{\int_0^{\xi_1} d\xi_2 \int_0^{\xi_2} \mathscr{L}_c{}^*(\xi_3)d\xi_3}{\bar{B}(\xi_1)}\right\} \tag{58}$$

where

$$\mathscr{L}_c{}^*(\xi) = \frac{\mathscr{L}_c(\xi)}{Q_c l}; \qquad \bar{B}(\xi) = \frac{B(\xi)}{Q_c l^4} \tag{59}$$

are non-dimensional loading and stiffness distributions.

When $\alpha_{ec}(\xi)$ has been calculated from equation (58), the required angle of attack distribution $\alpha_d(\xi)$ for the undeformed wing at the design C_L may be determined from equation (54). Thus

$$\alpha_d(\xi) = \alpha_c(\xi) - \alpha_{0c}{}' - \alpha_{ec}(\xi). \tag{60}$$

The lift distribution for the undeformed wing at the design C_L is calculable from

$$\{L_{\alpha d}(\xi)\}_{Q=Q_c} = \{L_{\alpha c}(\xi) - L_{\alpha_{0c}{}'}(\xi) - L_{\alpha_{ec}}(\xi)\}_{Q=Q_c} \tag{61}$$

on the assumption that $\{L_{\alpha c}(\xi)\}_{Q=Q_c}$ and $\{L_{\alpha_{0c}{}'}(\xi)\}_{Q=Q_c}$ $\{= Q_c l\alpha_{0c}{}'\phi_0(\xi)\}$ have been specified at the outset and that $\{L_{\alpha_{ec}}(\xi)\}_{Q=Q_c} = Q_c l\phi_{ec}(\xi)$ has been calculated by substituting the function $\phi_{ec}(\xi)$ {see equation (8) with $\alpha_e(\xi) = \alpha_{ec}(\xi)$} appropriate to the particular aerodynamic theory employed. With $\{L_{\alpha d}(\xi)\}_{Q=Q_c} = Q_c l\phi_d(\xi)$ {see equation (7)} now known, the function $\phi_d(\xi)$ can be determined for the cruising Mach number. If calculations are to be made for other Mach numbers, $\phi_d(\xi)$ may have to be modified (depending on the aerodynamic assumptions made in a particular application).

3. *Summary of Computations Required for Trim and Manoeuvrability Analysis of a Specific Design.*

The following *data* are assumed to be given:

(i) Planform of configuration [l, s_T, S, $s(\xi)$].

(ii) Weight and stiffness distributions, $W(\xi)$ and $B(\xi)$.

(iii) The kinetic pressure Q_c and the required lift distribution $\{L_{\alpha c}(\xi)\}_{Q=Q_c}$ in the design cruising condition. It is also assumed that the additional angle of attack α_{0c}' and the corresponding lift distribution $\{L_{\alpha_{0c}'}(\xi)\}_{Q=Q_c}$ are specified, so that the function $\phi_0(\xi)$ in equation (7) is effectively defined.

(iv) The function $\phi_\eta(\xi)$ defining the lift distribution due to control deflection in equation (7).

The following *computations* must be performed for the cruising Mach number M_c:

(i) Calculation of $\alpha_{ec}(\xi)$ from equation (58) and hence $\{L_{\alpha_{ec}}(\xi)\}_{Q=Q_c} = Q_c l \phi_{ec}(\xi)$.

(ii) Calculation of $\{L_{\alpha d}(\xi)\}_{Q=Q_c}$ from equation (61), followed by the determination of the function $\phi_d(\xi)$ from the relation

$$\phi_d(\xi) = \frac{1}{Q_c l}\{L_{\alpha d}(\xi)\}_{Q=Q_c}.$$

(iii) For a range of values of Q, obtain

$$\frac{\partial \alpha_e(\xi)}{\partial n}, \quad \alpha_{ed}(\xi), \quad \frac{\partial \alpha_e(\xi)}{\partial \alpha_0'}, \quad \frac{\partial \alpha_e(\xi)}{\partial \hat{q}}, \quad \text{and} \quad \frac{\partial \alpha_e(\xi)}{\partial \eta}$$

as solutions of the differential equation (15), with the right-hand side replaced in turn by $l^3 W(\xi)$, $-Ql^4\phi_d(\xi)$, $-Ql^4\phi_0(\xi)$, $-Ql^4\phi_q(\xi)$ and $-Ql^4\phi_\eta(\xi)$, and subject to the boundary conditions prescribed in equations (16), (17b) and (18).

(iv) Evaluation of $\bar{C}_{L0}$ and $\bar{C}_{m0}$ from equations (41) and of the partial derivatives of $\bar{C}_L$ and $\bar{C}_m$ with respect to α_0', η, $\hat{q}$ and n from equations (42) and (43), for the selected range of values of Q.

(v) Evaluation of K_m and $K_{m\eta}$ {equations (47)}, H_t and $H_{t\eta}$ {equations (48)} and H_m and $H_{m\eta}$ {equations (52)}.

(vi) Evaluation of the additional angle of attack α_{0t}' and control deflection η_t to trim, from equations (46).

(vii) Evaluation of the additional angle of attack and the incremental control deflection per g, ($d\alpha_0'/dn$ and $d\eta/dn$ respectively) from equations (51).

If computations are required for Mach numbers other than M_c, it may be necessary to modify some or all of the functions $\phi_d(\xi)$, $\phi_0(\xi)$, $\phi_q(\xi)$, $\phi_\eta(\xi)$, (depending on the particular aerodynamic assumptions associated with each). The operations (iii) to (vii) listed above must then be repeated wholly or in part for the other Mach number(s).

4. *Numerical Application of the Method.*

4.1. *General.*

The original aims of the numerical work undertaken in connection with this report were threefold:

(i) It was required to assess the practicability of the method, from the purely computational point of view, when stiffness and mass distributions typical of actual aircraft are introduced. Programmes had to be devised for the performance and checking, by digital computer, of the various computations listed in Section 3.

(ii) Realistic assessments of the aeroelastic effects in question were required for possible layouts of the Supersonic Transport Aircraft which were under consideration when the calculations were initiated.

(iii) It was hoped to derive general information as to the influence of such parameters as planform, and weight and stiffness distributions, and to assess the extent to which results are influenced by the aerodynamic assumptions.

At the time relevant to aim (ii), the R.A.E.'s ideas as to possible shapes for the Supersonic Transport Aircraft had crystallised around three distinct planforms discussed by Küchemann and Spence in an unpublished Memorandum. It seemed appropriate to make an aircraft with one of these planforms the subject of the pilot calculations needed to achieve aim (i), since the same calculations would partially achieve aim (ii). Subsequent repetition of the calculations for aircraft having the other two planforms, and additional computations in each case, made with modified stiffness and/or mass distributions, and possibly with alternative aerodynamic assumptions, would complete the second task and go a considerable way towards the completion of the third.

The planform selected for the pilot calculations had been the subject of a detailed project study by J. F. Holford, which yielded a realistic mass distribution for an aircraft of this layout. A fairly extensive set of calculations has been completed for such an aircraft. This included calculations for various stiffness and mass distributions, but the effect of changing the aerodynamic assumptions was not investigated, slender-wing theory being used in all cases to estimate the lift distributions due to elastic camber and to induced camber due to pitching.

A number of unexpected and puzzling difficulties were encountered in the course of the computations and although these have now been resolved, the process has been so time-consuming that it has not been possible, so far, to tackle the other items of the programme.

4.2. *Data for the Selected Aircraft.*

4.2.1. *Geometrical data.*—The selected aircraft embodies what is essentially a delta wing with rounded (streamwise) tips and a discrete body, protruding a relatively small distance ahead of the wing apex*. The planform is illustrated, roughly to scale, in Fig. 1 and the leading particulars are:

Overall length:	$l = 168$ ft
Semi-span at trailing edge:	$s_T = 42$ ft
Ratio: semi-span/length:	$s_T/l = 0{\cdot}25$
Body overhang/overall length:	$l_B/l = \xi_B = 0{\cdot}328$.

Planform shape:

For
$$0 \leqslant \xi \leqslant 0{\cdot}328, \left|\frac{s(\xi)}{s_T}\right| = 0{\cdot}68\xi - 1{\cdot}7\xi^3 + 0{\cdot}476\xi^4;$$
For
$$0{\cdot}328 \leqslant \xi \leqslant 1\dagger, \left|\frac{s(\xi)}{s_T}\right| = 1{\cdot}1(1{\cdot}26\xi - 0{\cdot}26) - 0{\cdot}1(1{\cdot}26\xi - 0{\cdot}26)^{11}. \qquad (62)$$

* In contrast, one of the other configurations incorporated a much longer nose, while the third consisted of an ogee wing with no discrete body.

† Referred to the wing apex, the wing planform is defined by

$$s(\xi_W)/s_T = 1{\cdot}1\ \xi_W - 0{\cdot}1\ \xi_W{}^{11};\ 0 \leqslant\ \xi_W \leqslant 1.$$

Gross plan area:

$$S = 2l \int_0^1 s(\xi) d\xi = 6376 \text{ ft}^2.$$

Planform shape parameter:

$$p = \frac{S}{2ls_T} = 0{\cdot}452.$$

Aspect ratio:

$$A = \frac{4{s_T}^2}{S} = 1{\cdot}107.$$

4.2.2. *Weight distributions.*—A detailed estimate of the weight distribution in the 'all-up' condition (take-off with full fuel- and pay-loads) was provided by J. F. Holford. This was approximated by Curve X of Fig. 2, which is composed of the minimum number of straight-line segments, consistent with preserving the essential features of the actual distribution*.

Some aeroelastic calculations were made with the weight distribution 'X', but it was considered appropriate to make the bulk of the aeroelastic calculations for a 'middle of the cruise' condition, with half of the fuel used; the corresponding weight distribution is shown as Curve Y in Fig. 2. In normal operation, fuel is consumed in such a way as to leave the c.g. position undisturbed, and accordingly the c.g.'s corresponding to Curves X and Y are practically coincident. To examine the effect of a shift of c.g., some calculations have been made using the weight distribution shown by Curve Z in Fig. 2, which corresponds to a condition (not occurring in normal operation) where all fuel ahead of the c.g. has been used, but the rear tanks remain full. The total weight in this case is approximately the same as for Case Y. The actual weights and c.g. positions for the three cases are tabulated below.

Distribution Curve in Fig. 2	Total weight (lb)	c.g. position $\bar{\xi}$
X	350 928	0·650
Y	271 111	0·6475
Z	277 804	0·6742

4.2.3. *Structural data and assumptions.*—For the purposes of this investigation the aircraft was idealised as a beam of varying cross-section, subjected to distributed transverse loading, which produced bending in planes parallel to the vertical plane of symmetry, but no spanwise deformations. Accordingly the only structural data to be specified was the distribution of bending rigidity $B(\xi) = EI(\xi)$ along the representative beam.

No detailed structural analysis had been made for the layout under consideration, but a simple approximate method of deducing the required stiffness distribution, given the mass distribution, was suggested by G. E. Smith (R.A.E.). This was based on the assumption that overall strength

* It should be remembered that the deformation of the aircraft is produced by the generally small and self-equilibrating distribution of loading resulting from the combination of the (large) aerodynamic and weight loading distributions. Accordingly, in assessing aeroelastic effects for a specific design, it may be important to ensure that 'peaks' in the weight distribution, due to local concentrations of mass, such as engines, are accurately represented.

requirements would be dictated by the dynamic loading imposed in a heavy landing at maximum weight. On the further assumption that the landing wheels would be situated at the c.g., this implied that the maximum bending rigidity would be required at the section through the c.g., while typical calculations indicated a steep fall-off in sectional rigidity on either side of this section. When applied to some S.T.A. layouts of Bristol Aircraft Limited and Handley Page Limited, which had been the subject of more detailed structural analysis, this procedure was seen to provide a good approximation to the required rigidity in the vicinity of the c.g., but to underestimate it for sections far removed from the c.g. This, of course, was due to the fact that the heavy landing case was critical only for the part of the structure near the c.g. and that elsewhere, various other stressing cases dictated the required strength (and hence stiffness). Thus Smith's method does no more than define the maximum sectional rigidity (which is required at or near the c.g.) and a curve representing a lower bound to the rigidity required elsewhere.

This lower bound to sectional rigidity was computed for the present layout and its form compared with the more accurate distributions for Bristol and Handley Page layouts referred to above. On this basis it was possible to suggest, for the present investigation, a mathematically simple but plausible generalized stiffness distribution, depending on two parameters, as indicated in the sketch:

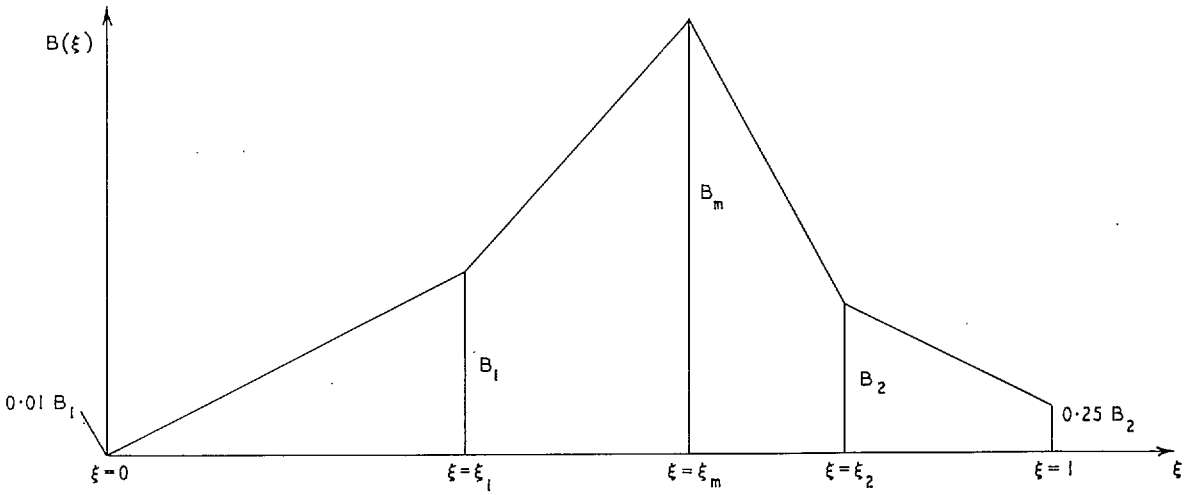

The maximum sectional rigidity B_m and the station $\xi = \xi_m$ at which it occurs are kept fixed. The distribution is then determined by specifying the rigidities B_1, B_2, respectively, at two other fixed stations $\xi = \xi_1$, $\xi = \xi_2$, and taking the rigidities at $\xi = 0$ and $\xi = 1$ to be fixed proportions (0·01 and 0·25) of B_1 and B_2 respectively. Thus the forward 'half' of the distribution is determined by the value of the parameter B_1/B_m, and the rear 'half' by the value of B_2/B_m; a variety of stiffness distributions can thus be examined by assuming different combinations of values of the two parameters.

In the present work, three values of each parameter were considered:

$$\frac{B_1}{B_m} = \frac{1}{4}, \frac{1}{3}, \frac{5}{12};$$

$$\frac{B_2}{B_m} = \frac{2}{15}, \frac{4}{15}, \frac{2}{5};$$

while ξ_1, ξ_m and ξ_2 were taken as 0·4045, 0·6824 and 0·8015 respectively*. The corresponding distributions are illustrated in Fig. 3, which also shows the 'lower bound' curve determined by Smith's method.

It is thought that the distribution corresponding to $B_1/B_m = 1/3$, $B_2/B_m = 4/15$ probably approximates most closely to that which would actually be required for our layout and this has been adopted as a datum, (subsequently termed the 'basic stiffness distribution') to which other distributions are referred.

4.2.4. *Aerodynamic data and assumptions.*—For the purposes of this investigation the design cruising condition is specified as:

Mach number $M = 2{\cdot}2$, at height 63 600 feet, with weight $W = 271\,111$ lb and c.g. position $\bar{\xi} = 0{\cdot}6475$.

Other related data for this condition are:

Lift coefficient: $\bar{C}_{Lc} = 0{\cdot}1$

Kinetic pressure: $Q_c = 425{\cdot}3$ lb/ft².

The optimum longitudinal load distribution for this condition (denoted by $\{L_{\alpha c}(\xi)\}_{Q=Q_c}$ in our notation) was worked out by J. H. B. Smith of R.A.E., and is presented non-dimensionally in Fig. 4a. It was compounded of two contributions—one corresponding to the design $\bar{C}_L$ of 0·05 and the other to the additional angle of attack (α_{0c}') required to produce the overall $\bar{C}_L$ of 0·1 in the cruise. This second contribution (which is $\{L_{\alpha_{0c}'}(\xi)\}_{Q=Q_c}$ in our notation) is shown non-dimensionally in Fig. 4b.

On the assumption that $dC_L/d\alpha_0' = 0{\cdot}025$ per degree for $M = 2{\cdot}2$, α_{0c}' was estimated to be 2 degrees and thus it was possible to derive the function $\phi_0(\xi)$ of equation (7); this is shown in Fig. 5. Of the remaining four non-dimensional lift distribution functions defined by equation (7), $\phi_a(\xi)$ had to be determined by the procedure described in Section 2.8, and is shown in Fig. 6, while for all the calculations covered by this report, $\phi_q(\xi)$ and $\phi_e(\xi)$ were assumed to be in accordance with slender-wing theory. Consequently the detailed mathematical analysis of the aeroelastic effects followed the lines of Sections 2.5.2 and 2.6 of the main text and Section A1.2 of Appendix I. In seeking to specify the remaining function $\phi_\eta(\xi)$, (defining the loading due to control deflection) so as to be reasonably representative of practicable control-surface layouts we have made calculations employing linearized supersonic theory and compared the results with experimental data obtained by Bristol Aircraft Limited in connection with one of their S.T.A. project studies. As a result, we have defined $\phi_\eta(\xi)$ for this investigation, (which has been restricted to supersonic Mach numbers) by

$$\phi_\eta(\xi) = 0\,;\, 0 \leqslant \xi \leqslant 0{\cdot}92$$

$$\phi_\eta(\xi) = \frac{1}{\sqrt{(M^2-1)}}\,;\, 0{\cdot}92 \leqslant \xi \leqslant 1\,. \tag{63}$$

This represents roughly the distribution one would expect to derive from the wing-tip elevons illustrated in Fig. 1, with $E = 0{\cdot}08$ and $s_\eta/s_T = 0{\cdot}5$.

* This apparently odd choice of values for ξ_1, ξ_m and ξ_2 is explained by the fact that the analysis was originally referred to an origin at the wing apex, with the wing root chord taken as reference length. In this system ξ_1, ξ_m and ξ_2 had the values 0·25, 0·6 and 0·75.

4.3. *Calculations Performed.*

The procedure of Section 2.8 was first applied to determine the distribution of elastic camber $\alpha_{ec}(\xi)$ in the design cruising condition defined in Section 4.2.4, assuming the 'basic stiffness distribution' specified at the end of Section 4.2.3. [The configuration of the aircraft in which the weight distribution of the design cruising condition (Curve Y in Fig. 2) is combined with the basic stiffness distribution will henceforth be referred to as the 'standard configuration'.] The calculated distribution $\alpha_{ec}(\xi)$ is shown in Fig. 7 and, as already mentioned in Section 4.2.4, the function $\phi_d(\xi)$ to which the subsequent analysis of Section 2.8 leads, is shown in Fig. 6.

The remaining calculations covered by this report have all been made for a Mach number of 2·2, as being relevant to the constant Mach number, 'cruise-climb' phase of the flight plan envisaged for a supersonic transport aircraft. A range of values of kinetic pressure Q, corresponding to flight at $M = 2{\cdot}2$ at various altitudes, has been considered. A plot of Q against altitude is given in Fig. 8, which also shows the variation of trimmed lift coefficient $\bar{C}_{Lt}$ and aircraft relative density μ with altitude, for the standard configuration*.

The calculations fell into two sets. In the first, the weight distribution was kept fixed, (as Distribution Y of Fig. 2) while the seven different stiffness distributions tabulated on page 26 were considered.

As originally defined, distributions 6 and 7 exhibited discontinuities at $\xi = \xi_2$. However, when applied with such distributions, the 'Mercury' programmes then in use, yielded incorrect (non-checking) results and since, at the time, the reasons for this were not understood, the modified distributions defined above were substituted. (*See* Discussion: Section 5.1.)

The second set of calculations was designed to illustrate the effects of total weight and c.g. position. The three weight distributions shown in Fig. 2 were considered in conjunction with the basic stiffness distribution.

For each configuration considered in the two sets, calculations were made for $Q/Q_c = 0{\cdot}5$, $1{\cdot}0$, $1{\cdot}5$, $2{\cdot}0$ and $2{\cdot}5$. Although, as indicated in Section 2.6.1, the deformations and associated 'modified' derivatives, corresponding to changes in individual parameters, have no physical significance, it has been thought worthwhile to present, for the standard configuration, a complete set of results to illustrate the sequence of calculations which leads to the physically meaningful quantities, $\alpha_{el}(\xi)$ {or $z_{el}(\xi)$}, α_{0l}', η_l, and $d\alpha_e(\xi)/dn$ (or $dz_e(\xi)/dn$), $d\alpha_0'/dn$, $d\eta/dn$. Such results are given in Figs. 9 to 14. For the remaining configurations only the overall results are presented. (*See* Figs. 15 to 24.)

5. *Discussion.*

5.1. *Some Observations on the Practical Working of the Method.*

The complete sequence of computations listed in Section 3 was programmed for the 'Mercury' digital computer. The empirically defined lift function $\phi_0(\xi)$ was fitted by a polynomial as was the function $\phi_d(\xi)$, determined from the first two operations of the sequence.

The main programme was concerned with the solution of the differential equations (30.r) and the processing of the resulting $\{\alpha_e(\xi)\}_r$ distributions, in accordance with equations (64) to (66)

* It should be remarked that in the normal operation of such an aircraft, the cruise-climb would commence with a weight considerably in excess of that applying to the standard configuration, and would terminate with a weight much lower than that. Thus, for aeroelastic calculations to be strictly applicable to the cruise climb, we should have to vary the weight distribution (and consequently C_{Lt} and μ) with Q. We have not, in fact, done this, because of the additional complications that it would entail in the computations.

Stiffness Distributions

Ref. No. in Fig. 15	Relationship to basic distribution	Values of stiffness parameters of Section 4.2.3		Reference to Fig. 3
		B_1/B_m	B_2/B_m	
1	Basic distribution	$\frac{1}{3}$	$\frac{4}{15}$	Middle curve
2	Increased throughout ..	$\frac{5}{12}$	$\frac{2}{5}$	Top curve
3	Decreased throughout ..	$\frac{1}{4}$	$\frac{2}{15}$	Bottom curve
4	Increased over rear 'half' ..	$\frac{1}{3}$	$\frac{2}{5}$	Front: Middle curve Rear: Top curve
5	Decreased over rear 'half' ..	$\frac{1}{3}$	$\frac{2}{15}$	Front: Middle curve Rear: Bottom curve
6	Increased over rear 'quarter'	$\frac{B_1}{B_m} = \frac{1}{3}$	The line corresponding to $\frac{B_2}{B_m} = \frac{2}{5}$ was produced forward of $\xi = \xi_2$ to meet the basic curve for $\frac{B_2}{B_m} = \frac{4}{15}$. (*See* sketch below.)	
7	Decreased over rear 'quarter'	$\frac{B_1}{B_m} = \frac{1}{3}$	The basic curve for $\frac{B_2}{B_m} = \frac{4}{15}$ was produced beyond $\xi = \xi_2$ to meet the line corresponding to $\frac{B_2}{B_m} = \frac{2}{15}$. (*See* sketch below.)	

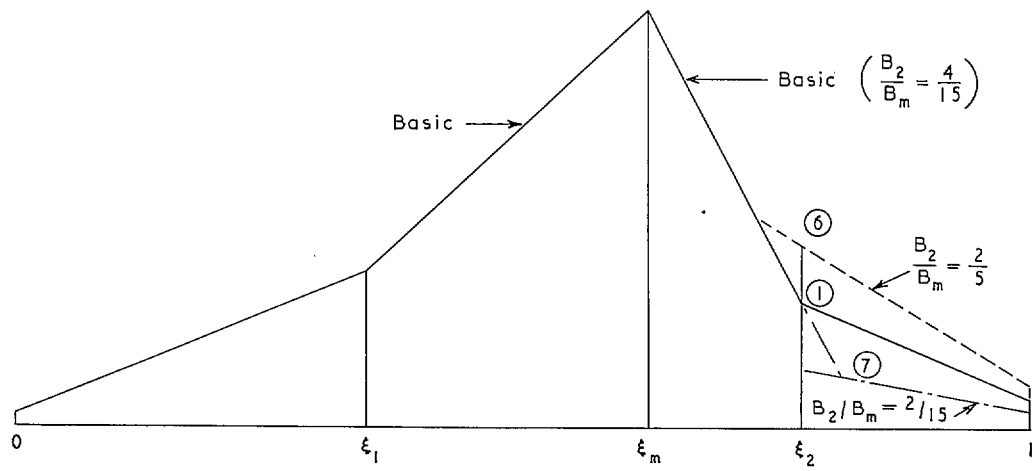

(which appear in Appendix I), to obtain the 'modified' aerodynamic coefficients and partial derivatives, and hence, *via* equations (47), (48) and (46), and (52) and (51), the quantities α_{0t}', η_t for the trim condition and $d\alpha_0'/dn$, $d\eta/dn$ for the pull-up manoeuvre respectively.

A note on the technique of solving the differential equations was given in Section 2.5.3. The derivations of the five elementary solutions $\{\alpha_{e0}(\xi)\}_r$ of equations (30.r), with boundary conditions $\alpha_e(0) = [d\alpha_e(\xi)/d\xi]_{\xi=0} = 0$, were programmed into separate chapters, and a further chapter solved the equation (32) with boundary conditions (33) and (16), $\{\alpha_2$ being taken as $0{\cdot}01745$ radian $(1°)\}$ to obtain $\alpha_e'(\xi)$. The parameter k was then determined from equation (37) and hence $\{\alpha_e(\xi)\}_r$ followed from the equation $\{\alpha_e(\xi)\}_r = \{\alpha_{e0}(\xi)\}_r + k\alpha_e'(\xi)$. A 'processing' chapter provided the final solutions for α_{0t}', η_t, $d\alpha_0'/dn$ and $d\eta/dn$.

The complete programme is inevitably lengthy and of a type that does not readily allow for the incorporation of 'built-in' checks en route. Moreover, as the results deducible from individual chapters are lacking in physical significance, they provide little clue as to the correctness of the relevant parts of the programme. Consequently, the most economical way of insuring against errors is probably to have two programmers working in parallel, and to apply an overall check of results in the manner described in Section A.1.3 of Appendix I. If this fails, then a similar check may be applied to the results of the individual chapters.

Most of our calculations have been made using an integration step length, for the Runge-Kutta process embodied in the Mercury Autocode 'INT STEP' routine, of $\Delta\xi = 0{\cdot}002$. With this step size, the main programme achieves the complete solution for a particular value of Q in 7 minutes. The influence of reducing step size to $0{\cdot}0005$ was investigated, but although the effect on the results was not entirely negligible, it was considered that, having regard to the numerous approximations involved in the method as a whole, the additional accuracy achieved by using the smaller step, would not justify the multiplication of machine production time by four.

An unexpected difficulty was encountered in calculations for the cases involving stiffness modifications over the rear 'quarter' of the aircraft length, i.e. Cases 6 and 7 in the Table of Stiffness Distributions in Section 4.3. As mentioned there, the stiffness distributions originally assumed for these cases involved discontinuities at $\xi = \xi_2$, where the stiffness 'jumped' from the 'basic' curve to either the 'increased stiffness' or the 'decreased stiffness' curve. The results obtained for these distributions failed to satisfy the check programme, although those for the modified distributions (Cases 6 and 7) were quite satisfactory. The reason for the failure of the 'Mercury' programme, which was not apparent to the authors at the time, has since been revealed by D. J. Eckford of R.A.E. A step in the stiffness function implies a singularity in a function appearing in one of the set of equations to be solved by the 'Mercury Intstep' routine. The integral of this function over a vanishingly small interval containing the singularity is finite and non-zero, so that there is a step in one of the dependent variables at the point in question. However, the 'Intstep' routine will not recognize the existence of such a step and will accordingly produce incorrect answers if allowed to continue operating, without modification, through such a singular point. To obtain correct answers in such circumstances, the magnitude of the step must be determined analytically, and the 'Mercury' programme modified to take account of it. A more detailed discussion is given in Appendix II.

With the programme thus modified, the method should work satisfactorily for all stiffness distributions. Once the programme for a particular layout has been proved, results for a range of values of Q, and for various combinations of mass and stiffness distributions, may quickly be produced.

5.2. *Discussion of Numerical Results.*

5.2.1. *General.*—In view of the lack of any real physical significance attaching to the deformations and associated partial derivatives which correspond to changes in individual parameters, Figs. 9 to 12 call for little comment. It may, however, be noted from Figs. 10 and 11, (as a point of academic interest) that with the exception of $\partial \bar{C}_L/\partial n$ and $\partial \bar{C}_m/\partial n$ all the 'modified' quantities tend to the rigid aircraft values as Q tends to zero. As regards the n-derivatives, $Q\ \partial \bar{C}_L/\partial n$ and $Q\ \partial \bar{C}_m/\partial n$ tend to zero as Q tends to zero, so that the actual lift and pitching moment (as distinct from the coefficients) which result from the deformations occurring when n is varied, both tend to zero with Q.

From Fig. 12 it will be observed that K_m and H_m (which correspond to the restoring and manoeuvre margins of classical stability theory) exhibit singularities at $Q/Q_e \approx 0{\cdot}56$ and are negative over parts of the range of Q/Q_e considered. Because these parameters relate to unbalanced states of the aircraft, however, and have had to be calculated with the aircraft arbitrarily constrained, their behaviour alone tells us nothing about the stability and controllability of the aircraft.

The physically meaningful results to which those of Figs. 9 to 12 lead, are the resultant deformation curves shown in Figs. 13 and 14 and the curves of α_{0t}', $d\alpha_0'/dn$, η_t and $d\eta/dn$ which are shown (labelled 'basic stiffness') in Figs. 16, 17, 18 and 19 respectively.

It is seen from Fig. 13 that the shape of the deflection curve for trimmed flight changes considerably as Q increases. Examination of Figs. 2 and 4a indicates that in the design cruising condition ($Q/Q_e = 1$) the resultant of the weight and aerodynamic load distributions will, broadly speaking, consist of regions of net downward loading towards the nose and trailing edge, with net upward loading in between. The deflection curve for $Q/Q_e = 1{\cdot}0$ in Fig. 13 is consistent with such loading. We see from Figs. 16 and 18, that as Q increases, α_{0t}' decreases (eventually becoming negative) while η_t increases. This implies a transfer of (upward) aerodynamic loading from the middle part of the beam to the region of the controls near the trailing edge, which would account for the indicated changes of shape in the deflection curves*.

The main indications of Fig. 14 are that although, in the pull-up manoeuvre, the amplitude of the incremental deformation curve increases considerably with increasing Q, changes in its (normalised) shape are quite small. This reflects the fact, illustrated by Figs. 17 and 19, that $d\alpha_0'/dn$ and $d\eta/dn$ both decrease in magnitude (albeit at somewhat different rates) as Q increases, so that the shape of the incremental aerodynamic load distribution (and hence that of the resultant incremental load distribution) in the pull-up varies much less with Q than does the shape of the load distribution in trimmed flight.

5.2.2. *The influence of stiffness distribution.*—The overall effects of varying stiffness are illustrated in Figs. 15 to 19. Fig. 15, which relates to the design cruising condition ($Q = 425{\cdot}3$ lb/ft^2) shows deformation curves calculated for the seven stiffness distributions specified in the Table on page 26. As might be anticipated, increasing the stiffness (relative to the basic) over the whole of the beam, decreases the amplitudes of the deformation curves, without very much affecting their (normalised) shapes; the reverse (as regards amplitudes) is true for decreasing stiffness. In the manoeuvre case (Fig. 15a), changing the stiffness over the rear 'half' or even over the rear 'quarter' only, produces a large proportion of the effect produced by stiffening throughout the length. The

* The argument is somewhat crude, inasmuch as it neglects the further changes in aerodynamic loading, consequent upon the deflection of the beam.

powerful influence of stiffness changes over the rear part of the beam is brought out even more strongly in Figs. 16 to 19. In particular, the curves of η_t and $d\eta/dn$ (Figs. 18 and 19) calculated for the cases with stiffening over the rear 'half' and rear 'quarter' only, are virtually indistinguishable from those for the case with stiffening throughout, while reducing stiffness over the rear 'quarter' is nearly as effective as reducing it throughout.

The range of elevon angles required to trim the aircraft at $M = 2{\cdot}2$ for a given range of altitude, increases progressively with decreasing stiffness. Thus for the range 50 000 ft to 78 000 ft, the required ranges of η_t are:

Rigid aircraft:		$5{\cdot}5° > \eta_t > -12{\cdot}2°$
Flexible aircraft	Stiffer throughout	$8{\cdot}7° > \eta_t > -13{\cdot}3°$
	Basic stiffness	$11° > \eta_t > -13{\cdot}8°$
	Less stiff throughout	$29° > \eta_t > -15{\cdot}5°$

The effects of stiffness variations on manoeuvrability, as illustrated by the curves of $d\eta/dn$ vs. Q in Fig. 19, are shown in an alternative way by the curves of relative control effectiveness versus Q in Fig. 25. (Relative control effectiveness is here defined as the ratio of the value of $dn/d\eta$ for the flexible aircraft to the value for the rigid aircraft.) These curves are very nearly linear and are readily extrapolated to determine, for each stiffness distribution, the kinetic pressure Q_R at which control reversal would theoretically occur*. Thus, for the basic stiffness distribution, Q_R is about 1750 lb/ft²; this figure is increased to about 2400 lb/ft² for all the cases of increased stiffness which have been considered, while it is reduced to the region of 1060 lb/ft² when the stiffness is reduced over the rear 'quarter', and to 980 lb/ft² when the stiffness is reduced throughout.

The precise significance of these figures in relation to a supersonic transport aircraft, under normal operating conditions, depends upon the detailed flight plan prescribed for the aircraft. Ideas on this subject had not crystallised when the calculations for this report were initiated, and in relation to current ideas, which suggest an altitude range of 58 000 ft to 62 000 ft for the cruise-climb at $M = 2{\cdot}2$, our assumed 'middle-of-the-cruise' height of 63 600 ft (corresponding to $Q_c = 425{\cdot}3$ lb/ft²) is somewhat high. For the more realistic height of 60 000 ft, the curves of Fig. 25 indicate a relative control effectiveness of just under $0{\cdot}7$ for the standard configuration; this falls to rather less than $0{\cdot}5$ for the configurations of reduced stiffness which have been considered. Although these values suggest that the effects of longitudinal elastic camber on manoeuvrability should not be unacceptably large under normal operating conditions, note should be taken of the potential dangers of an inadvertent dive at $M = 2{\cdot}2$, to altitudes lower than those envisaged for that Mach number in the flight plan. Thus, for $M = 2{\cdot}2$ at 40 000 feet, the relative control effectiveness for the standard configuration would be rather less than $0{\cdot}25$, while for the configurations of reduced stiffness, control reversal would already have occurred.

5.2.3. *The influence of weight distribution.*—Results of the calculations for the three different weight distributions (X, Y, Z in Fig. 2) are shown in Figs. 20 to 24 and 26. Fig. 20 indicates that, starting with the 100% Fuel (maximum weight) case (X), only small changes in the deformation

* In practice, as Q is increased, the deformations increase without limit, so that the assumptions of linearity on which the theory has been based are invalidated well before Q_R is reached. It would, in fact, be impossible to trim the aircraft at $Q = Q_R$.

curves result when half the fuel is assumed to have been consumed in the normal way (i.e. symmetrically with regard to the c.g.). When a similar quantity of fuel is assumed to have been consumed from tanks ahead of the c.g. (so that an aft shift of c.g. of roughly 2·5% l is simulated), there are considerably more pronounced changes (of opposite sign) in the deformations.

The effects of flexibility on α_{0t} and $d\alpha_0/dn$ are little affected by these changes in weight distribution, being generally small in all cases (Figs. 21 and 23). It should be remembered that the curves of α_{0t} and $d\alpha_0/dn$, and also those of η_t and $d\eta/dn$, for the rigid aircraft change with weight distribution. Thus in considering the extent to which weight distribution influences the aeroelastic effect on η_t and $d\eta/dn$ (Figs. 22 and 23) we have to compare the various 'flexible' curves with their corresponding 'rigid' curves, rather than with one another. This point is brought out better by Fig. 26, which shows the relative control effectivenesses for the three weight distributions, and demonstrates that in fact, the changes of weight distribution considered have only a small influence on the aeroelastic effect. In particular the control reversal speeds for the three cases are identical*.

Taking the standard configuration (Loading Y) as datum, we see from Fig. 22 that the main effect of increasing the weight (Loading X) is to increase the value of Q at which the elevator angle to trim is zero, by about 100 lb/ft² for both rigid and flexible aircraft, while the effect of the c.g. shift represented by Loading Z is to reduce the value of Q at which $\eta_t = 0$ by about 100 lb/ft². Fig. 24 shows that increasing the weight increases the elevon angles per g, as we might expect from the second of formulae (51), since $\bar{C}_{Lt}$ for a given value of Q is increased. Shifting the c.g. aft (Loading Z) reduces $d\eta/dn$, as we would expect, because of the generally destabilising effect of such a shift.

5.3. *Limitations of the Work.*

The relevance of the present investigation to the actual aeroelastic behaviour of a slender delta aircraft may be limited by the assumptions upon which it has been based. Other investigations mentioned in the Introduction have suggested that while longitudinal bending will undoubtedly exert the major influence on longitudinal trim and manoeuvrability, the effects of spanwise deformation may not be entirely negligible. Such effects were, however, automatically excluded from consideration in the present instance; this was the price that had to be paid for the privilege—comparatively rare in aeroelastic work—of being able to compute a deformed shape directly, without recourse to iterative procedures or to assumed modes and strain-energy methods.

Other limitations stem from the aerodynamic assumptions. The possible effects of non-linearity were alluded to in the Introduction, in relation to Hancock's work. Such effects should, however, be fairly small at the moderate angles of attack obtaining in the design cruising condition, although they could become more pronounced in 'off-design' conditions. Hodges' work, at Bristol Aircraft Limited, has suggested that slender-wing theory may give unreliable estimates of aeroelastic effects for the type of slender configuration which we have considered. In our numerical work, we have restricted the use of this theory to the computation of the loading contributions due to elastic camber and to the induced camber produced by pitching. These should be relatively small compared with loading due to additional angle of attack etc., but an examination of the effect on overall results, of computing the loadings in question by piston theory, would be an informative exercise.

---

* In Ref. 5, Hancock and Milne showed that the control reversal speed (called 'maximum trim speed' by them) is independent of the weight distribution.

It will have been noted that in considerations of the effects of varying stiffness and weight distributions, the relevant parameters have been varied independently of one another. In considering the results of such studies, however, it is well to bear in mind that in the search for the optimum layout to meet a given specification, it is seldom practicable for the designer to vary one of the parameters influencing aeroelastic behaviour, independently of all others. Changes in stiffness and weight distributions tend to go hand in hand, while a change of weight distribution, if it involves a shift of c.g., necessitates a change in wing warp distribution or planform configuration in order to keep the centre of pressure coincident with the c.g. in the design condition. The danger of drawing false conclusions is inherent in any trend study which fails to take due account of any essential interdependence of the several parameters upon which a particular aircraft characteristic depends.

6. *Conclusions and Suggestions for Further Work.*

(1) A method has been established for estimating the effects of longitudinal bending on the trim and manoeuvrability of slender aircraft. The degree of relevance of results obtained by this method is dependent on the extent to which spanwise deformations would influence these characteristics in an actual aircraft. The work of other investigators has suggested that while longitudinal bending is probably the dominating source of aeroelastic effects on longitudinal characteristics, the influence of spanwise deformations will not be entirely negligible. In this context it should be emphasised that the present method was conceived, and the work of earlier investigators such as Broadbent was performed, at a time when attention was focussed on the 'completely integrated' slender-wing configuration, rather than on the alternative configuration involving a discrete fuselage plus slender wing. For the latter type of layout, the effects of spanwise deformation are likely to be of relatively greater importance than the calculations suggested they would be for the completely integrated layout.

Apart from excluding non-linear effects, the method permits of some freedom as regards aerodynamic assumptions, inasmuch as loadings corresponding to the distribution of effective local angle of attack for the undeformed aircraft may be specified in any convenient theoretical or empirical manner. As regards the chordwise loading due to elastic camber, the method assumes that this is expressible as a function of $\alpha_e(\xi)$ and ξ which is linear in $\alpha_e(\xi)$ and its derivatives with respect to ξ; detailed development of the method is given using functions appropriate to slender-wing theory and piston theory respectively.

(2) For application to a possible design for a Supersonic ($M = 2{\cdot}2$) Transport Aircraft, the method was programmed for the 'Mercury' digital computer and a fairly comprehensive set of calculations was performed for $M = 2{\cdot}2$ over a range of altitudes, representing different kinetic pressures, Q. In this instance, loading due to elastic camber was assumed to be given by slender-wing theory. The calculations were made for a so-called 'standard configuration' (with realistically estimated weight and stiffness distributions) and also for configurations modified in respect of either weight or stiffness distribution.

This numerical work has demonstrated the practicability of the method and the results suggest that for a supersonic transport of the type considered, the aeroelastic effects should not be prohibitively large under normal operating conditions, at the cruising Mach number of $2{\cdot}2$. An inadvertent dive at $M = 2{\cdot}2$ to altitudes lower than that envisaged in the flight plan could, however, result in a reduction of control effectiveness to a dangerously low value. The possibility that aeroelastically critical combinations of M and Q might occur in the flight plan, at altitudes lower than the minimum permitted for $M = 2{\cdot}2$, would require separate investigation.

In general, stiffening of the structure will reduce the aeroelastic effects, but the results show that stiffening of the rear-most portions is far more effective than stiffening elsewhere along the length (see, for example, Fig. 19, in association with Fig. 3). The weight and c.g. changes considered, had little influence on the aeroelastic effects.

(3) Further numerical work would be required to achieve completely the aims originally prescribed for this investigation.

It is intended to examine the effect of using piston theory instead of slender-wing theory for the loading due to elastic camber, so as to indicate the degree to which refinement of the aerodynamics may be required.

It would also be desirable to apply the method to a completely integrated shape and also to one in which the discrete body is more pronounced. This would add to our knowledge of the effect of various parameters on the problems which have been studied. In each of these extensions of the work, a certain amount of re-writing of computer programmes would be involved.

A further extension of the work could readily be made in the field of Loading Actions, by computing the longitudinal distributions of shear force and bending moment for manoeuvres corresponding to points on the Flight Envelope. Comparison with the distributions for the rigid aircraft would indicate the likely order of aeroelastic effects on loading actions.

(4) Views as to the general applicability and usefulness of the method will probably vary from reader to reader according to technical upbringing. The numerical work has shown that for incremental loading resulting from control deflection, the deformation mode shape changes very little with kinetic pressure (Q); from this it may be argued that, for a determination of structural stiffness requirements, (depending on control reversal considerations) a modal-type analysis will provide a more rapid solution, which will be sufficiently accurate if the (incremental) mode shape is determined accurately at the outset, for a particular Q, and thereafter assumed constant. However, the *overall* deformation shape in steady or quasi-steady flight changes considerably with Q and load factor n, so that an investigation of equilibrium configurations and of the corresponding load distributions could not proceed on the basis of a single, invariant mode.

The method is rather restrictive in its assumptions, particularly as regards its neglect of spanwise deformations, so that it may not be well suited to the study of the aeroelastic behaviour of an actual aircraft, whose aerodynamic and structural properties are completely determined. Because of the emphasis placed on realism in the representation of the stiffness and weight distributions in the present investigation, the programmes evolved for the numerical work do not lend themselves immediately to general parametric studies. By idealising the distributions of stiffness and weight, however, it would be possible to devise programmes better suited to this purpose.

It might be argued that other methods, such as the modal type of analysis, are more versatile for this kind of work. However, providing as it does, a unified solution of the equations expressing the equilibrium of the elastic aeroplane, the present approach has the undoubted merit that it yields an accurate solution of an idealised problem which may be used as a check on other methods.

SYMBOLS

A		Aspect ratio of gross planform
$B(\xi)$	$\equiv$	$EI(\xi)$, bending rigidity at station ξ:lb/ft^2
$\bar{B}(\xi)$	$=$	$\dfrac{B(\xi)}{Q_c l^4}$, non-dimensionalstiffness parameter
B_m		Maximum value of $B(\xi)$ in range $0 \leqslant \xi \leqslant 1$
B_1, B_2		Values of $B(\xi)$ at stations ξ_1, ξ_2, used to define stiffness distribution
$\bar{C}_L$	$=$	$\dfrac{\bar{L}}{QS}$, overall lift coefficient
$\bar{C}_{L0}$		'Modified' lift coefficient corresponding to angle-of-attack distribution $\alpha_d(\xi)$: a function of Q
$\bar{C}_{Lt}$		Overall lift coefficient in trimmed level flight
$\bar{C}_m$	$=$	$\dfrac{\bar{M}}{QSl}$, overall pitching-moment coefficient
$\bar{C}_{m0}$		'Modified' pitching-moment coefficient corresponding to angle-of-attack distribution $\alpha_d(\xi)$: a function of Q
D	$\equiv$	$\dfrac{d}{d\xi}$, differential operator
E		Young's modulus: lb/ft^2
$F_1(\xi)$, $F_2(\xi, Q)$, $F_3(\xi, Q)$, $F_4(\xi, Q)$, $F_5(\xi, Q)$		Forcing functions in the differential equations (30) {Defined by equations (29)}
$f_1(\xi)$, $f_2(\xi, Q)$		Variable coefficients of the differential equations (30) {Defined by equations (28)}
g		Gravitational acceleration
H_m, $H_{m\eta}$		Defined by equations (52)
H_t, $H_{t\eta}$		Defined by equations (48)
K_m, $K_{m\eta}$		Defined by equations (47)
k		Coefficient to be evaluated from equation (37)
$I(\xi)$		Second moment of area of beam section at station ξ (about neutral axis): ft^4
$L(\xi)$		Total aerodynamic lift per unit chord at station ξ:lb/ft
$L_\alpha(\xi)$, $L_\eta(\xi)$		Contributions to $L(\xi)$ due to distribution of local angle-of-attack and elevon deflection respectively: lb/ft
$L_{\alpha_d}(\xi)$, $L_{\alpha_0}{}'(\xi)$, $L_{\alpha_q}(\xi)$, $L_{\alpha_e}(\xi)$		Contributions to $L_\alpha(\xi)$ due to angle-of-attack distributions $\alpha_d(\xi)$, $\alpha_0{}'$, $\alpha_q(\xi)$, $\alpha_e(\xi)$ respectively: lb/ft
$\bar{L}$		Total aerodynamic lift on aircraft: lb

SYMBOLS—*continued*

$\mathscr{L}(\xi)$		Total transverse loading per unit length at station ξ (positive upwards): lb/ft
$\mathscr{L}^*(\xi)$	$=$	$\dfrac{\mathscr{L}(\xi)}{Q_c l}$, non-dimensionalised loading per unit length
l		Total length of aircraft at centreline: ft
l_B		Length of body ahead of wing leading edge (*see* Fig. 1): ft
M		Mach number
$\overline{M}$		Total aerodynamic moment about c.g.: lb. ft
ng		Incremental normal acceleration in pull-up manoeuvre
p	$=$	$\dfrac{S}{2ls_T}$, planform shape parameter
Q	$=$	$\frac{1}{2}\rho V^2$, kinetic pressure: lb/ft^2
Q_R		Theoretical value of Q for control reversal
q		Pitching velocity: rad/sec
$\hat{q}$	$=$	$\dfrac{ql}{V}$, non-dimensionalised pitching velocity
S		Gross planform area: ft^2
$s(\xi)$		Semi-span of planform at station ξ: ft
s_T	$=$	$s(1)$, semi-span at trailing edge: ft
V		Speed of flight: ft/sec
$W(\xi)$		Weight per unit length at station ξ: lb/ft
$\overline{W}(\xi)$	$=$	$l\int_0^{\xi} W(\xi)d\xi$: lb
$\overline{W}$	$=$	$\overline{W}(1)$, total weight of aircraft: lb
$z'(\xi)$		Normal displacement of neutral axis from centre-section chord at station ξ: ft
$z_b'(\xi)$, $z_e'(\xi)$		Parts of $z'(\xi)$ due to built-in camber and elastic camber respectively
$\alpha(\xi)$		Total effective local angle of attack at station ξ
α_1, α_2		Arbitrarily assigned values of $\alpha_{e0}(\xi)$ and $\alpha_e'(\xi)$ respectively at $\xi = 0$ (Section 2.5.3)
$\alpha_b(\xi)$		Contribution to $\alpha(\xi)$ from built-in camber relative to centre-section chord
$\alpha_d(\xi)$		Local angle of attack at station ξ for the undeformed wing at the design C_L

$\alpha_e(\xi)$		Contribution to $\alpha(\xi)$ from elastic camber
α_0		Angle of attack of centre-section chord
α_0'	$=$	$\alpha_0 - \alpha_{0d}$
α_{0d}		Angle of attack of the centre-section chord of the undeformed wing at the design C_L
$\alpha_q(\xi)$		Contribution to $\alpha(\xi)$ from induced camber due to pitching velocity
$\alpha_{\epsilon 0}(\xi)$, $\alpha_e'(\xi)$		Particular solutions of equations (30.r) and (32). (*See* Section 2.5.3)
$\zeta'(\xi)$		Normal displacement of neutral axis from centre-section chord at station ξ (as fraction of l) positive upwards
$\zeta_e'(\xi)$		Part of $\zeta'(\xi)$ due to elastic deformation
η		elevon deflection, positive downwards
μ	$=$	$\dfrac{\overline{W}}{g\rho Sl}$, aircraft relative density
ξ	$\approx$	ξ', distances from the nose, measured as fractions of l, along the direction of flight and the centre-section chord line, respectively
ξ_B	$=$	l_B/l
ξ_1, ξ_2, ξ_m		Stations to which the stiffnesses B_1, B_2, B_m apply
$\bar{\xi}$		Distance of c.g. from nose as fraction of l
ρ		Air density: slugs/ft^3
$\phi_d(\xi)$, $\phi_e(\xi)$, $\phi_0(\xi)$, $\phi_q(\xi)$, $\phi_\eta(\xi)$		Non-dimensional lift functions—*see* equation (7)
$\bar{\phi}_d(\xi)$	$=$	$\int_0^\xi \phi_d(\xi)d\xi$
$\bar{\phi}_0(\xi)$	$=$	$\int_0^\xi \phi_0(\xi)d\xi$
$\bar{\phi}_\eta(\xi)$	$=$	$\int_0^\xi \phi_\eta(\xi)d\xi$
$\Psi_1(\xi)$, $\Psi_2(\xi, Q)$, $\Psi_3(\xi, Q)$, $\Psi_4(\xi, Q)$, $\Psi_5(\xi, Q)$		Forcing functions in the differential equations (78); {defined by equations (77)}
$\psi_1(\xi)$, $\psi_2(\xi)$, $\psi_3(\xi, Q)$		Variable coefficients of the differential equations (78); {defined by equations (76)}

Suffices

c	Relating to design cruising condition
d	Relating to design C_L lift distribution
t	Relating to trimmed level flight

REFERENCES

No.	*Author(s)*	*Title, etc.*
1	G. J. Hancock	The static aeroelastic deformation of slender configurations, Part II: Some calculations on slender-plate aircraft, including non-linear aerodynamics. *Aeronautical Quarterly*, Vol. XII. November, 1961.
2, 3	G. J. Hancock	The static aeroelastic deformation of slender configurations, Part III: Static stability. *Aeronautical Quarterly*, Vol. XIV. February, 1963. Part IV: Manoeuvre theory. *Aeronautical Quarterly*, Vol. XIV. November, 1963.
4	G. J. Hancock	Some static aeroelastic considerations of slender aircraft. AGARD Report 352. April, 1961.
5	G. J. Hancock and R. D. Milne	The stability and control of flexible slender aircraft. A.R.C. 24 090. October, 1962.
6	R. D. Milne	Dynamics of the deformable aeroplane. Part I—The equations of motion. Part II—A study of the trim state and longitudinal stability of the slender integrated aeroplane configuration. A.R.C. R. & M. 3345. September, 1962.

APPENDIX I

Detailed Development of the Mathematical Analysis for Two Particular Cases

A1.1. *General.*

In the main text we developed the differential equation defining the deflected shape of the beam in the form

$$\frac{d^2}{d\xi^2}\left\{B(\xi)\frac{d\alpha_e}{d\xi}\right\} + Ql^4\phi\{\alpha_e(\xi), \xi\} = (n+1)l^3W(\xi) - Ql^4\{\phi_d(\xi) + \alpha_0'\phi_0(\xi) + \hat{q}\phi_{\hat{q}}(\xi) + \eta\phi_\eta(\xi)\}, \quad (15)\text{ bis}$$

wherein the lift distribution due to elastic camber is represented in the generalised functional form $Ql\phi\{\alpha_e(\xi), \xi\}$. The formulae {equations (41) to (43)} for $\bar{C}_{L0}$ and $\bar{C}_{m0}$ and the 'modified' partial derivatives of $\bar{C}_L$ and $\bar{C}_m$ were also expressed in terms of $\phi_e(\xi) = \phi\{\alpha_e(\xi), \xi\}$. We have already considered in Section 2.5.2 of the main text, the particular form assumed by equation (15) and the method of solving it, when $\phi_e(\xi)$ is appropriate to slender-wing theory. We now give, in Section A1.2, the development from equations (41) to (43) of the formulae for the modified derivatives, appropriate to the assumption of slender-wing theory. Section A1.3 gives the mathematical basis of the overall check which has been applied to the digital computer results. Finally, Section A1.4 gives details of the mathematical analysis for the case when the loading due to elastic camber is assumed to be in accordance with piston theory.

A1.2. *Formulae for the Modified Derivatives Appropriate to the Assumption of Slender-wing Theory.*

Equations (41) to (43) may be developed to the forms appropriate to this case, by substituting for $\phi_{\hat{q}}(\xi)$ from equation (22b) and for $\phi_{ed}(\xi)$, $\partial\phi_e(\xi)/\partial\alpha_0'$, etc. in accordance with equation (21b) {i.e. substituting $\alpha_{ed}(\xi)$, $\partial\alpha_e(\xi)/\partial\alpha_0'$, etc. for $\alpha_e(\xi)$ in that formula}. The resulting formulae, expressed in terms of aspect ratio $A = 4s_T^2/S$ are:

$$\left.\begin{aligned}
\bar{C}_{L0} &= \frac{A}{4}\left(\frac{l}{s_T}\right)^2\bar{\phi}_d(1) + \frac{\pi A}{2}\alpha_{ed}(1) \\
\bar{C}_{m0} &= \bar{C}_{L0}\bar{\xi} - \frac{A}{4}\left(\frac{l}{s_T}\right)^2\int_0^1\phi_d(\xi)\xi\,d\xi - \frac{\pi A}{2}\left[\alpha_{ed}(1) - \int_0^1\alpha_{ed}(\xi)\left\{\frac{s(\xi)}{s_T}\right\}^2 d\xi\right].
\end{aligned}\right\} \quad (64)$$

$$\left.\begin{aligned}
\frac{\partial\bar{C}_L}{\partial\alpha_0'} &= \frac{A}{4}\left(\frac{l}{s_T}\right)^2\bar{\phi}_0(1) + \frac{\pi A}{2}\frac{\partial\alpha_e(1)}{\partial\alpha_0'} \\
\frac{\partial\bar{C}_L}{\partial\eta} &= \frac{A}{4}\left(\frac{l}{s_T}\right)^2\bar{\phi}_\eta(1) + \frac{\pi A}{2}\frac{\partial\alpha_e(1)}{\partial\eta} \\
\frac{\partial\bar{C}_L}{\partial\hat{q}} &= \frac{\pi A}{2}\left\{1 - \bar{\xi} + \frac{\partial\alpha_e(1)}{\partial\hat{q}}\right\} \\
\frac{\partial\bar{C}_L}{\partial n} &= \frac{\pi A}{2}\frac{\partial\alpha_e(1)}{\partial n}.
\end{aligned}\right\} \quad (65)$$

$$\left.\begin{aligned}
\frac{\partial\bar{C}_m}{\partial\alpha_0'} &= \frac{\partial\bar{C}_L}{\partial\alpha_0'}\bar{\xi} - \frac{A}{4}\left(\frac{l}{s_T}\right)^2\int_0^1\phi_0(\xi)\xi\,d\xi - \frac{\pi A}{2}\left[\frac{\partial\alpha_e(1)}{\partial\alpha_0'} - \int_0^1\frac{\partial\alpha_e(\xi)}{\partial\alpha_0'}\left\{\frac{s(\xi)}{s_T}\right\}^2 d\xi\right] \\
\frac{\partial\bar{C}_m}{\partial\eta} &= \frac{\partial\bar{C}_L}{\partial\eta}\bar{\xi} - \frac{A}{4}\left(\frac{l}{s_T}\right)^2\int_0^1\phi_\eta(\xi)\xi\,d\xi - \frac{\pi A}{2}\left[\frac{\partial\alpha_e(1)}{\partial\eta} - \int_0^1\frac{\partial\alpha_e(\xi)}{\partial\eta}\left\{\frac{s(\xi)}{s_T}\right\}^2 d\xi\right] \\
\frac{\partial\bar{C}_m}{\partial\hat{q}} &= \frac{\partial\bar{C}_L}{\partial\hat{q}}\bar{\xi} - \frac{\pi A}{2}\left[1 - \bar{\xi} - \int_0^1(\xi-\bar{\xi})\left\{\frac{s(\xi)}{s_T}\right\}^2 d\xi + \frac{\partial\alpha_e(1)}{\partial\hat{q}} - \int_0^1\frac{\partial\alpha_e(\xi)}{\partial\hat{q}}\left\{\frac{s(\xi)}{s_T}\right\}^2 d\xi\right] \\
\frac{\partial\bar{C}_m}{\partial n} &= \frac{\partial\bar{C}_L}{\partial n}\bar{\xi} - \frac{\pi A}{2}\left[\frac{\partial\alpha_e(1)}{\partial n} - \int_0^1\frac{\partial\alpha_e(\xi)}{\partial n}\left\{\frac{s(\xi)}{s_T}\right\}^2 d\xi\right].
\end{aligned}\right\} \quad (66)$$

A1.3. *The Basis for an Overall Check of Results.*

The end-products of the calculations for a configuration with particular mass and stiffness distributions, operating at a specific value of Q, are:

(1) the values of the additional angle of attack α_{0l}' and the control deflection η_l to trim {calculated from equation (46)}, together with the distribution of elastic camber $\alpha_{el}(\xi)$, calculated from the equation

$$\alpha_{el}(\xi) = \alpha_{ed}(\xi) + \frac{\partial \alpha_e(\xi)}{\partial n} + \alpha_{0l}' \frac{\partial \alpha_e(\xi)}{\partial \alpha_0'} + \eta_l \frac{\partial \alpha_e(\xi)}{\partial \eta}. \tag{44 bis}$$

(2) the increments of root angle of attack and control deflection, per g, $d\alpha_0'/dn$ and $d\eta/dn$ respectively, {calculated from equations (51)} together with the incremental distribution of elastic camber $d\alpha_e(\xi)/dn$, calculated from the equation

$$\frac{d\alpha_e(\xi)}{dn} = \frac{\partial \alpha_e(\xi)}{\partial n} + \frac{d\alpha_0'}{dn} \frac{\partial \alpha_e(\xi)}{\partial \alpha_0'} + \frac{\bar{C}_{Ll}}{2\mu} \frac{\partial \alpha_e(\xi)}{\partial \hat{q}} + \frac{d\eta}{dn} \frac{\partial \alpha_e(\xi)}{\partial n}. \tag{49 bis}$$

With the elastic camber distributions $\alpha_{el}(\xi)$ and $d\alpha_e(\xi)/dn$ known, the resultant load distributions which are purported to have produced them may be written down as

$$\begin{aligned} \mathscr{L}_l(\xi) &= L_l(\xi) - (n+1)W(\xi) \\ &= Ql\left[\phi_d(\xi) + \alpha_{0l}'\phi_0(\xi) + \eta_l\phi_\eta(\xi) + 2\pi\left(\frac{s_T}{l}\right)^2 \frac{d}{d\xi}\left\{\alpha_{el}(\xi)\left[\frac{s(\xi)}{s_T}\right]^2\right\}\right] - (n+1)W(\xi) \end{aligned} \tag{67}$$

and

$$\begin{aligned} \frac{d\mathscr{L}(\xi)}{dn} &= \frac{dL(\xi)}{dn} - W(\xi) \\ &= Ql\left[\frac{d\alpha_0'}{dn}\phi_0(\xi) + \frac{d\eta}{dn}\phi_\eta(\xi) + \right. \\ &\quad \left. + 2\pi\left(\frac{s_T}{l}\right)^2 \left\{\frac{\bar{C}_{Ll}}{2\mu}\frac{d}{d\xi}\left[(\xi-\bar{\xi})\left\{\frac{s(\xi)}{s_T}\right\}^2\right] + \frac{d}{d\xi}\left[\frac{d\alpha_e}{dn}\left\{\frac{s(\xi)}{s_T}\right\}^2\right]\right\}\right] - W(\xi). \end{aligned} \tag{68}$$

The deflection of the beam under the known loadings (67) and (68) may be calculated by direct integration of the differential equation

$$\frac{d^2}{d\xi^2}\left\{B(\xi)\frac{d\alpha_e}{d\xi}\right\} = -l^3\mathscr{L}(\xi),$$

(cf. the calculation of $\alpha_{ec}(\xi)$, described in Section 2.8). Thus we may calculate

$$\alpha_{el}'(\xi) = \int_0^1 d\xi \int_0^\xi d\xi_1 \left\{\frac{\int_0^{\xi_1} d\xi_2 \int_0^{\xi_2} \mathscr{L}_l^*(\xi_3)d\xi_3}{\bar{B}(\xi_1)}\right\} - \int_0^\xi d\xi_1 \left\{\frac{\int_0^{\xi_1} d\xi_2 \int_0^{\xi_2} \mathscr{L}_l^*(\xi_3)d\xi_3}{\bar{B}(\xi_1)}\right\} \tag{69}$$

and

$$\left(\frac{d\alpha_e(\xi)}{dn}\right)' = \int_0^1 d\xi \int_0^\xi d\xi_1 \left\{\frac{\int_0^{\xi_1} d\xi_2 \int_0^{\xi_2} \frac{d\mathscr{L}^*(\xi_3)}{dn} d\xi_3}{\bar{B}(\xi_1)}\right\} - \int_0^\xi d\xi_1 \left\{\frac{\int_0^{\xi_1} d\xi_2 \int_0^{\xi_2} \frac{d\mathscr{L}^*(\xi_3)}{dn} d\xi_3}{\bar{B}(\xi_1)}\right\} \tag{70}$$

where

$$\mathscr{L}_l^*(\xi) = \frac{\mathscr{L}_l(\xi)}{Q_c l} \quad \text{and} \quad \frac{d\mathscr{L}^*(\xi)}{dn} = \frac{d\mathscr{L}(\xi)}{dn} \Big/ Q_c l. \tag{71}$$

Then, if all calculations have been correctly performed, we should have

$$\alpha_{et}'(\xi) \equiv \alpha_{et}(\xi); \qquad \left(\frac{d\alpha_e(\xi)}{dn}\right)' \equiv \frac{d\alpha_e(\xi)}{dn} \tag{72}$$

within the limits of accuracy of whatever numerical methods have been employed.

A1.4. *Details of Mathematical Analysis when the Loading Due to Elastic Camber is in Accordance with Linearized Piston Theory.*

A1.4.1. *Form of the Differential Equation.*

In this case, we have

$$L_{\alpha_e}(\xi) = Q\frac{4}{M}\alpha_e(\xi) \times 2s(\xi) \tag{73a}$$

where M is the Mach number, so that

$$\phi_e(\xi) = \frac{8}{M}\left(\frac{s_T}{l}\right)\left\{\frac{s(\xi)}{s_T}\right\}\alpha_e(\xi). \tag{73b}$$

For consistency we will assume the loading due to $\alpha_q(\xi)$ also to be in accordance with piston theory, writing

$$L_{\alpha_q}(\xi) = Q\frac{4}{M}\alpha_q(\xi) \times 2s(\xi) \tag{74a}$$

or

$$\phi_q(\xi) = \frac{8}{M}\left(\frac{s_T}{l}\right)\left\{\frac{s(\xi)}{s_T}\right\}(\xi - \bar{\xi}). \tag{74b}$$

The form of $\phi_e(\xi)$ in this case does not permit the reduction of the order of equation (15) from third to second by direct integration. Since

$$\frac{d^2}{d\xi^2}\left\{B(\xi)\frac{d\alpha_e}{d\xi}\right\} = B(\xi)\frac{d^3\alpha_e}{d\xi^3} + 2\frac{dB(\xi)}{d\xi}\frac{d^2\alpha_e}{d\xi^2} + \frac{d^2B(\xi)}{d\xi^2}\frac{d\alpha_e}{d\xi},$$

equation (15), when divided through by $B(\xi)$, assumes the form

$$\begin{aligned}&\{D^3 + \psi_1(\xi)D^2 + \psi_2(\xi)D + \psi_3(\xi, Q)\}\alpha_e(\xi)\\ &\quad = (n+1)\Psi_1(\xi) + \Psi_2(\xi, Q) + \alpha_0'\Psi_3(\xi, Q) + \hat{q}\Psi_4(\xi, Q) + \eta\Psi_5(\xi, Q)\end{aligned} \tag{75}$$

with

$$\left.\begin{aligned}\psi_1(\xi) &= \frac{2}{\bar{B}(\xi)}\frac{d\bar{B}(\xi)}{d\xi}; \qquad \psi_2(\xi) = \frac{1}{\bar{B}(\xi)}\frac{d^2\bar{B}(\xi)}{d\xi^2};\\ \psi_3(\xi, Q) &= \frac{8}{M}\frac{1}{\bar{B}(\xi)}\frac{Q}{Q_c}\left(\frac{s_T}{l}\right)\left\{\frac{s(\xi)}{s_T}\right\}\end{aligned}\right\} \tag{76}$$

and

$$\left.\begin{aligned}\Psi_1(\xi) &= \frac{W(\xi)}{\bar{B}(\xi)Q_c l};\\ \Psi_2(\xi, Q) &= -\frac{Q}{Q_c}\frac{\phi_a(\xi)}{\bar{B}(\xi)};\\ \Psi_3(\xi, Q) &= -\frac{Q}{Q_c}\frac{\phi_0(\xi)}{\bar{B}(\xi)};\\ \Psi_4(\xi, Q) &= -\Psi_3(\xi, Q)(\xi - \bar{\xi});\\ \Psi_5(\xi, Q) &= -\frac{Q}{Q_c}\frac{\phi_\eta(\xi)}{\bar{B}(\xi)}.\end{aligned}\right\} \tag{77}$$

The solution of (75) may be expressed in the form (19) where $\partial\alpha_e(\xi)/\partial n$, $\alpha_{ed}(\xi)$, $\partial\alpha_e(\xi)/\partial\alpha_0'$, $\partial\alpha_e(\xi)/\partial\hat{q}$ and $\partial\alpha_e(\xi)/\partial\eta$ are now the respective solutions of

$$\{D^3 + \psi_1(\xi)D^2 + \psi_2(\xi)D + \psi_3(\xi, Q)\}\alpha_e(\xi) = \Psi_r(\xi, Q), \qquad r = 1, \ldots 5 \tag{78.r}$$

with forcing functions $\Psi_r(\xi, Q)$ as defined in equation (77), and with boundary conditions (16), (17b), (18).

In the solution of equations (78.r) by digital computer, the technique described in Section 2.5.3 may again be used to overcome the difficulty arising from the fact that the value of $\alpha_e(0)$ is not specified.

A1.4.2. *Formulae for the Modified Derivatives.*

With appropriate substitutions for $\phi_q(\xi)$, $\phi_{ed}(\xi)$, etc. equations (41) to (43) now become:

$$\left.\begin{aligned}
\bar{C}_{L0} &= \frac{A}{4}\left(\frac{l}{s_T}\right)^2 \bar{\phi}_d(1) + \frac{2A}{M}\frac{l}{s_T}\int_0^1 \alpha_{ed}(\xi)\left\{\frac{s(\xi)}{s_T}\right\} d\xi \\
\bar{C}_{m0} &= \bar{C}_{L0}\bar{\xi} - \frac{A}{4}\left(\frac{l}{s_T}\right)^2 \int_0^1 \phi_d(\xi)\xi\, d\xi - \frac{2A}{M}\frac{l}{s_T}\int_0^1 \alpha_{ed}(\xi)\left\{\frac{s(\xi)}{s_T}\right\}\xi\, d\xi.
\end{aligned}\right\} \tag{79}$$

$$\left.\begin{aligned}
\frac{\partial\bar{C}_L}{\partial\alpha_0'} &= \frac{A}{4}\left(\frac{l}{s_T}\right)^2 \bar{\phi}_0(1) + \frac{2A}{M}\frac{l}{s_T}\int_0^1 \frac{\partial\alpha_e(\xi)}{\partial\alpha_0'}\left\{\frac{s(\xi)}{s_T}\right\} d\xi \\
\frac{\partial\bar{C}_L}{\partial\eta} &= \frac{A}{4}\left(\frac{l}{s_T}\right)^2 \bar{\phi}_\eta(1) + \frac{2A}{M}\frac{l}{s_T}\int_0^1 \frac{\partial\alpha_e(\xi)}{\partial\eta}\left\{\frac{s(\xi)}{s_T}\right\} d\xi \\
\frac{\partial\bar{C}_L}{\partial\hat{q}} &= \frac{2A}{M}\frac{l}{s_T}\left[\int_0^1 \xi\left\{\frac{s(\xi)}{s_T}\right\} d\xi - \bar{\xi}\int_0^1 \left\{\frac{s(\xi)}{s_T}\right\} d\xi + \int_0^1 \frac{\partial\alpha_e(\xi)}{\partial\hat{q}}\left\{\frac{s(\xi)}{s_T}\right\} d\xi\right] \\
\frac{\partial\bar{C}_L}{\partial n} &= \frac{2A}{M}\frac{l}{s_T}\int_0^1 \frac{\partial\alpha_e(\xi)}{\partial n}\left\{\frac{s(\xi)}{s_T}\right\} d\xi.
\end{aligned}\right\} \tag{80}$$

$$\left.\begin{aligned}
\frac{\partial\bar{C}_m}{\partial\alpha_0'} &= \frac{\partial\bar{C}_L}{\partial\alpha_0'}\bar{\xi} - \frac{A}{4}\left(\frac{l}{s_T}\right)^2 \int_0^1 \phi_0(\xi)\xi\, d\xi - \frac{2A}{M}\frac{l}{s_T}\int_0^1 \frac{\partial\alpha_e(\xi)}{\partial\alpha_0'}\left\{\frac{s(\xi)}{s_T}\right\}\xi\, d\xi \\
\frac{\partial\bar{C}_m}{\partial\eta} &= \frac{\partial\bar{C}_L}{\partial\eta}\bar{\xi} - \frac{A}{4}\left(\frac{l}{s_T}\right)^2 \int_0^1 \phi_\eta(\xi)\xi\, d\xi - \frac{2A}{M}\frac{l}{s_T}\int_0^1 \frac{\partial\alpha_e(\xi)}{\partial\eta}\left\{\frac{s(\xi)}{s_T}\right\}\xi\, d\xi \\
\frac{\partial\bar{C}_m}{\partial\hat{q}} &= \frac{\partial\bar{C}_L}{\partial\hat{q}}\bar{\xi} - \frac{2A}{M}\frac{l}{s_T}\left[\int_0^1 \xi^2\left\{\frac{s(\xi)}{s_T}\right\} d\xi - \bar{\xi}\int_0^1 \xi\left\{\frac{s(\xi)}{s_T}\right\} d\xi + \int_0^1 \frac{\partial\alpha_e(\xi)}{\partial\hat{q}}\left\{\frac{s(\xi)}{s_T}\right\}\xi\, d\xi\right] \\
\frac{\partial\bar{C}_m}{\partial n} &= \frac{\partial\bar{C}_L}{\partial n}\bar{\xi} - \frac{2A}{M}\frac{l}{s_T}\int_0^1 \frac{\partial\alpha_e(\xi)}{\partial n}\left\{\frac{s(\xi)}{s_T}\right\}\xi\, d\xi.
\end{aligned}\right\} \tag{81}$$

APPENDIX II

The Effect of Discontinuities in the Stiffness Distribution or in the Slope of the Stiffness Distribution

Reference was made in Section 5.1 to the computing difficulties that arose in the calculations using slender-wing theory, when the stiffness distribution was discontinuous. Similar difficulties will arise when piston theory is employed if either the stiffness distribution or its slope is discontinuous. We will discuss this somewhat more complicated case in detail; results for the simpler slender-wing theory case then follow easily.

The equations by which equation (78.r) is replaced for solution by the 'Mercury Intstep' routine are:

$$\begin{aligned} f_4 &= \frac{dy_4}{d\xi} = -\psi_1 y_4 - \psi_2 y_3 - \psi_3 y_2 + \Psi_r', \\ f_3 &= \frac{dy_3}{d\xi} = y_4, \\ f_2 &= \frac{dy_2}{d\xi} = y_3, \\ f_1 &= \frac{dy_1}{d\xi} = y_2, \end{aligned} \tag{82}$$

where

$$y_1 = -\zeta, \quad y_2 = \alpha_e, \quad y_3 = \frac{d\alpha_e}{d\xi}, \quad y_4 = \frac{d^2\alpha_e}{d\xi^2}. \tag{83}$$

Also, if we write, for a linear segment of the stiffness distribution curve:

$$\bar{B}(\xi) = \bar{B}_1 + \bar{B}_0 \xi, \tag{84}$$

we have

$$\psi_1(\xi) = \frac{2}{\bar{B}(\xi)} \frac{d\bar{B}(\xi)}{d\xi} = \frac{2\bar{B}_0}{\bar{B}}, \tag{85}$$

$$\psi_2(\xi) = \frac{1}{\bar{B}} \frac{d^2\bar{B}}{d\xi^2} = \frac{1}{\bar{B}} \frac{d\bar{B}_0}{d\xi}, \tag{86}$$

$$\psi_3(\xi) = \frac{2}{M} \frac{Q}{Q_c} \left\{ \frac{s(\xi)}{s_T} \right\} \frac{1}{\bar{B}}, \tag{87}$$

$$\Psi_r'(\xi) \propto \frac{1}{\bar{B}} \{\textit{see} \text{ equation (77)}\}. \tag{88}$$

Now consider a point ξ_0 such that the stiffness is given by (84) for $\xi < \xi_0$, and by

$$\bar{B}'(\xi) = \bar{B}_1' + \bar{B}_0' \xi \tag{89}$$

for $\xi > \xi_0$. Write

$$\Delta\bar{B} = \bar{B}'(\xi_0) - \bar{B}(\xi_0), \tag{90}$$

and

$$\Delta\bar{B}_0 = \bar{B}_0' - \bar{B}_0. \tag{91}$$

We assume that in general $\Delta\bar{B} \neq 0$, $\Delta\bar{B}_0 \neq 0$, i.e. both the stiffness and its slope are discontinuous at $\xi = \xi_0$. Now $\bar{B}(\xi)$, and hence $\psi_3(\xi)$ and $\Psi_r(\xi)$, remain bounded throughout any (small) interval containing ξ_0, but $\psi_1(\xi)$ and $\psi_2(\xi)$ will each have a singularity at $\xi = \xi_0$. It will follow that in the integration of equations (82) through $\xi = \xi_0$, steps should occur in the values of y_4 and y_3 at $\xi = \xi_0$.

However, the 'Intstep' routine will not recognize the existence of such steps, and will accordingly produce incorrect answers if allowed to continue operating without modification through such a point.

The existence of the steps in y_3 and y_4 may be confirmed, and their magnitudes calculated more easily, perhaps, by invoking physical considerations than by using purely mathematical arguments. For remembering that bending moment and shear must be continuous across $\xi = \xi_0$ and noting that

$$\text{B.M. } (\xi) = Q_c l^3 \bar{B}(\xi) y_3, \tag{92}$$

and

$$\text{Shear } (\xi) = Q_c l^2 \{\bar{B}(\xi) y_4 + \bar{B}_0 y_3\}, \tag{93}$$

we have at once

$$\bar{B}(\xi_0) y_3(\xi_0 - 0) = \bar{B}'(\xi_0) y_3(\xi_0 + 0)$$

whence

$$y_3(\xi_0 + 0) = \frac{\bar{B}(\xi_0)}{\bar{B}'(\xi_0)} y_3(\xi_0 - 0) \tag{94a}$$

or

$$\Delta y_3(\xi_0) = -\frac{\Delta \bar{B}}{\bar{B}'(\xi_0)} y_3(\xi_0 - 0), \tag{94b}$$

and

$$\bar{B}(\xi_0) y_4(\xi_0 - 0) + \bar{B}_0 y_3(\xi_0 - 0) = \bar{B}'(\xi_0) y_4(\xi_0 + 0) + \bar{B}_0' y_3(\xi_0 + 0),$$

whence, using (94a) we obtain

$$y_4(\xi_0 + 0) = \frac{\bar{B}(\xi_0)}{\bar{B}'(\xi_0)} y_4(\xi_0 - 0) + \frac{\bar{B}_0 \bar{B}'(\xi_0) - \bar{B}_0' \bar{B}(\xi_0)}{\{\bar{B}'(\xi_0)\}^2} y_3(\xi_0 - 0) \tag{95a}$$

or

$$\Delta y_4(\xi_0) = -\frac{\Delta \bar{B}}{\bar{B}'(\xi_0)} y_4(\xi_0 - 0) + \frac{\bar{B}_0' \Delta \bar{B} - \bar{B}'(\xi_0) \Delta \bar{B}_0}{\{\bar{B}'(\xi_0)\}^2} y_3(\xi_0 - 0). \tag{95b}$$

In the particular case where the stiffness $\bar{B}(\xi)$ is continuous at $\xi = \xi_0$ and only B_0 discontinuous, we have $\Delta \bar{B} = 0$ and $\bar{B}'(\xi_0) = \bar{B}(\xi_0)$, so that

$$y_3(\xi_0 + 0) = y_3(\xi_0 - 0) = y_3(\xi_0), \quad \text{or} \quad \Delta y_3(\xi_0) = 0, \tag{96}$$

and

$$\left.\begin{aligned} y_4(\xi_0 + 0) &= y_4(\xi_0 - 0) - \frac{\Delta \bar{B}_0}{\bar{B}(\xi_0)} y_3(\xi_0) \\ \text{or} \qquad \Delta y_4(\xi_0) &= -\frac{\Delta \bar{B}_0}{\bar{B}(\xi_0)} y_3(\xi_0). \end{aligned}\right\} \tag{97}$$

In order that the 'Mercury' programme should cope with stiffness distributions exhibiting discontinuities of the stiffness itself or of its slope, it is necessary to make provision for adding increments to y_3 and y_4 in accordance with equations (94b) and (95b) at any point where such discontinuities occur*.

The reader may easily check for himself that when, as in the calculations described in this report, slender-wing theory is employed, and the equation to be solved by the computer is the second-order equation (30.r) rather than the third-order equation (78.r), singular behaviour occurs only if the stiffness itself is discontinuous. This may be dealt with by adding the increment $\Delta y_3(\xi_0)$, given by equation (94b), to $y_3(\xi_0 - 0)$ at any point $\xi = \xi_0$ where such a discontinuity occurs.

* A point of interest to programmers is that the relevant instructions must not be included within the 'Intstep' auxiliary sequence itself.

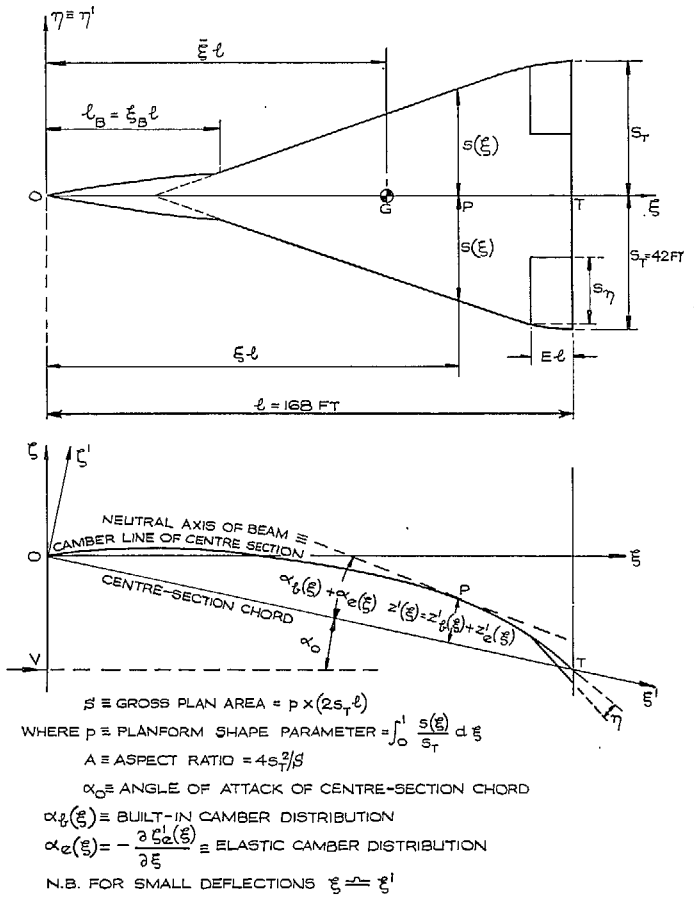

FIG. 1. Illustrations of planform assumed for calculations, and general geometric notation.

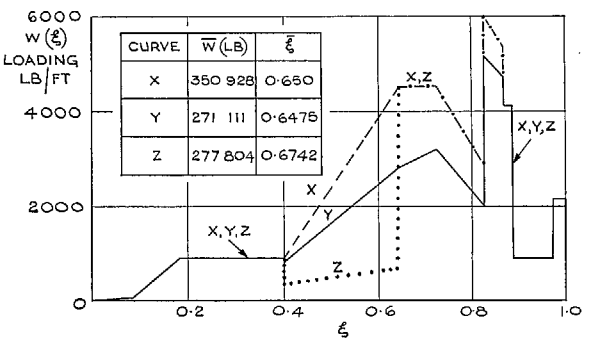

FIG. 2. Weight distributions.

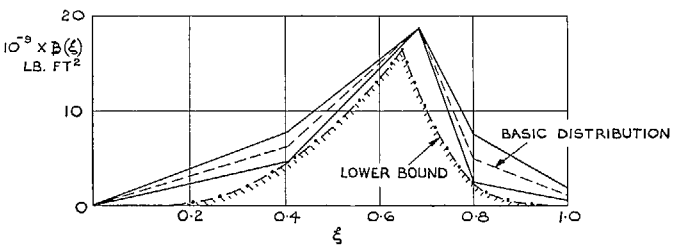

FIG. 3. Stiffness distributions.

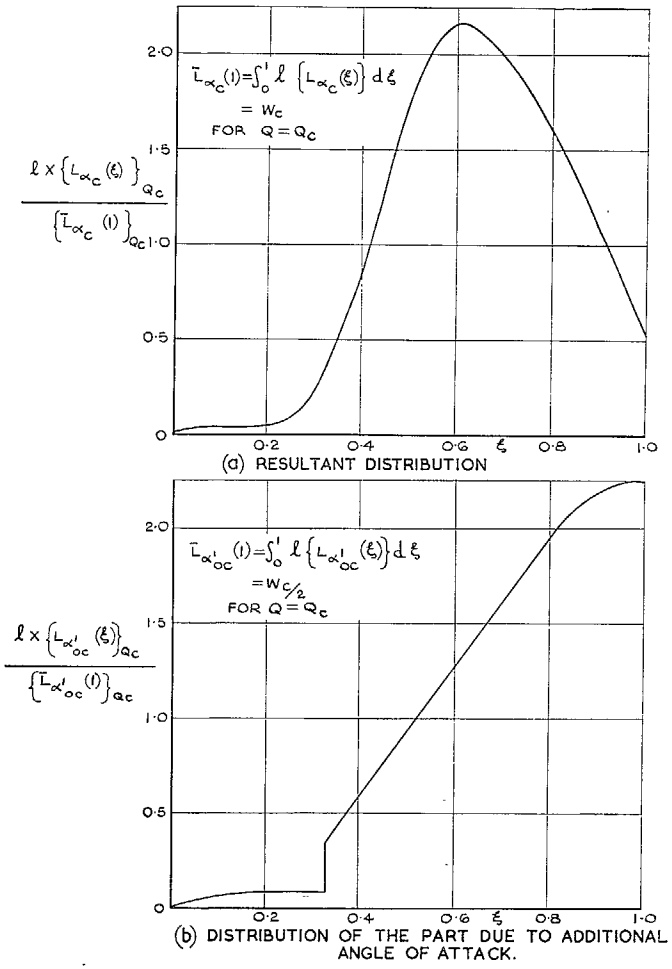

FIG. 4. Longitudinal load distributions for design cruising condition ($C_{L\,\text{cruise}} = 2C_{L\,\text{design}}$).

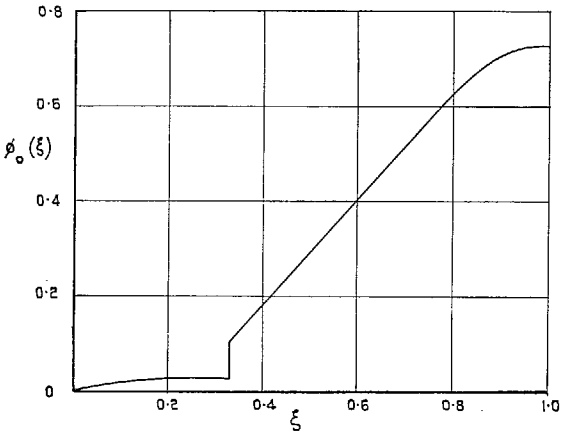

FIG. 5. Lift distribution function $\phi_0(\xi)$ for additional angle of attack.

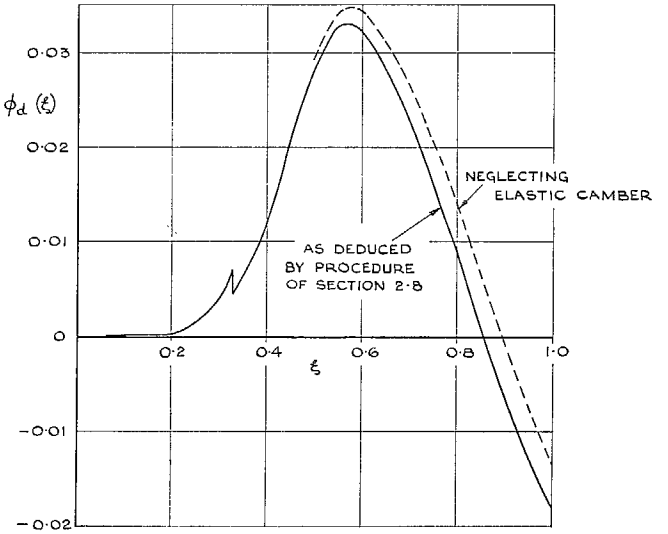

FIG. 6. Lift distribution function $\phi_d(\xi)$ for design case.

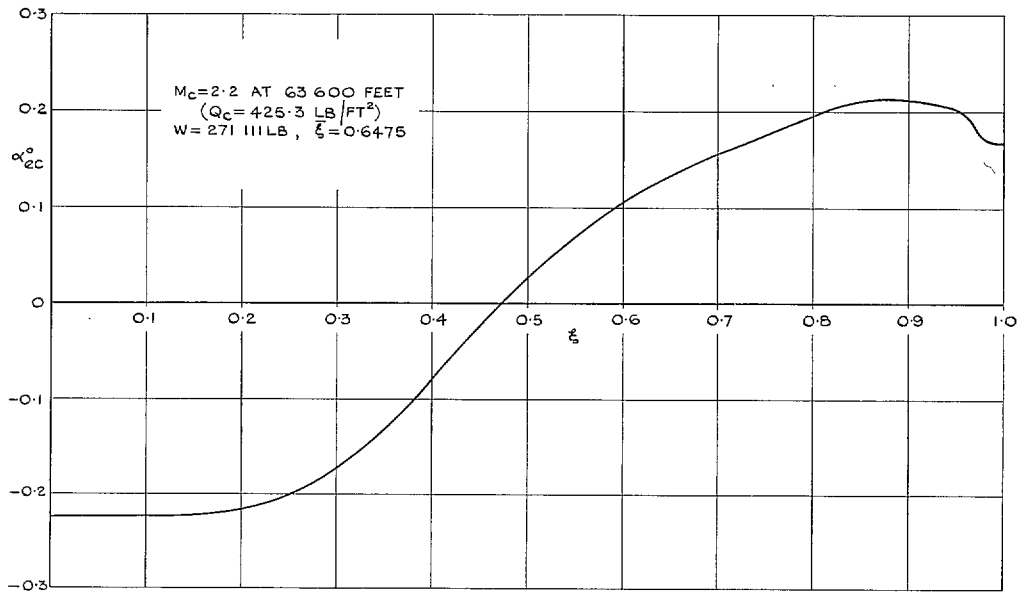

FIG. 7. Distribution of elastic camber for standard configuration in design cruise condition.

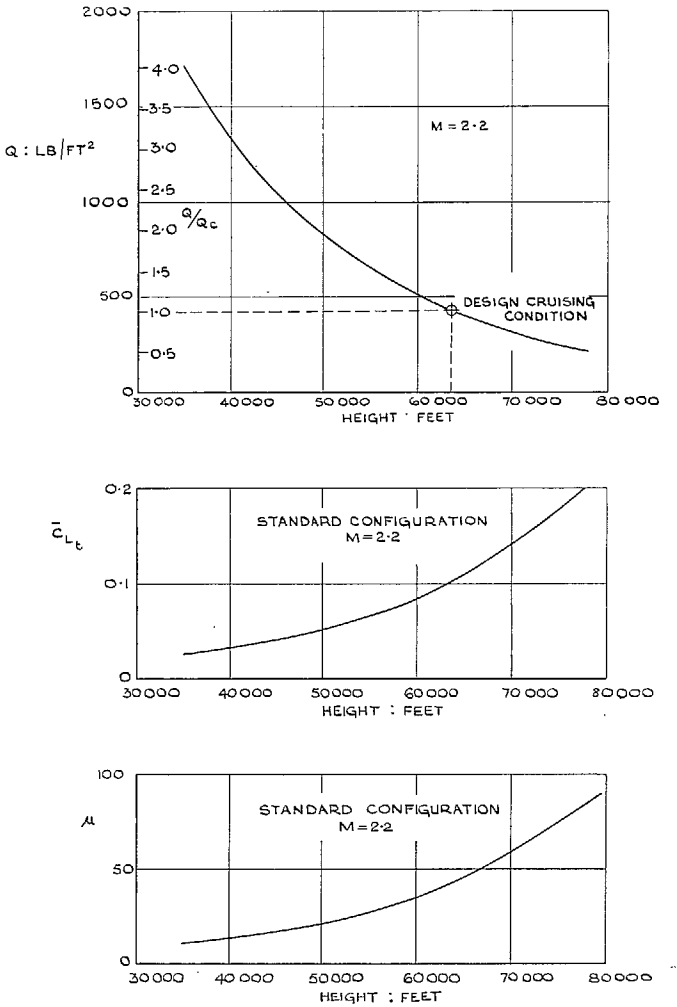

FIG. 8. Variation with height, of kinetic pressure, and of trimmed lift coefficient and aircraft relative density for the standard configuration, at $M = 2{\cdot}2$.

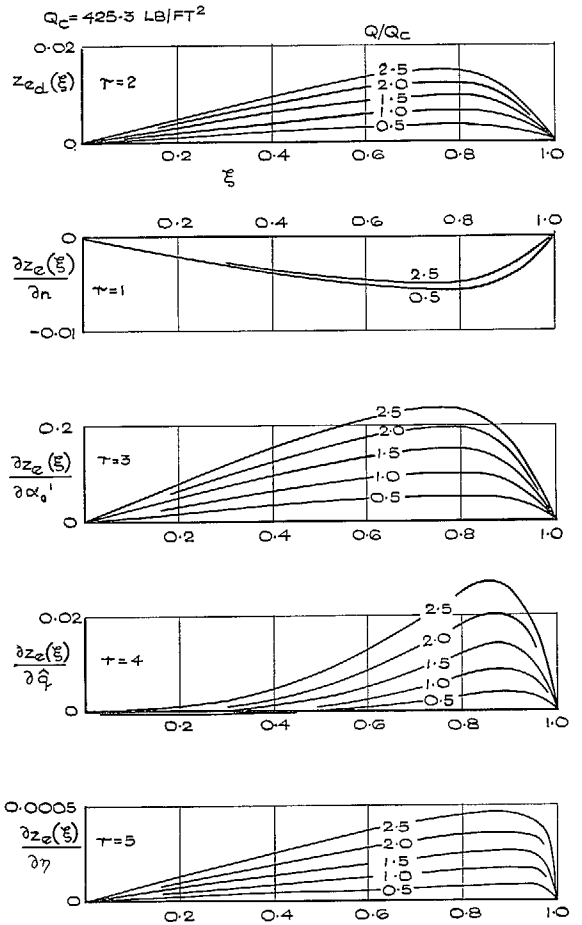

FIG. 9. Deformations computed from solutions of the equations $\{D^2 + f_1(\xi)D + f_2(\xi,Q)\}\alpha_e(\xi) = F_r(\xi,Q)$, $r = 1 \ldots 5$: standard configuration, at $M = 2{\cdot}2$.

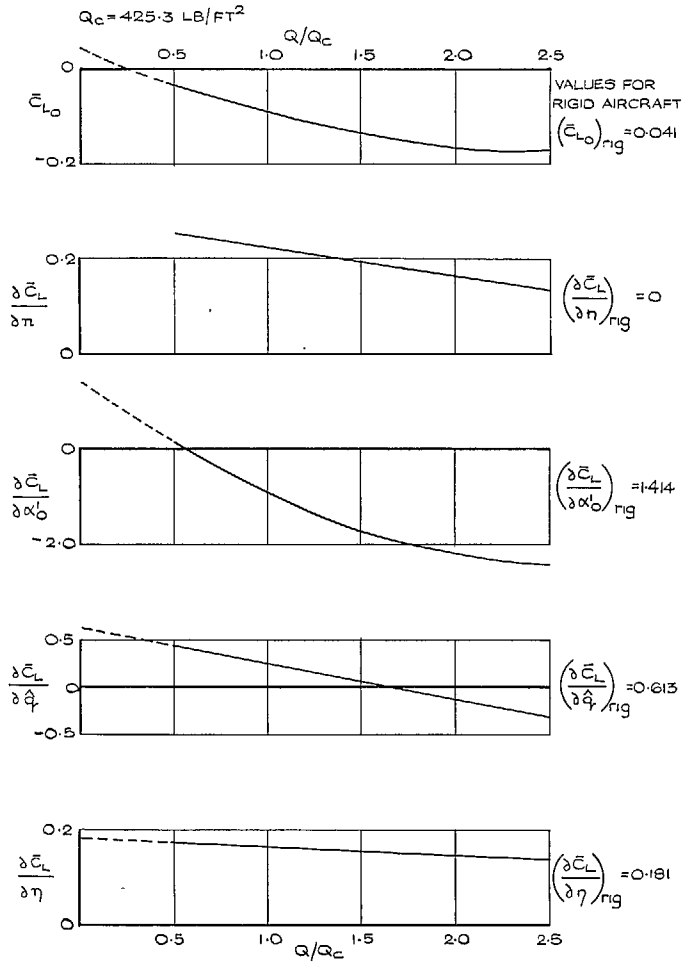

FIG. 10. 'Modified' partial derivatives of C_L for the standard configuration at $M = 2{\cdot}2$.

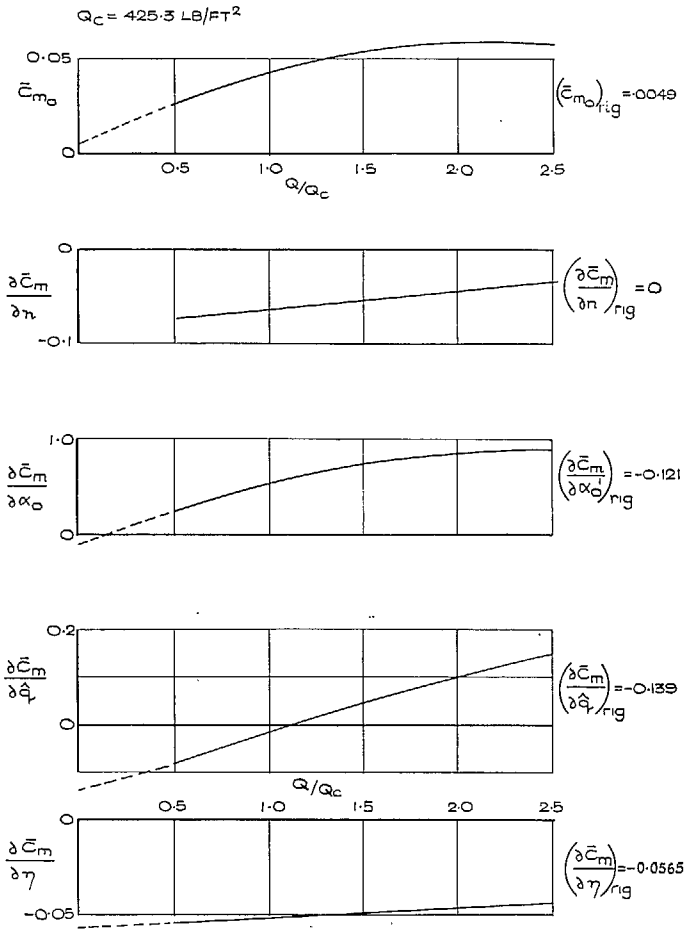

FIG. 11. Modified partial derivatives of $\bar{C}_m$ for the standard configuration at $M = 2{\cdot}2$.

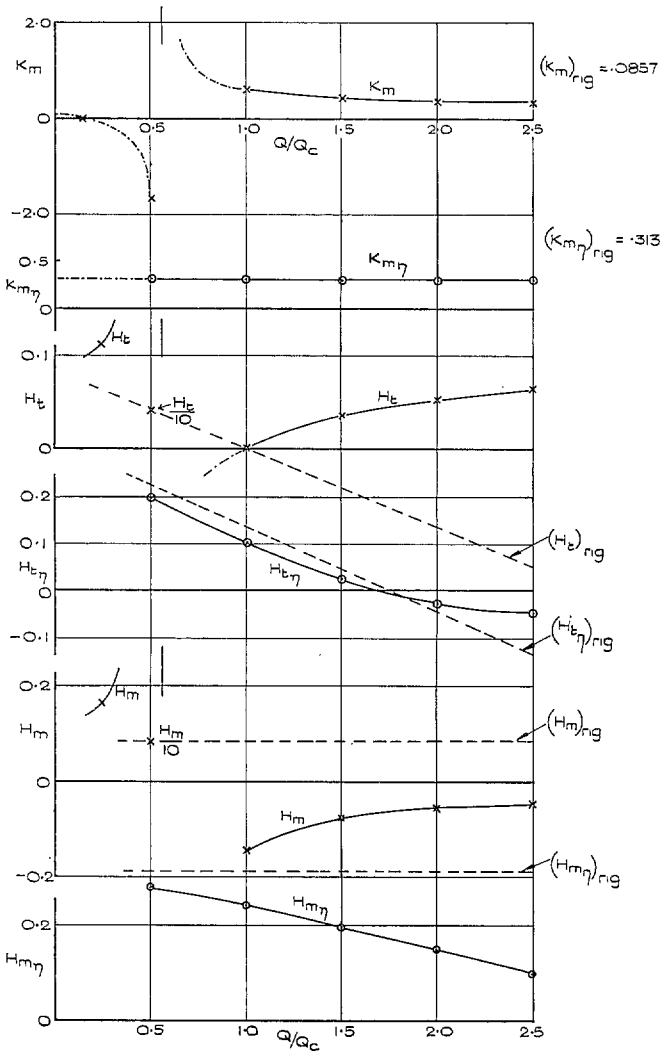

FIG. 12. Variation of the parameters K_m, $K_{m\eta}$, H_t, $H_{t\eta}$, H_m and $H_{m\eta}$ with Q for standard configuration at $M = 2{\cdot}2$.

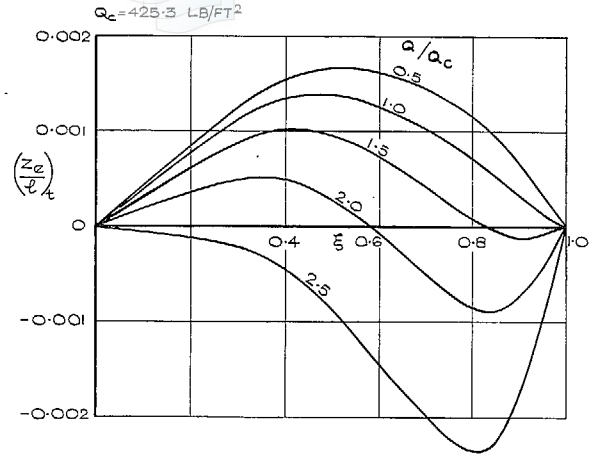

FIG. 13. Deformations for standard configuration in trimmed flight at $M = 2{\cdot}2$.

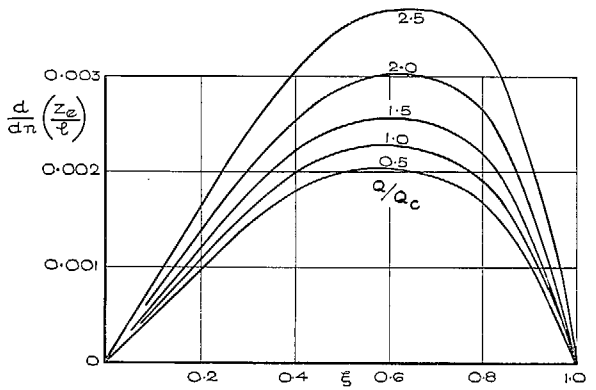

FIG. 14. Incremental deformations per g for standard configuration in steady pull-up manoeuvre at $M = 2{\cdot}2$.

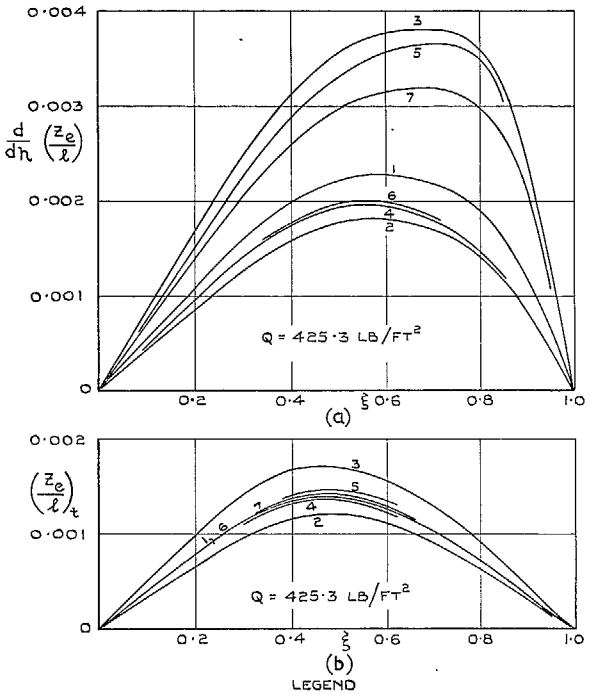

LEGEND

CURVES	STIFFNESS DISTRIBUTION (SEE TABLE SECT. 43)
1	BASIC STIFFNESS
2	INCREASED THROUGHOUT
3	DECREASED THROUGHOUT
4	INCREASED OVER REAR HALF
5	DECREASED OVER REAR HALF
6	INCREASED OVER REAR QUARTER
7	DECREASED OVER REAR QUARTER

FIG. 15. Incremental deformations per g (a) and deformations in trimmed flight (b) for standard weight distribution and various stiffness distributions at $M = 2{\cdot}2$.

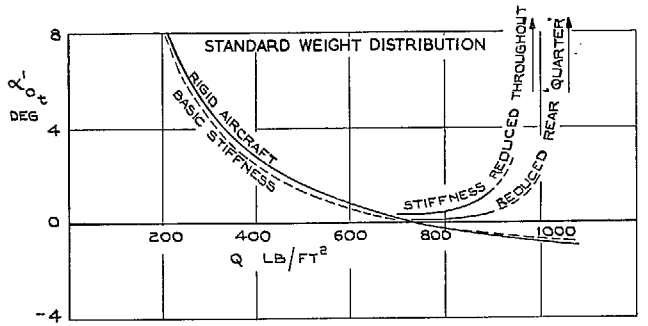

FIG. 16. Additional angle of attack required for trimmed flight at $M = 2{\cdot}2$.

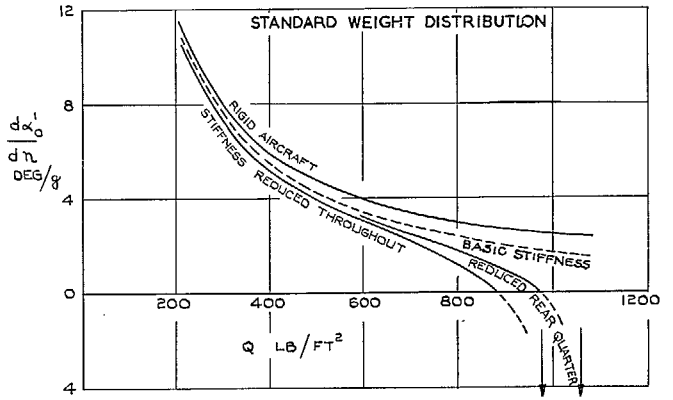

FIG. 17. Incremental angle of attack per g required for steady pull-up manoeuvre at $M = 2{\cdot}2$.

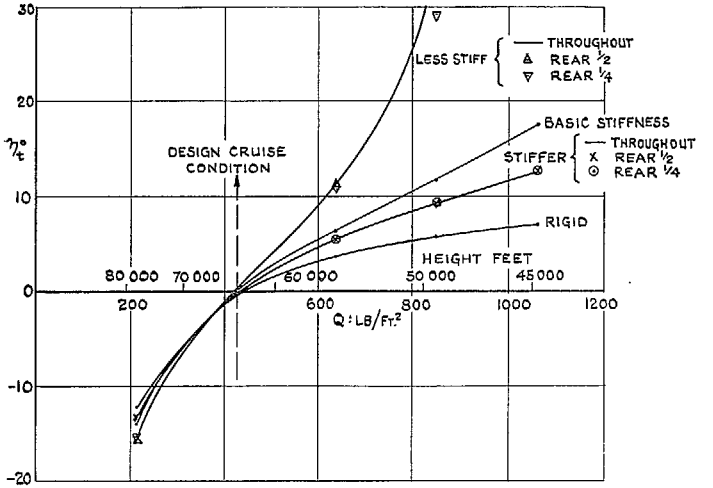

FIG. 18. Effect of stiffness on elevon angle to trim: standard weight distribution, $M = 2{\cdot}2$.

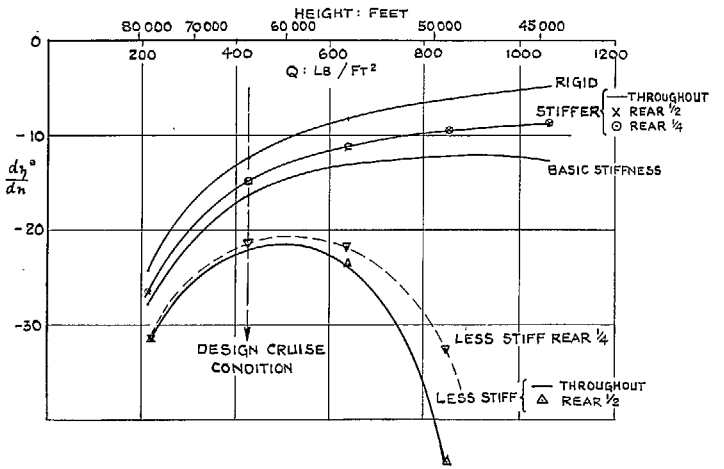

FIG. 19. Effect of stiffness on elevon angle per g in pull-up manoeuvre at $M = 2{\cdot}2$: standard weight distribution.

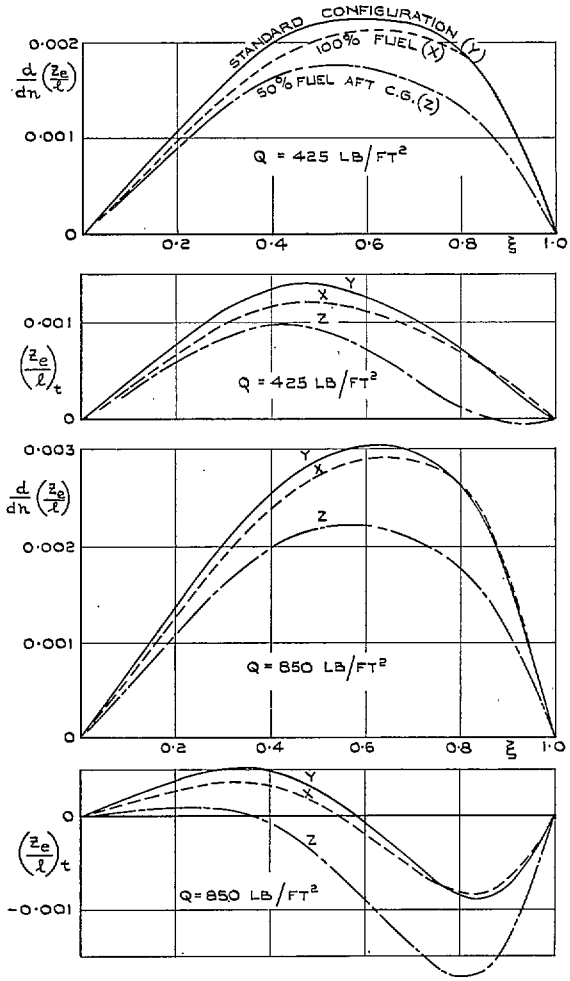

FIG. 20. Effect of weight and c.g. position on deformation modes (basic stiffness distribution) at $M = 2{\cdot}2$.

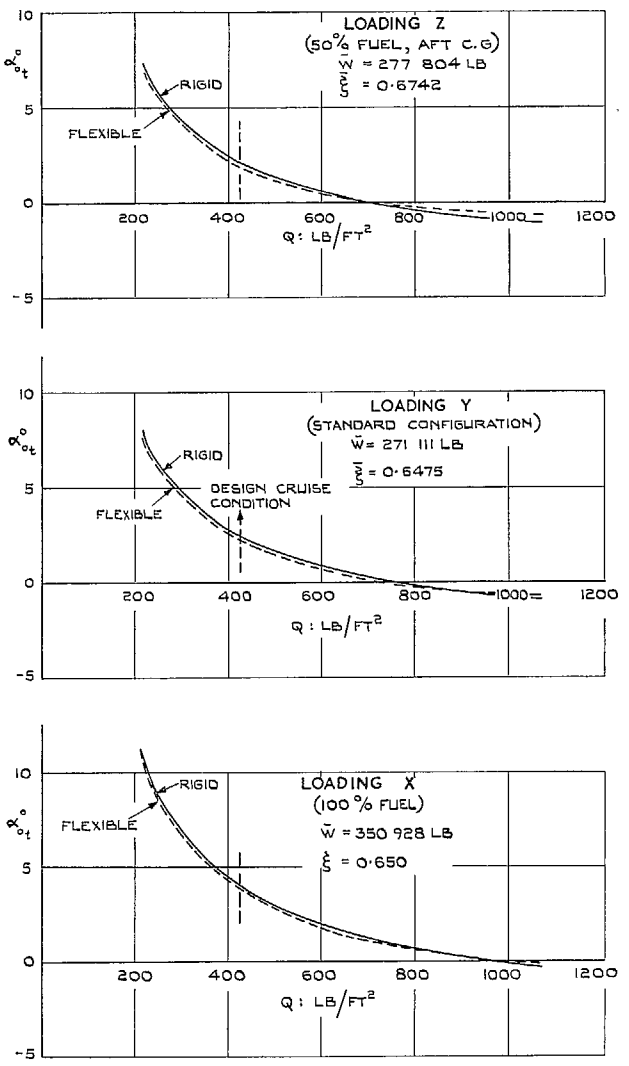

FIG. 21. Effect of weight and c.g. position on root angle of attack in trimmed flight (basic stiffness distribution) at $M = 2{\cdot}2$.

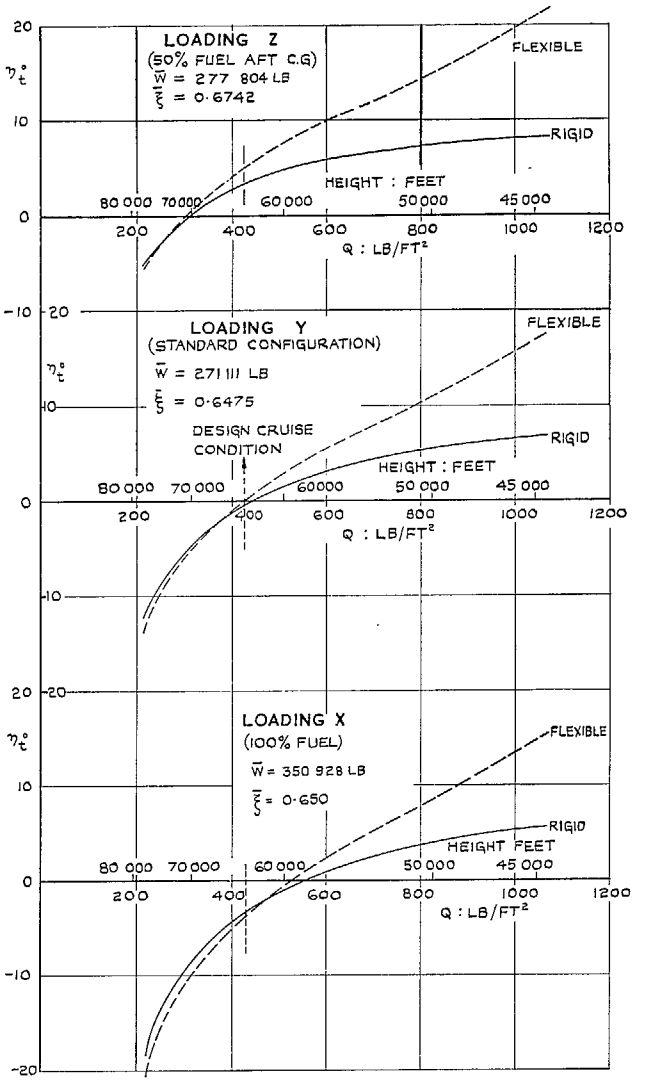

FIG. 22. Effect of weight and c.g. position on elevon angles to trim (basic stiffness distribution) at $M = 2{\cdot}2$.

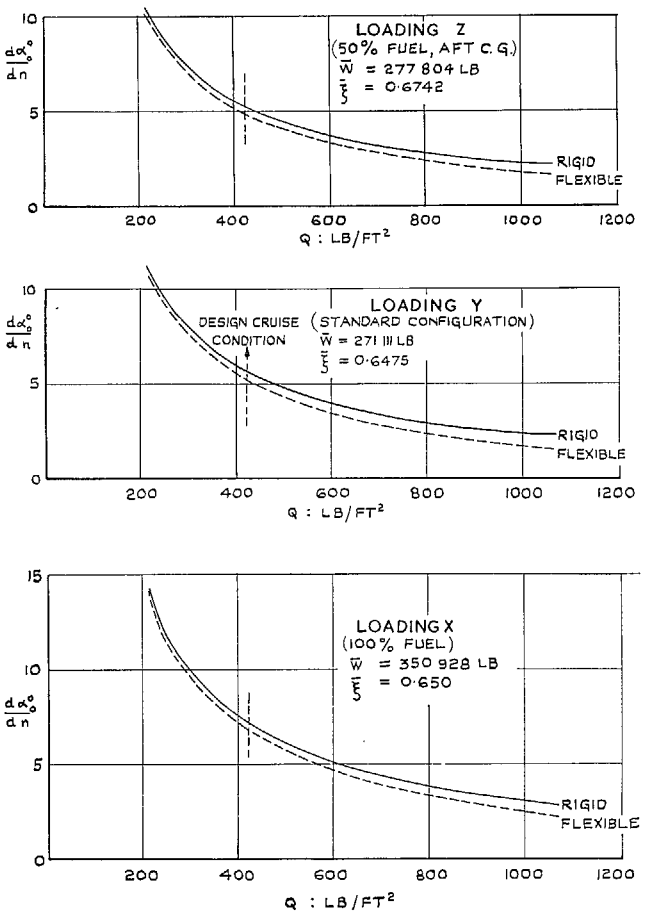

FIG. 23. Effect of weight and c.g. position on increment of root angle of attack per g (basic stiffness distribution) at $M = 2{\cdot}2$.

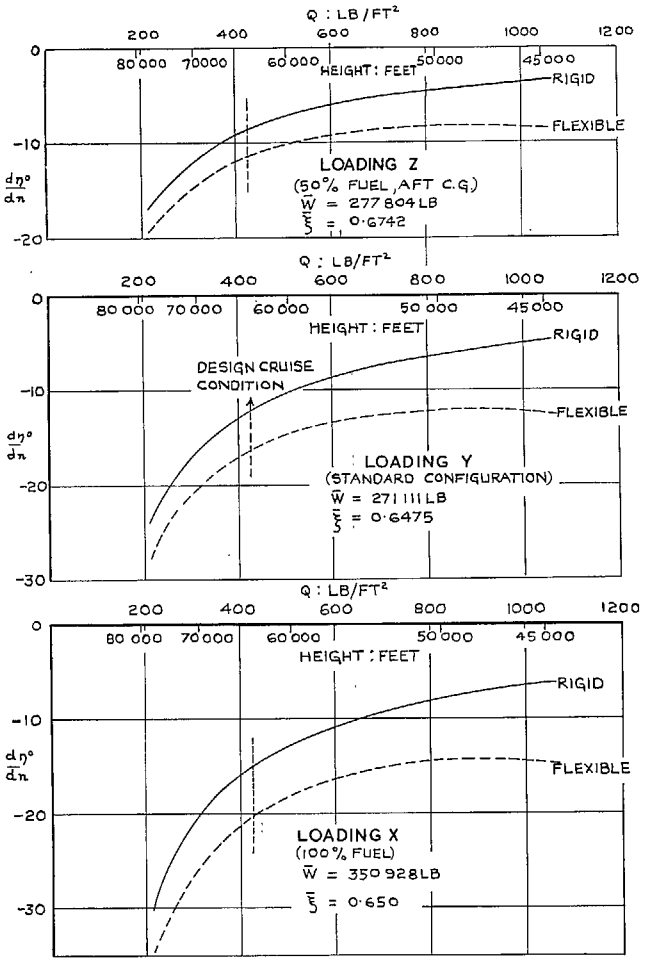

FIG. 24. Effect of weight and c.g. position on elevon angle per g (basic stiffness distribution) at $M = 2{\cdot}2$.

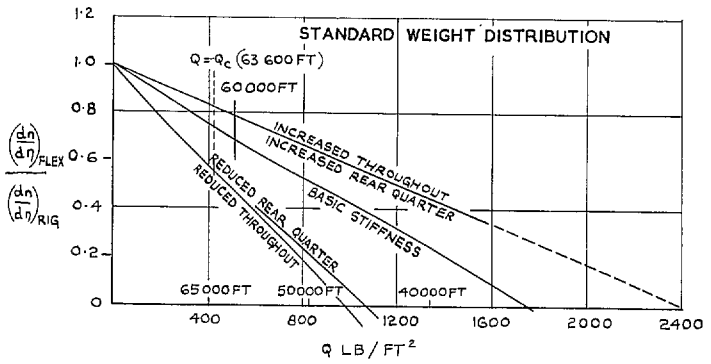

FIG. 25. Effect of stiffness on relative control effectiveness at $M = 2{\cdot}2$.

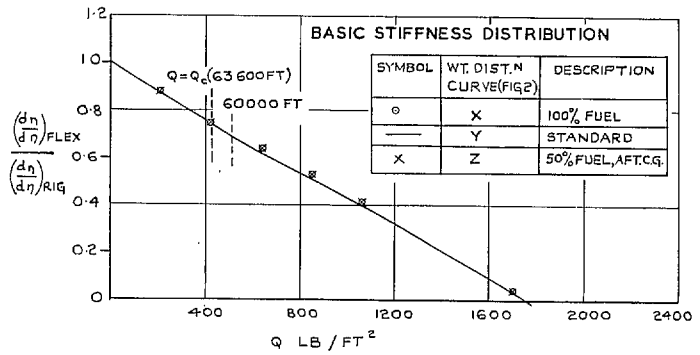

FIG. 26. Effect of weight distribution on relative control effectiveness at $M = 2{\cdot}2$.

PART II

A Further Investigation of the Effects of Longitudinal Elastic Camber on Slender Aircraft in Steady Symmetrical Flight Including Estimates of the Effect on Shear Forces and Bending Moments

By A. S. TAYLOR, M. Sc., A.F.R.Ae.S.

Summary.

The method developed in Part I for the estimation of the effect of longitudinal elastic camber on trim and manoeuvrability of slender aircraft has been used for further calculations relating to the design for a supersonic ($M = 2{\cdot}2$) transport aircraft, which was studied in that Part. Some of the earlier calculations have been repeated using piston theory instead of slender-wing theory for the estimation of the incremental loading due to elastic camber. In addition, estimates have been made of the effect of deformations on the longitudinal distributions of shear force and bending moment in quasi-steady symmetric manoeuvres.

The results have been used to demonstrate the importance of allowing for aeroelastic effects when computing loading actions on slender aircraft, and to draw attention to the need for a reliable method of specifying the loading on such aircraft due to arbitrary distributions of elastic warp, superposed on known initial incidence distributions.

LIST OF CONTENTS

LIST OF CONTENTS—*continued*

LIST OF ILLUSTRATIONS

LIST OF ILLUSTRATIONS—*continued*

Figure

LIST OF ILLUSTRATIONS—*continued*

Figure

---

1. *Introduction.*

In Part I the author and W. F. W. Urich developed an approximate method of estimating the effect of aeroelasticity on the longitudinal trim and quasi-steady manoeuvrability of slender aircraft. The method assumes that, structurally, the aircraft behaves as a 'free-free' beam, subject only to longitudinal bending, and that the total chordwise aerodynamic loading per unit length (including that due to elastic camber) varies linearly with the effective local angle of attack, $\alpha(\xi)$. The loading is thus calculable by superposition of 'elementary' distributions corresponding to the various contributions to $\alpha(\xi)$, together with the distribution due to elevon deflection. Subject to the assumption of linearity, the contributions to total aerodynamic loading, other than that due to elastic camber, may be specified in accordance with the best available experimental or theoretical data. For the specification of loading due to the elastic camber, however, recourse must be had to a simple (linearised) theory such as slender-wing or piston theory, since there is a dearth of experimental information concerning loading due to arbitrary camber modes and since, in any event, the elastic camber mode for a particular flight condition is unknown at the outset. Part I, in fact, gave the detailed mathematical development of the method appropriate to each of these theories, but in the numerical application described therein, only the slender-wing-theory version was used.

It was the original intention in the investigation begun in Part I that sufficient numerical work should be undertaken to accomplish the following three aims:

(i) To assess the practicability of the method, from the purely computational point of view, when stiffness and mass distributions typical of actual aircraft are introduced.

(ii) To make realistic assessments of the aeroelastic effects in question for various possible layouts of a supersonic ($M = 2{\cdot}2$) transport aircraft.

(iii) To derive general information as to the influence of such parameters as planform, and weight and stiffness distributions, and to assess the extent to which results are influenced by the aerodynamic assumptions.

The first aim was substantially achieved with the completion of the numerical work described in Part I, which related to a feasible layout for a $M = 2{\cdot}2$ transport aircraft with the planform illustrated in Fig. 1, and in which supposedly realistic mass and stiffness distributions, based on detailed project studies in progress at the time, were used. Thus, to the extent to which the assumed mass and stiffness distributions were, in fact, realistic, the work could also be said to have provided a partial realisation of the second objective, which would have been more fully realised if the original intention of studying two other configurations* had been put into effect.

---

* One of these would have had a much longer 'nose' than that shown in Fig. 1 while the other, representing the 'completely integrated planform' concept, would have consisted of an ogee wing with no discrete body.

It was of course recognised in Part I (Sections 5.3 and 6) that in some practical applications, the neglect of spanwise deformation which is implicit in the assumption of 'beam-like' behaviour might, in fact, be unrealistic. The method was originally conceived at a time when attention was focussed on the 'completely integrated' slender-wing configuration, rather than on configurations involving a discrete fuselage plus a thin slender wing, such as that adopted for the Anglo-French 'Concord' aircraft. Now that detailed structural analyses of the latter type of configuration by matrix methods have been made, it has become clear that the beam hypothesis is indeed untenable for such configurations. From an examination of the matrices of structural influence coefficients, and the deformation for representative flight conditions deduced therefrom, it would appear virtually impossible to prescribe an 'equivalent (EI) distribution' for use in our method, which would at all adequately represent the stiffness properties of the aircraft. Thus, for a quantitatively reliable assessment of aeroelastic effects in these circumstances it would appear to be essential to resort to a more sophisticated mathematical model of the structure*. Accepting this, it would appear pointless to pursue the second of the original aims any further, at least in respect of a Concord-type layout.

As regards the third aim, the numerical work in Part I included a limited investigation of the effects of varying the weight and stiffness distributions of the particular aircraft configuration under consideration, but did not examine the influence of aerodynamic assumptions. Even though doubt has now been cast on the applicability of the method for quantitative assessments of certain configurations, it still seemed useful to investigate the sensitivity of results to changes in the assumptions regarding the aerodynamic loading due to elastic camber. For in seeking any 'three-dimensional' adaptation of the present 'two-dimensional' method it would be of advantage to know at the outset what degree of refinement must be aimed at in specifying the aerodynamic loading due to elastic deformation, in order to achieve a reasonably accurate overall answer for the aeroelastic effects. Comparative results derived from the present method, using two such radically different theories as the slender-wing and piston theories, could provide valuable pointers in this direction.

One of the two main aims of the work described in this part of the report was therefore to repeat a selection of the calculations made for Part I, using piston theory instead of slender-wing theory, and to make a critical comparison of the two sets of results. This necessitated reprogramming the sequence of computations detailed in Section 3 of Part I and advantage was taken of this fact to implement a suggestion made in the concluding Section 6 of that Part, namely that the work be extended into the field of Loading Actions. The computer programme is readily adapted to yield the longitudinal distributions of shear force and bending moment for the flexible aircraft in quasi-steady symmetric manoeuvres, in addition to all the previously obtained output quantities, such as the elastic camber shape, the angle of attack and elevon deflection for trimmed level flight, and the incremental angle of attack and elevon deflection in pull-ups. The derivation and interpretation of comparative estimates of these loading actions quantities for the flexible and (hypothetical) rigid aircraft thus constituted a second main aim for the work described in this Part.

Section 2 is devoted to the mathematical theory upon which the investigation has been based. Apart from the portion dealing with the derivation of the shear and bending-moment distributions, this was fully developed in Part I, but to make the present Part reasonably self-contained an outline of the complete method is included here.

* BAC-Sud calculations for the 'Concord' have shown, for instance, that because of spanwise deformation of the wing, the relative effectiveness of the elevons (i.e. effectiveness on flexible aircraft/effectiveness on rigid aircraft) depends very much on their spanwise location.

Section 3 gives details of the numerical work, results of which are presented and discussed under two headings, relating respectively to the two main aims of the investigation, specified above.

Section 4 gives a more general discussion of this later phase of the work begun in Part I, and seeks to draw final conclusions from the work as a whole.

Acknowledgement.

The author is indebted to Miss S. France, who drafted the 'Mercury' computer programmes used in this investigation, and to Mr. D. J. Eckford who helped her to perfect them and to make the 'production runs'.

2. *Mathematical Theory.*

2.1. *General.*

The general mathematical theory underlying the calculations of both parts of the report was fully developed in Part I. For the convenience of the general reader, the main steps in the analysis are indicated below by quoting the essential equations from Part I, to which, however, the reader who is interested in detailed derivations should refer. The recapitulation of earlier equations is followed by the development of some additional analysis relating to the calculation of the 'loading actions' quantities considered in the present work.

2.2. *Recapitulation of Equations from Part I.*

2.2.1. *Basic assumptions.*—An aircraft of the configuration illustrated in Fig. 1 is considered in steady manoeuvring flight, (initiated from trimmed level flight at speed V and lift coefficient $\overline{C}_{Lt}$) with incremental normal acceleration ng.

Structurally, the aircraft is assumed to behave as a beam of varying cross-section, subject only to longitudinal bending; the distributions of weight and bending rigidity along the beam are denoted by $W(\xi)$ and $B(\xi) = EI(\xi)$, respectively.

Aerodynamically, it is assumed that the lift per unit length at station ξ may be expressed as

$$L(\xi) = Ql\{\phi_a(\xi) + \alpha_0'\phi_0(\xi) + \hat{q}\phi_q(\xi) + \phi_e(\xi) + \eta\phi_\eta(\xi)\}, \tag{1}$$

corresponding to a distribution of effective local angle of attack $\alpha(\xi)$ given by

$$\alpha(\xi) = \alpha_a(\xi) + \alpha_0' + \alpha_q(\xi) + \alpha_e(\xi), \tag{2}$$

together with a control deflection η. Here $\alpha_a(\xi)$ denotes the angle of attack distribution corresponding to the 'design C_L lift distribution', and α_0' is the 'additional angle of attack';

$$\alpha_q(\xi) = \hat{q}(\xi - \bar{\xi}) \tag{3}$$

is the effective camber distribution due to the non-dimensionalised pitching velocity $\hat{q} = ql/V$, which is related to n by

$$\frac{\hat{q}}{n} = \frac{\overline{C}_{Lt}}{2\mu} \quad \text{with} \quad \mu = \frac{\overline{W}}{g\rho Sl}, \tag{4}$$

$\overline{W} = l\int_0^1 W(\xi)d\xi$ being the total weight of the aircraft, S its gross plan area and ρ the air density; $\alpha_e(\xi)$ is the distribution of elastic camber.

In equation (1) $Q = \frac{1}{2}\rho V^2$ is the kinetic pressure and the $\phi(\xi)$ are all non-dimensional lift functions, which may in general depend on Mach number. For numerical work, $\phi_a(\xi)$, $\phi_0(\xi)$ and $\phi_\eta(\xi)$ have been prescribed on a semi-empirical basis, while the general theory of Part I has been developed for cases where $\phi_q(\xi)$ and $\phi_e(\xi)$ are in accordance with either slender-wing theory or piston theory.

2.2.2. *Equations of equilibrium for steady symmetric flight.*—For steady flight at fixed values of Q, M and n, the (deformed) configuration of the aircraft relative to the airstream, and hence the aerodynamic loading, is determined by three quantities—the 'additional angle of attack' α_0', the control deflection η and the distribution of elastic camber $\alpha_e(\xi)$. Three equations are available to determine these quantities, namely the two ordinary equations expressing the overall equilibrium of forces and moments acting on the aircraft, and the differential equation expressing the aeroelastic equilibrium of the beam representing the aircraft; with the last equation must be associated the boundary conditions appropriate to the 'free-free' condition of the beam.

The conditions of overall equilibrium are expressed in coefficient form as

$$\left.\begin{aligned} \bar{C}_L = \frac{\bar{L}}{QS} &= \frac{l^2}{S}\left\{\int_0^1 \phi_d(\xi)d\xi + \alpha_0' \int_0^1 \phi_0(\xi)d\xi + \hat{q}\int_0^1 \phi_q(\xi)d\xi + \right. \\ &\left. + \int_0^1 \phi_e(\xi)d\xi + \eta\int_0^1 \phi_\eta(\xi)d\xi\right\} = \frac{(n+1)\bar{W}}{QS} \\ \bar{C}_m = \frac{\bar{M}}{QSl} &= \bar{C}_L\xi - \frac{l^2}{S}\left\{\int_0^1 \phi_d(\xi)\xi\, d\xi + \alpha_0' \int_0^1 \phi_0(\xi)\xi\, d\xi + \hat{q}\int_0^1 \phi_q(\xi)\xi\, d\xi + \right. \\ &\left. + \int_0^1 \phi_e(\xi)\xi\, d\xi + \eta\int_0^1 \phi_\eta(\xi)\xi\, d\xi\right\} = 0. \end{aligned}\right\} \tag{5}$$

The differential equation of the deflected beam under the total chordwise loading per unit length $\mathscr{L}(\xi)$ where

$$\mathscr{L}(\xi) = L(\xi) - (n+1)W(\xi) \tag{6}$$

is developed in Part I, with the assumption $\phi_e(\xi) = \phi\{\alpha_e(\xi), \xi\}$, as

$$\begin{aligned} &\frac{d^2}{d\xi^2}\left\{B(\xi)\frac{d\alpha_e}{d\xi}\right\} + Ql^4\phi\{\alpha_e(\xi), \xi\} \\ &\qquad = (n+1)l^3W(\xi) - Ql^4\{\phi_d(\xi) + \alpha_0'\phi_0(\xi) + \hat{q}\phi_q(\xi) + \eta\phi_\eta(\xi)\} \end{aligned} \tag{7}$$

with boundary conditions

$$\left[\frac{d\alpha_e}{d\xi}\right]_{\xi=0} = \left[\frac{d^2\alpha_e}{d\xi^2}\right]_{\xi=0} = 0 \tag{8}$$

and

$$\int_0^1 \alpha_e(\xi)d\xi = 0. \tag{9}$$

The solution of (7) is expressible in the form

$$\alpha_e(\xi) = \sum_{r=1}^{5} \alpha_{er}(\xi) = (n+1)\frac{\partial\alpha_e(\xi)}{\partial n} + \alpha_{ed}(\xi) + \alpha_0'\frac{\partial\alpha_e(\xi)}{\partial\alpha_0'} + \hat{q}\frac{\partial\alpha_e(\xi)}{\partial\hat{q}} + \eta\frac{\partial\alpha_e(\xi)}{\partial\eta} \tag{10}$$

where $\partial\alpha_e(\xi)/\partial n$, $\alpha_{ed}(\xi)$, $\partial\alpha_e(\xi)/\partial\alpha_0'$, $\partial\alpha_e(\xi)/\partial\hat{q}$ and $\partial\alpha_e(\xi)/\partial\eta$ are the solutions of (7) with the right-hand side put equal to $l^3W(\xi)$, $-Ql^4\phi_d(\xi)$, $-Ql^4\phi_0(\xi)$, $-Ql^4\phi_q(\xi)$ and $-Ql^4\phi_\eta(\xi)$ respectively. The corresponding lift function can then be written

$$\phi_e(\xi) = (n+1)\frac{\partial\phi_e(\xi)}{dn} + \phi_{ed}(\xi) + \alpha_0'\frac{\partial\phi_e(\xi)}{\partial\alpha_0'} + \hat{q}\frac{\partial\phi_e(\xi)}{\partial\hat{q}} + \eta\frac{\partial\phi_e(\xi)}{\partial\eta}. \tag{11}$$

This form of solution permits equations (5) to be re-expressed in terms of 'modified' derivatives* of $\bar{C}_L$ and $\bar{C}_m$ with respect to α_0', η, q and n; regarded as simultaneous equations for the determination of the unknowns α_0' and η, equations (5) finally appear in the form

$$\left.\begin{aligned} \frac{\partial \bar{C}_L}{\partial \alpha_0'}\alpha_0' + \frac{\partial \bar{C}_L}{\partial \eta}\eta &= (n+1)\bar{C}_{Lt} - \bar{C}_{L0} - \frac{\partial \bar{C}_L}{\partial \hat{q}}\hat{q} - \frac{\partial \bar{C}_L}{\partial n}(n+1) \\ \frac{\partial \bar{C}_m}{\partial \alpha_0'}\alpha_0' + \frac{\partial \bar{C}_m}{\partial \eta}\eta &= -\bar{C}_{m0} - \frac{\partial \bar{C}_m}{\partial \hat{q}}\hat{q} - \frac{\partial \bar{C}_m}{\partial n}(n+1) \end{aligned}\right\} \tag{12}$$

where expressions for the 'modified' coefficients and partial derivatives, in terms of the various 'rigid body' lift functions $\phi(\xi)$ and the generalised 'elastic' lift function $\phi_e(\xi)$ are given in equations (41) to (43) of Part I. The particular forms which these expressions assume when $\phi_e(\xi)$ is appropriate to slender-wing theory and piston theory respectively, are given in Appendix I of Part I.

2.2.3. *Formal solutions for trimmed level flight and for the steady pull-up.*—For trimmed level flight ($n = \hat{q} = 0$) the formal solution of the equations of equilibrium is given in Part I as

$$\alpha_{et}(\xi) = \alpha_{e\bar{a}}(\xi) + \frac{\partial \alpha_e(\xi)}{\partial n} + \alpha_{0t}'\frac{\partial \alpha_e(\xi)}{\partial \alpha_0'} + \eta_t\frac{\partial \alpha_e(\xi)}{\partial \eta} \tag{13}$$

with

$$\alpha_{0t}' = \frac{\bar{C}_{Lt}H_{t\eta}}{\frac{\partial \bar{C}_m}{\partial \alpha_0'}\left(1 - \frac{K_{m\eta}}{K_m}\right)}; \qquad \eta_t = \frac{\bar{C}_{Lt}H_t}{\frac{\partial \bar{C}_m}{\partial \eta}\left(1 - \frac{K_m}{K_{m\eta}}\right)}; \tag{14}$$

where K_m, $K_{m\eta}$, H_t, $H_{t\eta}$ are functions of the 'modified' derivatives, defined in equations (47) and (48) of Part I.

For a steady pull-up, incremental solutions per g are expressed as

$$\frac{d\alpha_e(\xi)}{dn} = \frac{\partial \alpha_e(\xi)}{\partial n} + \frac{d\alpha_0'}{dn}\frac{\partial \alpha_e(\xi)}{\partial \alpha_0'} + \frac{\bar{C}_{Lt}}{2\mu}\frac{\partial \alpha_e(\xi)}{\partial \hat{q}} + \frac{d\eta}{dn}\frac{\partial \alpha_e(\xi)}{\partial \eta} \tag{15}$$

with

$$\frac{d\alpha_0'}{dn} = \frac{\bar{C}_{Lt}H_{m\eta}}{\frac{\partial \bar{C}_m}{\partial \alpha_0'}\left(1 - \frac{K_{m\eta}}{K_m}\right)}; \qquad \frac{d\eta}{dn} = \frac{\bar{C}_{Lt}H_m}{\frac{\partial \bar{C}_m}{\partial \eta}\left(1 - \frac{K_m}{K_{m\eta}}\right)}; \tag{16}$$

where H_m and $H_{m\eta}$ are defined in equations (52) of Part I.

2.2.4. *Treatment of the differential equation for particular forms of the function $\phi\{\alpha_e(\xi), \xi\}$.*—For the numerical work described in Part I, the function $\phi\{\alpha_e(\xi), \xi\}$ was given the form appropriate to slender-wing theory, and Sections 2.5.2 and 2.5.3 of that Part deal fully with the solution of the differential equation (7) in that case. The work described in the present Part has been principally concerned with the case where $\phi_e(\xi) = \phi\{\alpha_e(\xi), \xi\}$ and also $\phi_q(\xi)$ have the forms appropriate to piston theory. The analysis for this case is also developed in Part I (Appendix I) from which the following equations are quoted:

$$\left.\begin{aligned} \phi_e(\xi) &= \frac{8}{M}\left(\frac{s_T}{l}\right)\left\{\frac{s(\xi)}{s_T}\right\}\alpha_e(\xi) \\ \phi_q(\xi) &= \frac{8}{M}\left(\frac{s_T}{l}\right)\left\{\frac{s(\xi)}{s_T}\right\}(\xi - \bar{\xi}). \end{aligned}\right\} \tag{17}$$

* That is, derivatives modified to incorporate the effects of aeroelasticity on a quasi-static basis.

With these expressions for $\phi_e(\xi)$ and $\phi_q(\xi)$, the differential equation (7) is manipulated to the form (in which $D \equiv d/d\xi$):

$$\{D^3 + \psi_1(\xi)D^2 + \psi_2(\xi)D + \psi_3(\xi, Q)\}\alpha_e(\xi)$$
$$= (n+1)\Psi'_1(\xi) + \Psi'_2(\xi, Q) + \alpha_0'\Psi'_3(\xi, Q) + \hat{q}\Psi'_4(\xi, Q) + \eta\Psi'_5(\xi, Q). \tag{18}$$

The solution of (18) is expressible in the form (10) where $\partial\alpha_e(\xi)/\partial n$, $\alpha_{eq}(\xi)$, $\partial\alpha_e(\xi)/\partial\alpha_0'$, $\partial\alpha_e(\xi)/\partial\hat{q}$ and $d\alpha_e(\xi)/d\eta$ are the respective solutions of

$$\{D^3 + \psi_1(\xi)D^2 + \psi_2(\xi)D + \psi_3(\xi, Q)\}\alpha_e(\xi) = \Psi'_r(\xi, Q), \tag{19.r}$$
$$r = 1, \ldots 5$$

where

$$\left.\begin{aligned} \psi_1(\xi) &= \frac{2}{\bar{B}(\xi)}\frac{d\bar{B}(\xi)}{d\xi}; \qquad \psi_2(\xi) = \frac{1}{\bar{B}(\xi)}\frac{d^2\bar{B}(\xi)}{d\xi^2}; \\ \psi_3(\xi, Q) &= \frac{8}{M}\frac{1}{\bar{B}(\xi)}\frac{Q}{Q_c}\left(\frac{s_T}{l}\right)\left\{\frac{s(\xi)}{s_T}\right\}; \end{aligned}\right\} \tag{20}$$

and the forcing functions $\Psi'_r(\xi, Q)$ are given by

$$\left.\begin{aligned} \Psi'_1(\xi) &= \frac{W(\xi)}{\bar{B}(\xi)Q_c l}; \\ \Psi'_2(\xi, Q) &= -\frac{Q}{Q_c}\frac{\phi_d(\xi)}{\bar{B}(\xi)}; \\ \Psi'_3(\xi, Q) &= -\frac{Q}{Q_c}\frac{\phi_0(\xi)}{\bar{B}(\xi)}; \\ \Psi'_4(\xi, Q) &= -\Psi'_3(\xi, Q)(\xi - \bar{\xi}); \\ \Psi'_5(\xi, Q) &= -\frac{Q}{Q_c}\frac{\phi_\eta(\xi)}{\bar{B}(\xi)}. \end{aligned}\right\} \tag{21}$$

$\bar{B}(\xi)$ is the non-dimensional stiffness parameter defined by

$$\bar{B}(\xi) = \frac{B(\xi)}{Q_c l^4}, \tag{22}$$

where Q_c is the kinetic pressure in the design cruising condition.

In each case the equation (19.r) is to be solved with the boundary conditions (8) and (9).

2.3. *Extension of Analysis to Include the Evaluation of the Shear Force and Bending-Moment Distributions.*

2.3.1. *Basic formulae.*—If $\mathscr{M}(x')$, $\mathscr{S}(x')$ denote the bending moment and shear at distance $x' = \xi' l$ from the nose of the aircraft and if $z_e'(\xi') = \zeta_e'(\xi')l$ is the normal displacement of the neutral axis from the centre-section chord at station ξ', $(\approx \xi)$ due to elastic camber, then since $\alpha_e(\xi) = -dz_e'(\xi)/dx' \approx -dz_e'(\xi)/dx$ and $d/dx = (1/l)d/d\xi$, $\mathscr{M}(x) \approx -B(x)\,d^2z_e'/dx^2 = \{B(x)/l\}d\alpha_e/d\xi$ or, non-dimensionalising by dividing through by $Q_c l^3$,

$$\mathscr{M}^*(\xi) = \frac{\mathscr{M}(x)}{Q_c l^3} = \bar{B}(\xi)\frac{d\alpha_e}{d\xi}. \tag{23}$$

Now

$$\mathscr{S}(x) = \frac{d\mathscr{M}(x)}{dx} = \frac{1}{l}\frac{d}{d\xi}\left\{Q_c l^3 \bar{B}(\xi)\frac{d\alpha_e}{d\xi}\right\}$$

$$= Q_c l^2 \left\{\bar{B}(\xi)\frac{d^2\alpha_e}{d\xi^2} + \frac{d\bar{B}(\xi)}{d\xi}\frac{d\alpha_e}{d\xi}\right\}$$

or

$$\mathscr{S}^*(\xi) = \frac{\mathscr{S}(x)}{Q_c l^2} = \bar{B}(\xi)\frac{d^2\alpha_e}{d\xi^2} + \frac{d\bar{B}(\xi)}{d\xi}\frac{d\alpha_e}{d\xi}. \tag{24}$$

Note on sign conventions.

With the geometrical notation as given in Fig. 1, and the differential equation for the deflected beam as given in equation (14) of Part I (leading to equation (7) of the present Part), the sign conventions for $\mathscr{S}(\xi)$ and $\mathscr{M}(\xi)$ consistent with equations (23) and (24) are that $\mathscr{S}(\xi_0)$ is positive if the resultant of the forces between stations $\xi = 0$ and $\xi = \xi_0$ is downwards and that $\mathscr{M}(\xi_0)$ is positive if the resultant moment at $\xi = \xi_0$, of the loads acting between $\xi = 0$ and $\xi = \xi_0$, is anticlockwise.

2.3.2. *Bending moment and shear force in trimmed level flight.*—Corresponding to the five 'elementary' elastic camber distributions derived by solution of the equations (19.r), $r = 1, \ldots 5$, there will be five pairs of 'elementary' bending moment and shear force distributions $\mathscr{M}_r^*(\xi)$, $\mathscr{S}_r^*(\xi)$, calculated in accordance with equations (23) and (24). The resultant bending-moment and shear-force distributions for trimmed level flight, $\mathscr{M}_t^*(\xi)$ and $\mathscr{S}_t^*(\xi)$, corresponding to the resultant elastic camber distribution $\alpha_{et}(\xi)$ given by equation (13), will be obtained as

$$\begin{aligned}\mathscr{M}_t^*(\xi) &= \mathscr{M}_1^*(\xi) + \mathscr{M}_2^*(\xi) + \alpha_{0t}'\mathscr{M}_3^*(\xi) + \eta_t\mathscr{M}_5^*(\xi)\\ \mathscr{S}_t^*(\xi) &= \mathscr{S}_1^*(\xi) + \mathscr{S}_2^*(\xi) + \alpha_{0t}'\mathscr{S}_3^*(\xi) + \eta_t\mathscr{S}_5^*(\xi).\end{aligned} \tag{25}$$

2.3.3. *Incremental bending moment and shear force in the steady pull-up.*—The total incremental bending moment and shear force per g in the pull-up, $d\mathscr{M}^*(\xi)/dn$ and $d\mathscr{S}^*(\xi)/d\eta$, corresponding to the incremental elastic camber distribution $d\alpha_e(\xi)/d\xi$ given by equation (15), will be given by

$$\begin{aligned}\frac{d\mathscr{M}^*(\xi)}{dn} &= \mathscr{M}_2^*(\xi) + \frac{d\alpha_0'}{dn}\mathscr{M}_3^*(\xi) + \frac{\bar{C}_{Lt}}{2\mu}\mathscr{M}_4^*(\xi) + \frac{d\eta}{dn}\mathscr{M}_5^*(\xi)\\ \frac{d\mathscr{S}^*(\xi)}{dn} &= \mathscr{S}_2^*(\xi) + \frac{d\alpha_0'}{dn}\mathscr{S}_3^*(\xi) + \frac{\bar{C}_{Lt}}{2\mu}\mathscr{S}_4^*(\xi) + \frac{d\eta}{dn}\mathscr{S}_5^*(\xi).\end{aligned} \tag{26}$$

2.3.4. *Resultant bending-moment and shear-force distributions in pull-ups.*—For a pull-up under total load factor $\bar{n} = 1 + n$, from trimmed level flight, the quasi-steady bending-moment and shear-force distributions are given by

$$\begin{aligned}\mathscr{M}^*(\xi) &= \mathscr{M}_t^*(\xi) + n\frac{d\mathscr{M}^*(\xi)}{dn}\\ \mathscr{S}^*(\xi) &= \mathscr{S}_t^*(\xi) + n\frac{d\mathscr{S}^*(\xi)}{dn}.\end{aligned} \tag{27}$$

2.3.5. *A note on boundary conditions.*—When each of the equations (19.r) is solved with boundary conditions (8) and (9), the beam is in effect being considered with its forward end free, and subject to a distributed loading which is not self-equilibrating. Accordingly, while $\mathscr{M}_r^*(0)$ and

$\mathscr{S}_r^*(0)$ will be zero, ($r = 1, \ldots 5$) $\mathscr{M}_r^*(1)$ and $\mathscr{S}_r^*(1)$ will not in general vanish so that, in each case, application of a force and moment at the trailing edge must be postulated in order to maintain the beam in equilibrium. However, the resultant distributions given by equations (25) and (26) correspond (nominally) to equilibrium states of the aircraft in which the distributed loadings (aerodynamic + inertia) are self-equilibrating so that $\mathscr{M}_i^*(1)$, $\mathscr{S}_i^*(1)$, $d\mathscr{M}^*(1)/dn$ and $d\mathscr{S}^*(1)/dn$ should all be zero, consistent with the absence of constraint at the trailing edge.

The values of α_{0t}' and η_t for substitution in equations (25), and those of $d\alpha_0'/dn$ and $d\eta/dn$ for substitution in equations (26), may be obtained from equations (14) and (15) respectively. These equations, it may be recalled, were derived from the equations of overall equilibrium, expressed in terms of 'modified' derivatives of $\bar{C}_L$ and $\bar{C}_m$ {equations (12)}. Now in numerical applications it has been found that this procedure leads to residual values of the *resultant* bending moment and shear at the trailing edge {i.e. $\mathscr{M}_i^*(1)$ etc.} which are not always negligible in relation to the maximum values occurring over the length of the beam. This reflects the fact that the relatively small *resultant* loading actions quantities are evaluated, through equations (25) and (26), as the algebraic sums of terms of opposite signs which, individually, are much larger than their sums. The combination of the relatively small errors occurring in the calculated values of component distributions may result in a relatively much larger overall error.

To avoid producing bending-moment and shear-force distribution diagrams which manifestly fail to satisfy the end conditions for a 'free-free' beam, the values of α_{0t}', η_t, $d\alpha_0'/dn$ and $d\eta/dn$ for substitution in equations (25) and (26) may be chosen so as to satisfy directly the requirement of zero bending moment and shear force at the free trailing edge. Thus, equating the right-hand sides of equations (25), with $\xi = 1$, to zero and solving the resulting equations for α_{0t}' and η_t yields

$$\alpha_{0t} = \frac{\mathscr{M}_5^*(1)\{\mathscr{S}_1^*(1) + \mathscr{S}_2^*(1)\} - \mathscr{S}_5^*(1)\{\mathscr{M}_1^*(1) + \mathscr{M}_2^*(1)\}}{\mathscr{S}_5(1)\mathscr{M}_3(1) - \mathscr{S}_3(1)\mathscr{M}_5(1)}$$

and (28)

$$\eta_t = \frac{\mathscr{S}_3^*(1)\{\mathscr{M}_1^*(1) + \mathscr{M}_2^*(1)\} - \mathscr{M}_3^*(1)\{\mathscr{S}_1^*(1) + \mathscr{S}_2^*(1)\}}{\mathscr{S}_5^*(1)\mathscr{M}_3^*(1) - \mathscr{S}_3^*(1)\mathscr{M}_5^*(1)}.$$

Similarly, from equations (26), when $\xi = 1$,

$$\frac{d\alpha_0'}{dn} = \frac{\mathscr{M}_5^*(1)\left\{\mathscr{S}_2^*(1) + \frac{\bar{C}_{Lt}}{2\mu}\mathscr{S}_4^*(1)\right\} - \mathscr{S}_5^*(1)\left\{\mathscr{M}_2^*(1) + \frac{\bar{C}_{Lt}}{2\mu}\mathscr{M}_4^*(1)\right\}}{\mathscr{S}_5^*(1)\mathscr{M}_3^*(1) - \mathscr{S}_3^*(1)\mathscr{M}_5^*(1)}$$

(29)

$$\frac{d\eta}{dn} = \frac{\mathscr{S}_3^*(1)\left\{\mathscr{M}_2^*(1) + \frac{\bar{C}_{Lt}}{2\mu}\mathscr{M}_4^*(1)\right\} - \mathscr{M}_3^*(1)\left\{\mathscr{S}_2^*(1) + \frac{\bar{C}_{Lt}}{2\mu}\mathscr{S}_4^*(1)\right\}}{\mathscr{S}_5^*(1)\mathscr{M}_3^*(1) - \mathscr{S}_3^*(1)\mathscr{M}_5^*(1)}.$$

2.3.6. *Distributions of bending moment and shear force for the rigid aircraft.*—The distributions of bending moment and shear force for the (hypothetical) rigid aircraft may be obtained by direct integration of the chordwise loading. Thus for trimmed level flight, (having regard to the sign conventions defined in Section 2.3.1)

$$[\mathscr{S}_i^*(\xi)]_R = -\int_0^\xi [\mathscr{L}_i^*(\xi_1)]_R\, d\xi_1$$

$$[\mathscr{M}_i^*(\xi)]_R = -\int_0^\xi d\xi_1 \int_0^{\xi_1} [\mathscr{L}_i^*(\xi_2)]_R\, d\xi_2 \qquad (30)$$

where the non-dimensional load per unit length for the rigid aircraft in trimmed level flight, $[\mathscr{L}_l^*(\xi)]_R = (1/Q_c l)[\mathscr{L}_l(\xi)]_R$ is readily deduced from equations (6) and (1) as

$$[\mathscr{L}_l^*(\xi)]_R = \frac{Q}{Q_c}[\phi_d(\xi) + \{\alpha_{0t}'\}_R \phi_0(\xi) + \{\eta_t\}_R \phi_\eta(\xi)] - \frac{W(\xi)}{Q_c l}. \tag{31}$$

Similarly, for the steady pull-up,

$$\left[\frac{d\mathscr{S}^*(\xi)}{dn}\right]_R = -\int_0^\xi \left[\frac{d\mathscr{L}^*(\xi_1)}{dn}\right]_R d\xi_1$$
$$\left[\frac{d\mathscr{M}^*(\xi)}{dn}\right]_R = -\int_0^\xi d\xi_1 \int_0^{\xi_1} \left[\frac{d\mathscr{L}^*(\xi_2)}{dn}\right]_R d\xi_2 \tag{32}$$

where the non-dimensional incremental loading is given by

$$\left[\frac{d\mathscr{L}^*(\xi)}{dn}\right]_R = \frac{Q}{Q_c}\left[\left\{\frac{d\alpha_0'}{dn}\right\}_R \phi_0(\xi) + \left\{\frac{d\eta}{dn}\right\}_R \phi_\eta(\xi) + \frac{\bar{C}_{Lt}}{2\mu}\phi_q(\xi)\right] - \frac{W(\xi)}{Q_c l}. \tag{33}$$

The values of $\{\alpha_{0t}'\}_R$, $\{\eta_t\}_R$ in (31) and of $\{d\alpha_0'/dn\}_R$ and $\{d\eta/dn\}_R$ in (33) could be obtained from equations (14) and (15) respectively, using values of the various derivatives appropriate to the rigid aircraft. However, since the inherent inaccuracies of the numerical processes may lead to residual bending moments and shear forces at the trailing edge, it is again preferable to evaluate the angles of attack and control deflections directly from the conditions of zero bending moment and shear force at the trailing edge. Thus, for example, if the integrations of $[\mathscr{L}_l^*(\xi)]_R$ {equation (31)} involved in equations (30) are performed term by term, $[\mathscr{S}_l^*(1)]_R$ and $[\mathscr{M}_l^*(1)]_R$ are obtained as expressions involving the unknown $\{\alpha_{0t}'\}_R$ and $\{\eta_t\}_R$; equating these to zero provides a pair of simultaneous equations for the determination of the unknowns.

3. *Numerical Application.*

3.1. *General Aims.*

The numerical work undertaken in connection with the present Part of the report had two principal aims:

(1) to assess the extent to which the results of calculations of the effects of longitudinal elastic camber, by the general method developed in Part I, would be influenced by the aerodynamic assumptions involved in the assessment of the incremental loading due to elastic camber, and

(2) to obtain an idea of the order of magnitude of the changes in longitudinal bending-moment and shear-force distributions brought about by elastic camber.

For the accomplishment of these aims, further calculations have been made for the slender-aircraft configuration studied in Part I, to which the reader is referred for full details regarding aerodynamic data and assumptions, and the specification of representative weight and stiffness distributions. For convenience, some of the more essential data are reproduced here.

3.2. *Aerodynamic Design Data.*

The planform of the selected configuration is illustrated, roughly to scale, in Fig. 1. The design cruising condition for the aircraft (mid-cruise) is specified as:

Mach number $M = 2{\cdot}2$, at height 63 600 feet, with weight $W = 271\,111$ lb and c.g. position $\xi = 0{\cdot}6475$; the lift coefficient in this condition is $\bar{C}_{Lc} = 0{\cdot}1$ and the kinetic pressure $Q_c = 425{\cdot}3$ lb/ft^2.

The lift distribution functions, $\phi_d(\xi)$ for the design $\bar{C}_L$ ($= 0{\cdot}05$) and $\phi_0(\xi)$ for additional angle of attack, are shown in Figs. 2 and 3 respectively, while the lift function $\phi_\eta(\xi)$, corresponding to control deflection η at supersonic Mach numbers (to which the investigation has been restricted) is defined as

$$\begin{aligned} \phi_\eta(\xi) &= 0; && 0 \leqslant \xi \leqslant 0{\cdot}92 \\ \phi_\eta(\xi) &= \frac{1}{\sqrt{(M^2-1)}}; && 0{\cdot}92 \leqslant \xi \leqslant 1. \end{aligned} \tag{34}$$

3.3. *Weight and Stiffness Distributions.*

All of the calculations in the present series have been made for the weight distribution illustrated in Fig. 4, which is appropriate to the mid-cruise condition defined above. Calculations which were made in the earlier investigation, reported in Part I, for two other weight distributions, indicated that practicable weight and c.g. variations should have relatively little influence on the character and magnitude of the aeroelastic effects under consideration.

Of the various stiffness distributions studied in Part I (Section 4.2.3), three have been considered in the present investigation, namely the 'basic distribution', which is thought to approximate most closely to what would actually be required for a supersonic transport aircraft of the type considered, and two distributions of reduced stiffness. These are illustrated in Fig. 5.

3.4. *The Calculations Performed.*

As in Part I, calculations have been made for the fixed Mach number of $2{\cdot}2$, corresponding to the 'cruise-climb' phase of the flight plan envisaged for this type of aircraft. A range of values of kinetic pressure Q, corresponding to flight at $M = 2{\cdot}2$ at various altitudes, has again been considered. No account has been taken of variations, along the flight profile, of the weight, which has been kept fixed at the value appropriate to mid-cruise.

The sequence of computations required *for the flexible aircraft*, with a given stiffness distribution, at each value of Q is as follows:

(i) Determination of $\partial\alpha_e(\xi)/\partial n$, $\alpha_{ed}(\xi)$, $\partial\alpha_e(\xi)/\partial\alpha_0'$, $\partial\alpha_e(\xi)/\partial\hat{q}$ and $\partial\alpha_e(\xi)/\partial\eta$ as solutions of the differential equations (19.r) with boundary conditions (8) and (9). The corresponding displacements $\partial\zeta_e'(\xi)/\partial n$, $\zeta_{ed}'(\xi)$ etc. and the 'elementary' bending-moment and shear distributions $\mathscr{M}_r^*(\xi)$ and $\mathscr{S}_r^*(\xi)$ have also to be determined.

(ii) Evaluation of $\bar{C}_{L0}$ and $\bar{C}_{m0}$ and the partial derivatives of $\bar{C}_L$ and $\bar{C}_m$ with respect to α_0, η, $\hat{q}$ and n from equations (79) to (81) of Appendix I to Part I.

(iii) Evaluation of K_m, $K_{m\eta}$, H_t, $H_{t\eta}$, H_m, $H_{m\eta}$ from equations (47), (48) and (52) of Part I, which define these quantities as functions of the 'modified' derivatives evaluated in the preceding stage of the calculations.

(iv) Evaluation of (a) the additional angle of attack α_{0t}' and control deflection η_t to trim, from equations (14), and (b) the additional angle of attack and incremental control deflection per g ($d\alpha_0'/dn$ and $d\eta/dn$ respectively) from equations (16).

(v) Evaluation of the resultant elastic camber distributions $\alpha_{et}(\xi)$ and $d\alpha_e(\xi)/dn$ from equations (13) and (14) respectively, and of the corresponding displacement distributions $\zeta_{et}'(\xi)$ and $d\zeta_e'/dn$ from similar equations.

(vi) Evaluation of the resultant bending-moment and shear-force distributions for trimmed level flight, $\mathscr{M}_t^*(\xi)$ and $\mathscr{S}_t^*(\xi)$, from equations (25) and of the incremental distributions per g in the pull-up, $d\mathscr{M}^*(\xi)/dn$ and $d\mathscr{S}^*(\xi)/dn$, from equations (26).

(vii) Recalculation of α_{0t}, η_t from equations (28) and of $(d\alpha_0'/dn)\,d\eta/dn$ from equations (29), followed by the repetition of steps (v) and (vi), to obtain solutions satisfying exactly the conditions of vanishing bending moment and shear force at the trailing edge.

(viii) Evaluation of the resultant bending-moment and shear-force distributions in pull-ups under total load factor $\bar{n} = 1 + n$, for various n, using equations (27) in conjunction with the results of step (vii).

For the rigid aircraft, the distributions of bending moment and shear force, under the same flight conditions as considered for the flexible aircraft in (viii) above, are required and may be obtained by the direct integration procedures described in Section 2.3.6 followed by the combination of the trim and incremental solutions in accordance with equations (27).

3.5. *Programming of Computations for Digital Computer.*

The sequence of calculations (i) to (vii) detailed above for the flexible aircraft was programmed for the 'Mercury' digital computer by Miss S. France. The programme was of the same general pattern as that developed for the numerical work of Part I (*see* Section 5.1 of that Part). Modifications were required to cover the substitution of piston-theory aerodynamics for slender-wing theory, and extensions were needed to provide for the calculation of bending-moment and shear-force distributions. Provision was made to deal with the singularities which occur in certain of the functions involved in the Mercury 'Intstep' routines when there are discontinuities in the stiffness distribution or its slope. (See Appendix II of Part I).

In order to obtain comparative results using slender-wing theory, the original programme of Part I was revised and extended to bring it into line with the piston-theory programme.

3.6. *Presentation and Discussion of Results.*

3.6.1. *General scope.*—From the large volume of numerical results accumulated in the course of this investigation, a representative selection has been made and is presented in two groups of figures, 7 to 18 and 19 to 33, designed to permit the realisation of the two aims set out in Section 3.1.

Figs. 7 to 18 serve principally to illustrate the effects of using piston theory in place of slender-wing theory for the estimation of loading due to elastic camber when assessing trim and manoeuvrability characteristics of the flexible slender aircraft. Some of these figures also serve the subsidiary purpose of indicating the order of magnitude of the differences arising in the results, according to whether α_{0t}', η_t, $d\alpha_0'/dn$ and $d\eta/dn$ are evaluated from 'modified derivative' calculations of overall equilibrium, or from direct application of the conditions of zero bending moment and shear force at the trailing edge.

Figures 19 to 33 are relevant to the second aim of Section 3.1, with Figs. 25 to 33 illustrating the changes in the longitudinal bending-moment and shear-force distributions which result from elastic camber in various conditions of quasi-steady manoeuvring flight. Figs. 19 and 20 are included to indicate the order of magnitude of the residual shear forces and bending moments at the trailing edge, yielded by the 'modified derivative' calculations. Figs. 21 to 23 compare the deflections

computed, using piston theory and slender-wing theory, for the flight cases covered by Figs. 25 to 33. The additional angles of attack and elevon deflections required for these cases are shown in Fig. 24.

3.6.2. *Comparison of results obtained using the two different aerodynamic theories.*—Before considering the results of the aeroelastic calculations, we may with advantage examine Fig. 6, in which the lift distributions predicted by slender-wing theory and piston theory respectively, for two modes of angle of attack, are compared. In the lower part of the figure, the lift function $\phi(\xi)$ according to the two theories is shown for the constant angle of attack mode $\alpha(\xi) = 1$. Slender-wing theory predicts much less lift over the projecting fuselage portion of the planform than does piston theory while over most of the wing portion, the two theories give fairly similar results. Over the rearmost 10% of the length, however, there is a rapidly increasing discrepancy between the two because, for a wing with streamwise tips, slender-wing theory predicts zero lift per unit length at the trailing edge whereas, according to piston theory the load is proportional to local span right up to the trailing edge.

In the upper part of Fig. 6, the comparison is made for a sinusoidal mode of angle of attack which, as will be seen later, (e.g. Fig. 7) bears a rough resemblance to some of the computed elastic camber distributions*. It will be observed that the estimates of $\phi(\xi)$ by the two theories are more widely dissimilar in this case than in that of constant angle of attack, and that again the discrepancy is greatest near the trailing edge.

Thus, in going on to consider the comparative aeroelastic effects, we should bear in mind that the two aerodynamic theories which have been employed do, in fact, give estimates of the incremental loads due to elastic camber which are considerably different from one another. Unfortunately, it is not possible to say with certainty which theory provides the more accurate estimates of loading for the elastic camber modes corresponding to the various conditions of flight which have been considered. It may be recalled that the lift distribution function $\phi_0(\xi)$ for additional angle of attack, shown in Fig. 3, was deduced semi-empirically (using experimental data to modify slender-wing-theory calculations). Comparison of the lower part of Fig. 6 with Fig. 3 suggests that, for the constant angle of attack mode, piston theory, although grossly overestimating the loading over the nose portion of the planform, provides a rather more accurate assessment than slender-wing theory elsewhere. This is particularly so towards the trailing edge, where the latter theory, contrary to experimental evidence, predicts zero load. Away from the trailing edge both theories appear to over-estimate the loading somewhat. Intuition might now suggest that, for camber modes resembling the sinusoidal mode illustrated in Fig. 6, piston theory would again provide the more reliable estimate of loading, but there is no firm evidence to support or to refute such a suggestion.

Fig. 7, which relates to the aircraft with basic stiffness distribution in flight at the design cruising condition ($Q = 425 \cdot 3$ lb/ft^2) shows the distributions of elastic camber in trimmed level flight $(\alpha_e)_t$ and the distributions of incremental elastic camber per g in the pull-up, $d\alpha_e/dn$, as estimated using the two aerodynamic theories. Two sets of results are shown: (a) those derived when using the conditions of zero bending moment and shear at the trailing edge to determine the equilibrium angles of attack and elevon deflections; and (b) those derived when using the 'modified derivative' technique. It is seen that the choice of aerodynamic theory has negligible effect on the calculated

* Such a camber distribution should, in fact, satisfy boundary conditions (8) and (9) and also $[d\alpha_e/d\xi]_{\xi=1} = [d^2\alpha_e/d\xi^2]_{\xi=1} = 0$, whereas the sinusoidal mode satisfies only $[d\alpha_e/d\xi]_{\xi=0} = [d\alpha_e/d\xi]_{\xi=1} = \int_0^1 \alpha_e(\xi)d\xi = 0$.

distribution of elastic camber in trimmed level flight. For the pull-up, slender-wing theory predicts somewhat greater incremental camber than does piston theory, the difference being more pronounced towards the trailing edge than elsewhere. The method of satisfying the overall equilibrium conditions has very little effect on the results except in the vicinity of the trailing edge.

Fig. 8 gives results for a kinetic pressure of 1063 lb/ft² which is well outside the range to be encountered in the normal flight plan of the type of aircraft considered. The elastic camber is, of course, generally larger than in the design cruising condition, and the discrepancy between the results yielded by the two aerodynamic theories is now much larger.

Figs. 9 and 10 for $Q = 425 \cdot 3$ lb/ft² and Fig. 11 for $Q = 1063$ lb/ft² give the elastic displacements of the neutral axis corresponding to the camber distributions of Figs. 7 and 8 respectively, and as would be expected, they confirm the fact that increasing kinetic pressure accentuates the differences between the results derived from piston theory and slender-wing theory.

Figs. 12 and 13 compare estimates of the deflections, based on the two theories, for the three stiffness distributions considered in the present series of calculations. The kinetic pressures of $425 \cdot 3$ lb/ft² and $637 \cdot 8$ lb/ft² appropriate to the two figures should both be attainable in the normal flight plan. It can be seen that, except for the case of the deflections in trimmed level flight at the design condition, ($Q = 425 \cdot 3$ lb/ft²) reducing the stiffness tends to increase the differences between the results obtained with the two theories.

Figs. 14 and 16 (derived from piston-theory calculations), show how variations in Q and stiffness affect the 'additional' angle of attack and the elevon angle required in level flight, and the incremental angle of attack and elevon angle per g required in pull-ups. Figs. 15 and 17 compare the results for the basic stiffness distribution case with the corresponding results obtained using slender-wing theory. Probably the most significant fact to emerge from these figures is that, for a given stiffness, the ultimate divergence of the quantities α_{0t}', $d\alpha_0'/dn$, η_t and $d\eta/dn$ (corresponding to the condition of control reversal) is predicted by piston theory to occur at a much higher value of Q than that predicted by slender-wing theory. The fact that α_{0t}' and $d\alpha_0'/dn$, when estimated by piston theory, appear to diverge in directions opposite to those in which they respectively diverge when estimated by slender-wing theory, is mathematically interesting, but not of any profound significance as regards the prediction of the aircraft behaviour on its normal flight plan. At kinetic pressures associated with the latter (which are much lower than the pressure for control reversal) the angles of attack and elevon angles predicted by the two theories may differ appreciably, but they remain of comparable magnitudes.

The results for incremental elevon angle per g are presented in alternative form in Fig. 18, which shows relative control effectiveness (defined as the ratio of the value of $dn/d\eta$ for the flexible aircraft to the value for the rigid aircraft) plotted against Q. This brings out very clearly the large difference in the estimated kinetic pressure for control reversal, according to the two aerodynamic theories, while it also indicates that the respective values estimated for control effectiveness at values of Q attained on the flight envelope are not greatly at variance. Thus, while for the basic stiffness case, piston theory estimates a value of Q at reversal which is more than twice that deduced from slender-wing theory, the values of the relative control effectiveness at the design cruising condition ($Q = 425 \cdot 3$ lb/ft²) are given as $0 \cdot 836$ and $0 \cdot 743$ respectively.

3.6.3. *The effects of elastic camber on the distributions of longitudinal bending moment and shear force.*—Results illustrating how elastic camber affects the distributions of bending moment and shear force are presented in Figs. 25 to 33.

Reference was made in Section 2.3.5 to the fact that the original calculations of bending moment and shear force, employing values of the equilibrium angle of attack and elevon deflection obtained by the 'modified derivative' approach, yielded non-zero (albeit small) residual moments and shears at the trailing edge. To avoid this apparent violation of the physical boundary conditions, the alternative approach based on the direct satisfaction of the trailing-edge conditions was introduced and in general, the results presented in this Section have been obtained by that approach.

However, Figs. 19 and 20 have been included to show the order of magnitude of the discrepancies between results obtained by the two methods; at the same time they give some idea of the overall accuracy of the numerical procedures used in the method of this report. These figures give comparative results of piston-theory calculations for the aircraft with basic stiffness distributions, at the design cruising condition. Fig. 19 gives the non-dimensional shear-force $\{\mathscr{S}_i^*(\xi)\}$ and bending-moment $\{\mathscr{M}_i^*(\xi)\}$ distributions in trimmed flight, while Fig. 20 gives the corresponding incremental quantities $d\mathscr{S}^*(\xi)/dn$, $d\mathscr{M}^*(\xi)/dn$ in manoeuvring flight. It is seen that the residual bending moment at the trailing edge, according to the 'modified derivative' calculations, may be of the order of 15% of the maximum bending moment; residual shear forces are relatively smaller.

The remaining figures of this Section relate to flight at three values of the kinetic pressure Q ($283{\cdot}5$, $425{\cdot}3$ and $637{\cdot}8$ lb/ft^2) which, for a Mach number of $2{\cdot}2$, correspond to a height range from about 73 000 ft down to 55 000 ft; this probably covers the cruising phase of the flight plan for a typical supersonic ($M = 2{\cdot}2$) transport aircraft. For each value of Q, calculations have been made for three values of the total load factor $\bar{n}$, viz. $1{\cdot}0$, $2{\cdot}5$ and $-0{\cdot}5$, corresponding respectively to trimmed level flight and quasi-steady manoeuvres with incremental load factors $+1{\cdot}5$ and $-1{\cdot}5$. In each case, results for the bending-moment and shear-force distributions on the aircraft with basic stiffness distribution, according to the two aerodynamic theories, are compared with those for the (hypothetical) rigid aircraft.

Figs. 21 to 23 compare the deflections computed by the slender-wing and piston theories for the various flight conditions represented by the different combinations of Q and $\bar{n}$. They illustrate once again that the discrepancies between results obtained using the two theories increase with increasing Q.

Fig. 24 indicates that, in general, the elevon angles η required in quasi-steady manoeuvres are affected by flexibility to a relatively greater extent than are the additional angles of attack α_0'. The effect on η, in particular, becomes relatively larger as the kinetic pressure increases. The loading due to the increment of elevon deflection necessitated by flexibility is concentrated at the rear of the aircraft, whereas the equilibrating loadings, due to the increment of angle of attack and to the elastic camber, are distributed over its whole length. This fact would lead one to anticipate that the influence of flexibility on shear and bending-moment distributions would be more pronounced over the rearward half of the aircraft than over the forward half. An examination of Figs. 25 to 33 confirms that, in general, this is so. Other conclusions to be drawn from these figures are that:

(1) The inclusion of flexibility effects may result in considerable increases in the computed values of shear force and bending moment, particularly at the higher kinetic pressures. Thus, for the $\bar{n} = 2{\cdot}5$, $Q = 637{\cdot}8$ lb/ft^2. Case, (Fig. 32) the value of the maximum bending moment, according to the slender-wing theory calculations for the flexible aircraft, is about 22% greater than that calculated at the same chordwise station ($\xi \approx 0{\cdot}6$), neglecting aeroelastic effects. Further aft ($\xi \approx 0{\cdot}9$) the bending moment for the flexible aircraft exceeds that for the 'rigid' aircraft by as much as 75%.

It will be observed from Figs. 25 to 33 that the effect of flexibility is always to increase the magnitude of the bending moments. That this must be so may be deduced from physical considerations. It suffices to consider the positive load factor case. The net loading is upwards over the middle portion of the aircraft's length, where the aerodynamic lift exceeds the inertia loading, and predominantly downwards forward and aft of this region. This results in a 'hogging' deflection of the 'beam' (as illustrated by the curves of Figs. 21 to 23 for $\bar{n} = 1$ and $2 \cdot 5$) so that local angles of attack are reduced over the forward part of the aircraft and increased towards the rear. Thus the centre of lift due to wing incidence is moved aft by flexibility; this necessitates an increase in upward elevon deflection to bring the overall centre of aerodynamic lift again into coincidence with the c.g. The reduction in lift over the forward part of the flexible aircraft, as compared with the rigid aircraft, results in an increase in the net downward loading which clearly leads to a higher peak bending moment near mid-length.

(2) The differences in the values of η, α_0' and $\alpha_e(\xi)$ computed for a given flight condition of the flexible aircraft according to the two aerodynamic theories lead, as one might expect, to considerable differences in the shear and bending-moment distributions. In general, the slender-wing-theory calculations predict larger aeroelastic effects on these quantities than do the piston-theory calculations. Thus, for example, in the case quoted in (1) above, the bending moment at $\xi = 0 \cdot 9$, as predicted using piston theory, exceeds the value for the rigid aircraft by only 36% as against the 75% given by the slender-wing calculations. Nevertheless, the general order of magnitude of the effects computed by either theory is such as to indicate that their neglect could lead to a substantial underestimate of loading actions.

4. *General Discussion and Conclusions.*

The investigation of the effects of longitudinal elastic camber on the characteristics of slender aircraft in quasi-steady symmetrical flight, which was begun in Part I, has been taken a stage further by the present series of calculations. Part I established a method of computing the configuration {specified by α_0', η and $\alpha_e(\xi)$} which is assumed by the deformable aircraft in such a condition of flight, and applied it to a possible layout for a supersonic ($M = 2 \cdot 2$) transport aircraft, which embodied a low aspect ratio ($A = 1 \cdot 107$) delta wing with rounded (streamwise) tips, and a discrete body, protruding a relatively small distance ahead of the wing apex. For these calculations, which were restricted to the cruising Mach number of $2 \cdot 2$, associated with various kinetic pressures, (corresponding to different altitudes) and which covered variations in structural stiffness and weight distributions, the aerodynamic loading due to elastic camber $\{\alpha_e(\xi)\}$ was evaluated by slender-wing theory. Some of the calculations have now been repeated, using piston theory instead of slender-wing theory. Since these two theories predict considerably different load distributions for an arbitrary camber mode of a shape similar to that expected for the elastic camber, a comparison of the overall aeroelastic effects derived from the two series of calculations should give a good indication of the sensitivity of the method to changes in the aerodynamic assumptions.

The results in fact indicate that, in general, the aeroelastic effects as given by the slender-wing-theory calculations are larger than those given by piston-theory calculations, and that the differences between the two sets of results increase as the kinetic pressure Q increases (for a given stiffness distribution) or as the stiffness is reduced at a given Q. This, of course, simply reflects the fact that the aeroelastic effects themselves become larger as kinetic pressure is increased or stiffness reduced, so that the proportion of the total loading (i.e. the part due to elastic camber) which is estimated by

different aerodynamic theories in the two cases increases. It has been noted that, as a consequence of the increasing discrepancy between results as Q increases, estimates of the kinetic pressure for hypothetical* control reversal differ by a factor of more than 2, whereas differences in the estimated relative control effectiveness, at values of Q attainable on the normal flight plan, are of a lower order, although by no means negligible. Thus, for example, the values of the relative effectiveness, as calculated by piston theory and slender-wing theory respectively, for the design cruising condition, are 0·836 and 0·743.

As a further extension of the work of Part I, the longitudinal distributions of shear force and bending moment for the flexible aircraft have now been calculated (using the two aerodynamic theories) for various quasi-steady flight conditions, and compared with the corresponding distributions for the (hypothetical) rigid aircraft. The results indicate that inclusion of the aeroelastic effects may lead to considerable increases in these loading actions quantities at some longitudinal stations, particularly towards the rear of the aircraft, where the local concentration of loading due to the additional deflection of the elevons (necessitated by their loss of effectiveness) makes its presence felt. As was to be expected from the results for control effectiveness, slender-wing theory leads to estimates of the increases in bending moment and shear force due to aero-elasticity, which are in general larger than those derived using piston theory.

Before one seeks to draw any further inferences from the above facts, it is pertinent to make the following observations:

(a) As mentioned in the Introduction, evidence accruing since our investigation was originally launched has suggested that one underlying assumption of our method, namely that of 'beam-like' behaviour of the aircraft under load, is untenable for the 'Concord'-type slender-aircraft layout, which incorporates a discrete fuselage with a thin slender wing. It seems likely that for such configurations spanwise deformations of the wing (leading to appreciable washout towards the tip) will have a destabilising influence on the aircraft so that the true relative effectiveness of inboard elevons should be greater than would be estimated by our method. With outboard elevons, however, the elevon power†, as well as the aircraft stability, would be considerably reduced by elastic washout of the wing, so that in this case the true relative elevon effectiveness could be greater or less than that estimated by our method; however, the relative effectiveness of outboard elevons should certainly be less than that of inboard elevons. [The foregoing reasoning is somewhat intuitive, but leads to conclusions which are consistent with the results of unpublished BAC-Sud calculations.]

For a slender-aircraft configuration of the 'fully integrated' (all wing) type, which would have much greater spanwise stiffness than the 'Concord'-type layout, the assumption of 'beam-like' behaviour might still be reasonably valid, but a detailed structural analysis of an integrated design would be necessary to confirm this.

(b) The longitudinal distributions of shear force and bending moment in quasi-steady symmetric manoeuvres were quantities readily calculable as by-products of the trim and manoeuvrability investigation, and as such, they have been used to demonstrate the likely order of magnitude of

* 'hypothetical', because with deformations, angles of attack and control deflections tending to infinity as the critical pressure is approached, it would be impossible to fly the aircraft at the reversal speed. Assumptions of linear aerodynamic and structural behaviour made in the calculations would, of course, become untenable as the reversal condition was approached.

† As measured by the pitching moment about the c.g. produced by elevon deflection.

aeroelastic effects in the general field of loading actions problems for slender aircraft. A thorough exploration of that field requires the consideration of numerous loading cases; in particular, with reference to the symmetric flight cases, current airworthiness requirements would necessitate an investigation of dynamic response characteristics (including aeroelastic effects) to determine the critical loadings occurring during the manoeuvres associated with various points on the flight envelopes. In view of what has been said in (a), it is clear that for an accurate assessment of the loading actions on a flexible slender aircraft of the 'Concord' type, it is essential to adopt a 'three-dimensional' approach to both the structural and the aerodynamic aspects of the problem.

(c) From Fig. 24, in conjunction with Figs. 7 and 8, it may be deduced that in the manoeuvre cases for which loading actions have been calculated, local angles of attack could be as large as $+ 20°$ or $- 10°$. At such angles of attack, aerodynamic characteristics are likely to be markedly non-linear with incidence.

Bearing the above points in mind, we may return to the main line of discussion and suggest the following as the principal conclusions to be drawn from the present investigation:

(i) When the method of Part I is employed to estimate the effects of aeroelasticity upon the trim and manoeuvrability of a slender aircraft and upon the associated loading actions, the results may be significantly affected by the choice of theory whereby the incremental loading due to elastic camber is to be computed. Although, because of its simplifying assumptions, this particular method is thought to be inapplicable to a 'Concord'-type layout, it is evident that in any more sophisticated approach, allowing for the 'three-dimensional' structural and aerodynamic behaviour of such aircraft, results would again be fairly sensitive to changes in the assumptions regarding the incremental loading due to deformation.

(ii) In view of (i), there is an urgent need to establish an experimentally substantiated method of specifying the loading on slender configurations due to arbitrary distributions of elastic warp (camber + twist) superposed on known initial incidence distributions. Since, for loading actions considerations at least, the resultant attitudes of interest may involve local angles of attack up to 20°, for which non-linear effects may be pronounced, the problem is a formidable one, for the treatment of which the existing literature may provide some clues, but hardly the complete solution.

(iii) With the assumptions of Parts I and II of this report, it has been shown that aeroelasticity tends to increase the shear forces and bending moments along the length of the aircraft. The magnitude of the increases is such as to suggest that it is essential to allow for aeroelastic effects when estimating loading actions on slender aircraft; their neglect could lead to serious underestimates.

(iv) Unless there is a revival of interest in the integrated (all-wing) type of layout, in connection with which the method of the report was originally conceived, the practical possibilities of the method would appear to have been largely exhausted by the work described in the two parts.

SYMBOLS

A		Aspect ratio of gross planform
$B(\xi)$	$=$	$EI(\xi)$, bending rigidity at station ξ: lb/ft²
$\bar{B}(\xi)$	$=$	$\dfrac{B(\xi)}{Q_c l^4}$, non-dimensional stiffness parameter
$\bar{C}_L$	$=$	$\dfrac{\bar{L}}{QS}$, overall lift coefficient
$\bar{C}_{L0}$		'Modified' lift coefficient corresponding to angle-of-attack distribution $\alpha_d(\xi)$: a function of Q
$\bar{C}_{Lt}$		Overall lift coefficient in trimmed level flight
$\bar{C}_m$	$=$	$\dfrac{\bar{M}}{QS\bar{l}}$, overall pitching-moment coefficient
$\bar{C}_{m0}$		'Modified' pitching-moment coefficient corresponding to angle-of-attack distribution $\alpha_d(\xi)$: a function of Q
D	$\equiv$	$\dfrac{d}{d\xi}$, differential operator
E		Young's modulus: lb/ft²
g		Gravitational acceleration: ft/sec²
$H_m, H_{m\eta}, H_t, H_{t\eta}$ $K_m, K_{m\eta}$		Functions of the 'modified' aerodynamic derivatives, appearing in equations (14) and (16)
$I(\xi)$		Second moment of area of beam at station ξ (about neutral axis): ft⁴
$L(\xi)$		Total aerodynamic lift per unit chord at station ξ: lb/ft
$\bar{L}$		Total aerodynamic lift on aircraft: lb
$\mathscr{L}(\xi)$		Total transverse loading per unit length at station ξ (positive upwards): lb/ft
$\mathscr{L}^*(\xi)$	$=$	$\dfrac{\mathscr{L}(\xi)}{Q_c l}$, non-dimensionalised loading per unit length
l		Total length of aircraft at centreline: ft
l_B		Length of body ahead of wing leading edge (*see* Fig. 1): ft
M		Mach number
$\bar{M}$		Total aerodynamic moment about c.g.: lb. ft

SYMBOLS—*continued*

$\mathscr{M}(x)$ Bending moment at station x: lb. ft

$\mathscr{M}^*(\xi) = \dfrac{\mathscr{M}(x)}{Q_c l^3}$, non-dimensionalised bending moment

$\mathscr{M}_r^*(\xi), r = 1, 2, \ldots 5$ 'Elementary' bending-moment distributions corresponding to elementary elastic-camber distributions derived from equations (19.r)

$ng, \bar{n}g$ Incremental and total normal accelerations in pull-up manoeuvre

$Q = \frac{1}{2}\rho V^2$, kinetic pressure: lb/ft²

q Pitching velocity: rad/sec

$\hat{q} = \dfrac{ql}{V}$, non-dimensionalised pitching velocity

S Gross planform area: ft²

$\mathscr{S}(x)$ Shear force at station x: lb

$\mathscr{S}^*(\xi) = \dfrac{\mathscr{S}(x)}{Q_c l^2}$, non-dimensionalised shear force

$\mathscr{S}_r^*(\xi), r = 1, 2, \ldots 5$ 'Elementary' shear-force distributions corresponding to elementary elastic-camber distributions derived from equations (19.r)

$s(\xi)$ Semi-span of planform at station ξ: ft

$s_T = s(1)$, semi-span at trailing edge: ft

V Speed of flight: ft/sec

$W(\xi)$ Weight per unit length at station ξ: lb/ft

$\bar{W} = l\int_0^1 W(\xi)d\xi$, total weight of aircraft: lb

$z'(\xi)$ Normal displacement of neutral axis from centre-section chord at station ξ: ft

$z_b'(\xi), z_e'(\xi)$ Parts of $z'(\xi)$ due to built-in camber and elastic camber respectively

$\alpha(\xi)$ Total effective local angle of attack at station ξ

$\alpha_b(\xi)$ Contribution to $\alpha(\xi)$ from built-in camber relative to centre-section chord

SYMBOLS—*continued*

$\alpha_d(\xi)$		Local angle of attack at station ξ for the undeformed wing at the design C_L
$\alpha_e(\xi)$		Contribution to $\alpha(\xi)$ from elastic camber
α_0		Angle of attack of centre-section chord
α_0'	$=$	$\alpha_0 - \alpha_d$, 'additional' angle of attack
α_{0d}		Angle of attack of the centre-section chord of the undeformed wing at the design C_L
$\alpha_q(\xi)$		Contribution to $\alpha(\xi)$ from induced camber due to pitching velocity
$\zeta'(\xi)$		Normal displacement of neutral axis from centre-section chord at station ξ (as fraction of l) positive upwards
$\zeta_e'(\xi)$		Part of $\zeta'(\xi)$ due to elastic deformation
η		Elevon deflection, positive downwards
μ	$=$	$\dfrac{\overline{W}}{g\rho Sl}$, aircraft relative density
ξ	$\approx$	ξ', distances from the nose, measured as fractions of l, along the direction of flight and the centre-section chord line, respectively
ξ_B	$=$	l_B/l
$\bar{\xi}$		Distance of c.g. from nose as fraction of l
ρ		Air density: slugs/ft^3
$\phi_d(\xi), \phi_e(\xi), \phi_0(\xi), \phi_q(\xi), \phi_\eta(\xi)$		Non-dimensional lift functions—*see* equation (1)
$\Psi_1(\xi), \Psi_2(\xi, Q), \Psi_3(\xi, Q), \Psi_4(\xi, Q), \Psi_5(\xi, Q)$		Forcing functions in the differential equations (19) {defined by equations (21)}
$\psi_1(\xi), \psi_2(\xi), \psi_3(\xi, Q)$		Variable coefficients of the differential equations (19) {defined by equations (20)}

Suffices

c	Relating to design cruising condition
d	Relating to design C_L lift distribution
R	Relating to the (hypothetical) rigid aircraft
t	Relating to trimmed level flight

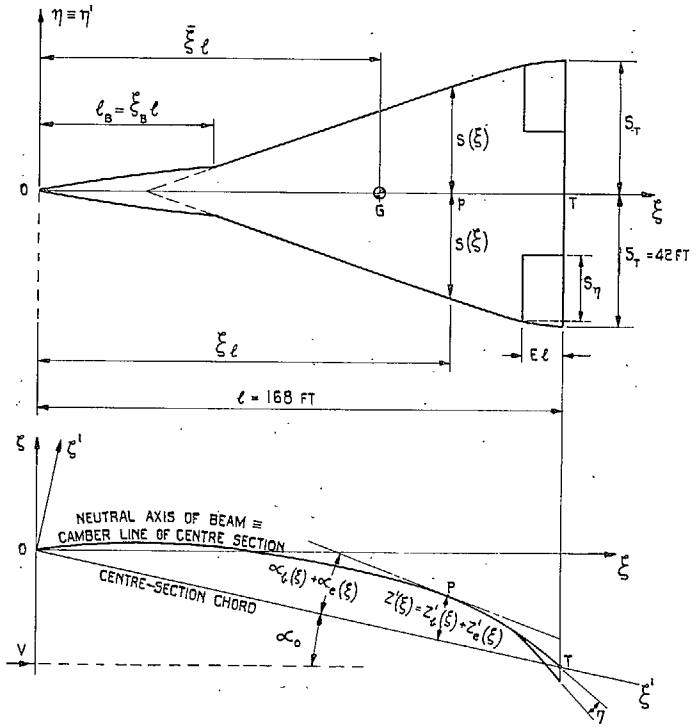

S ≡ GROSS PLAN AREA = p × (2 S_T ℓ)

WHERE p ≡ PLANFORM SHAPE PARAMETER = $\int_0^1 \frac{S(\xi)}{S_T} d\xi$

A ≡ ASPECT RATIO = $4 S_T^2 / S$

α_0 ≡ ANGLE OF ATTACK OF CENTRE-SECTION CHORD

$\alpha_b(\xi)$ ≡ BUILT-IN CAMBER DISTRIBUTION

$\alpha_e(\xi) = -\frac{\partial \zeta_e'(\xi)}{\partial \xi}$ ≡ ELASTIC CAMBER DISTRIBUTION

N.B. FOR SMALL DEFLECTIONS $\xi \triangleq \xi'$

FIG. 1. Illustrations of planform assumed for calculations, and general geometric notation.

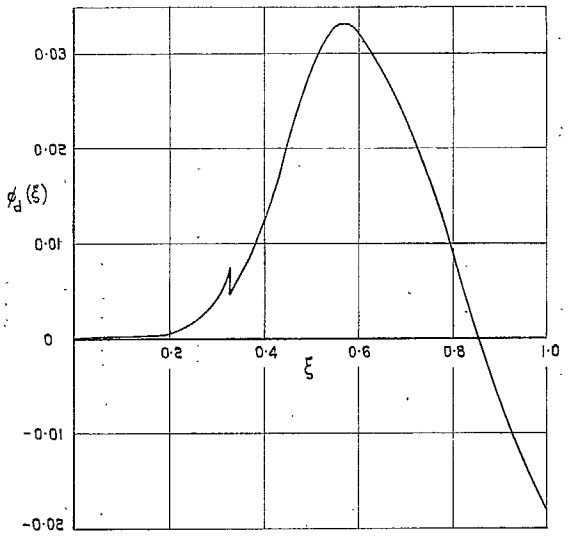

FIG. 2. Lift distribution function $\phi_d(\xi)$ for design case.

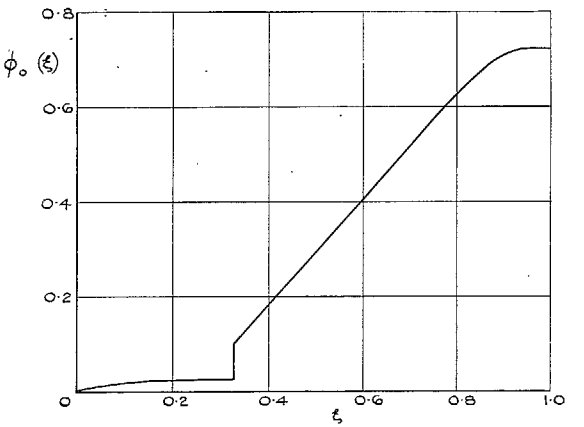

FIG. 3. Lift distribution $\phi_0(\xi)$ for additional angle of attack.

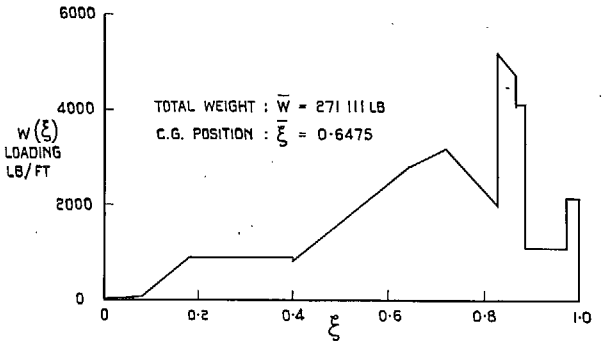

FIG. 4. Assumed weight distribution for mid-cruise.

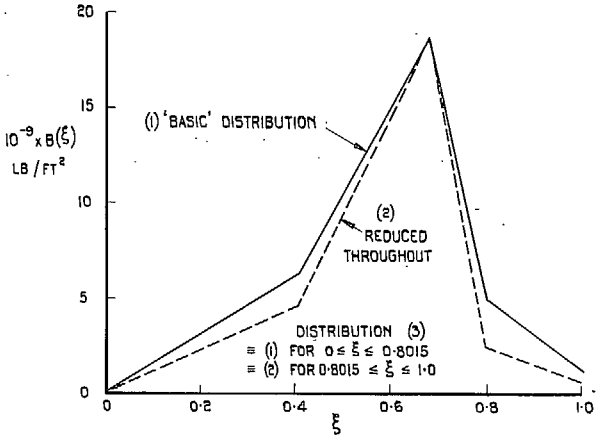

FIG. 5. Stiffness distributions.

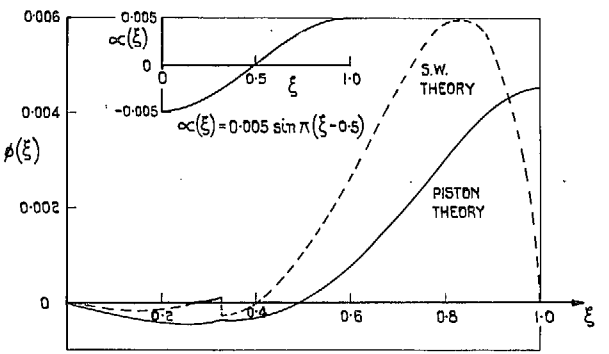

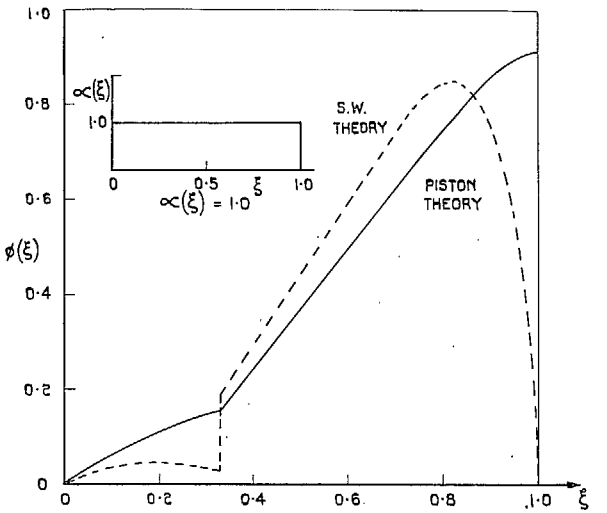

FIG. 6. Comparison of lift functions for two modes of angle of attack as derived from slender-wing and piston theories.

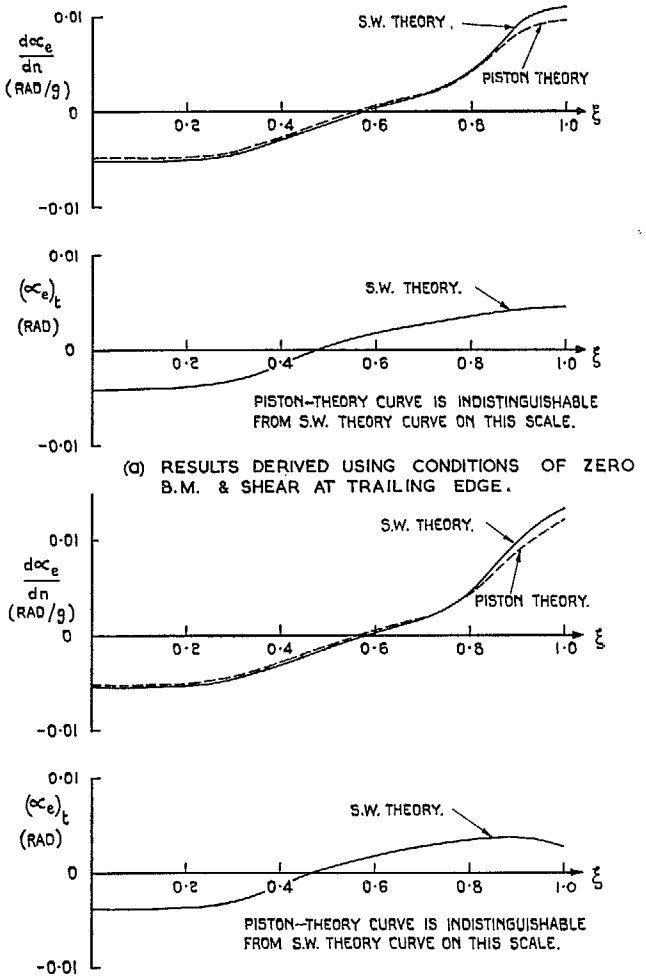

FIG. 7. Comparison of elastic camber distributions as estimated using slender-wing theory and piston theory at $M = 2{\cdot}2$, $Q = 425{\cdot}3$ lb/ft² (basic stiffness).

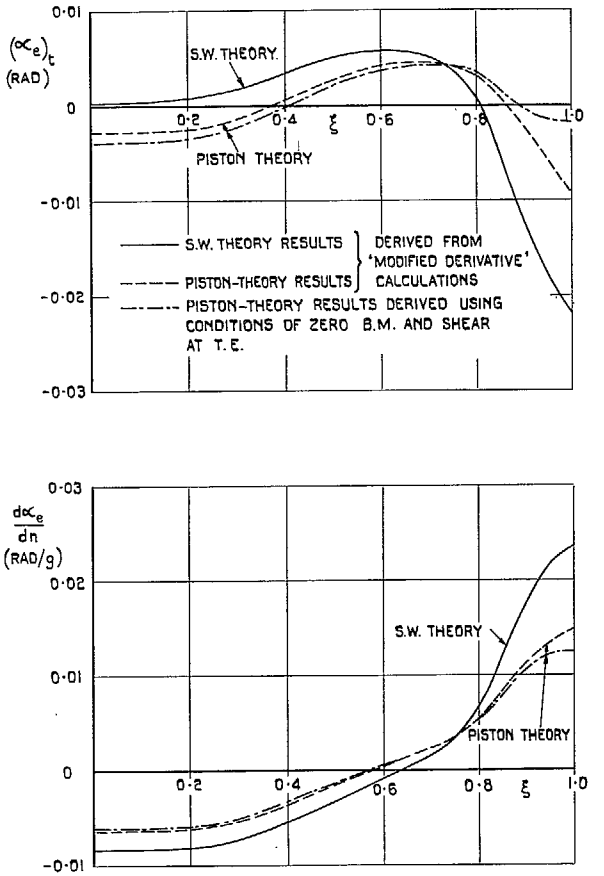

FIG. 8. Comparison of elastic camber distributions as estimated using slender-wing theory and piston theory at $M = 2{\cdot}2$, $Q = 1063$ lb/ft² (basic stiffness).

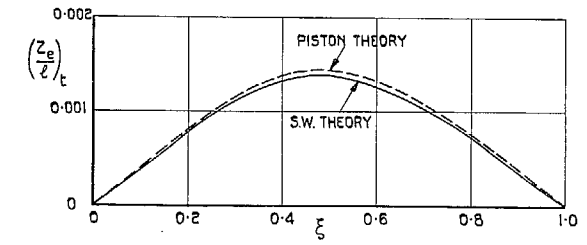

'MODIFIED DERIVATIVE' CALCULATIONS.

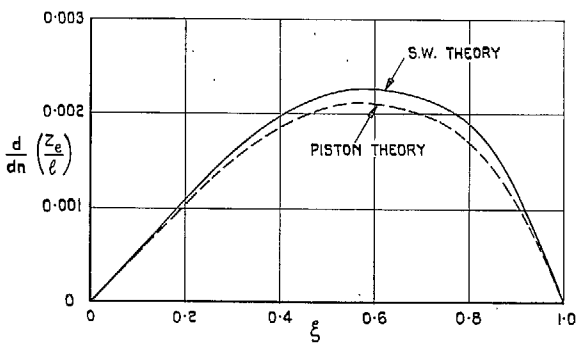

FIG. 9. Comparison of deflections as estimated using slender-wing theory and piston theory at $M = 2{\cdot}2$, $Q = 425{\cdot}3$ lb/ft² (basic stiffness).

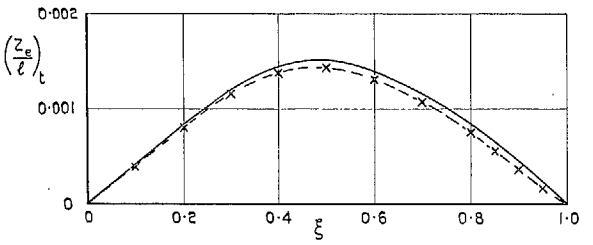

——— RESULTS DERIVED BY DIRECT USE OF CONDITIONS OF ZERO SHEAR AND BENDING MOMENT AT TRAILING EDGE

---×--- RESULTS DERIVED BY 'MODIFIED DERIVATIVE' CALCULATIONS

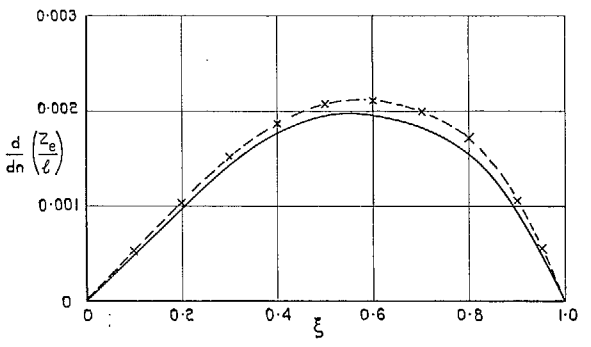

FIG. 10. Comparison of deflections calculated using piston theory when two different methods are used to evaluate equilibrium conditions at $M = 2{\cdot}2$, $Q = 425{\cdot}3$ lb/ft² (basic stiffness).

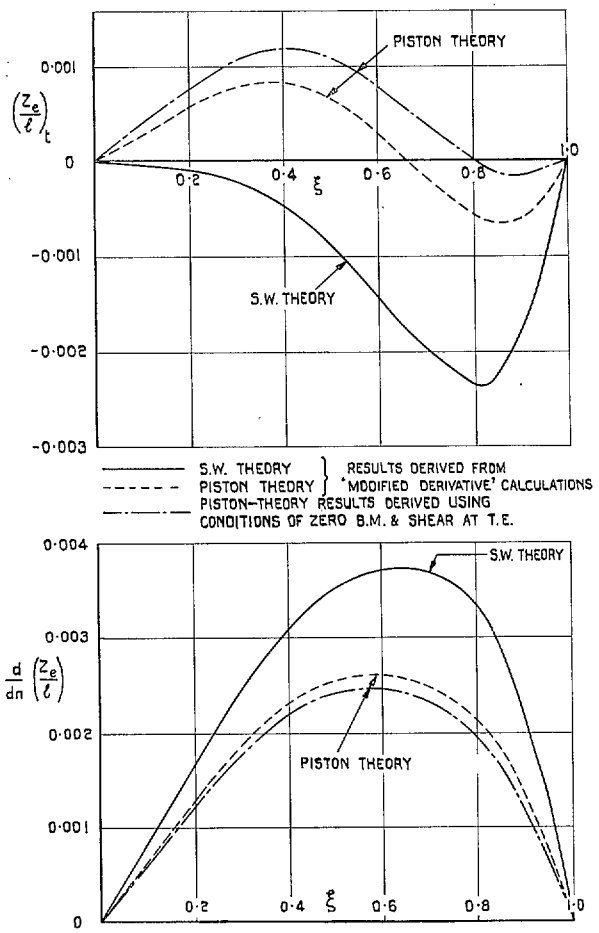

FIG. 11. Comparison of deflections as estimated using slender-wing theory and piston theory at $M = 2{\cdot}2$, $Q = 1063$ lb/ft² (basic stiffness).

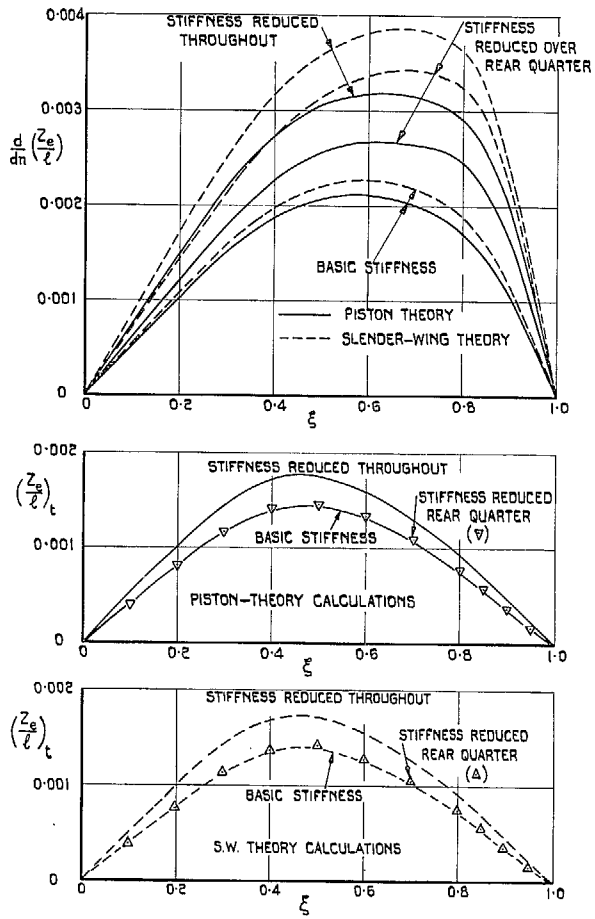

FIG. 12. Comparative ('Modified derivative') estimates of deflections for various stiffness distributions at $M = 2{\cdot}2$, $Q = 425{\cdot}3$ lb/ft².

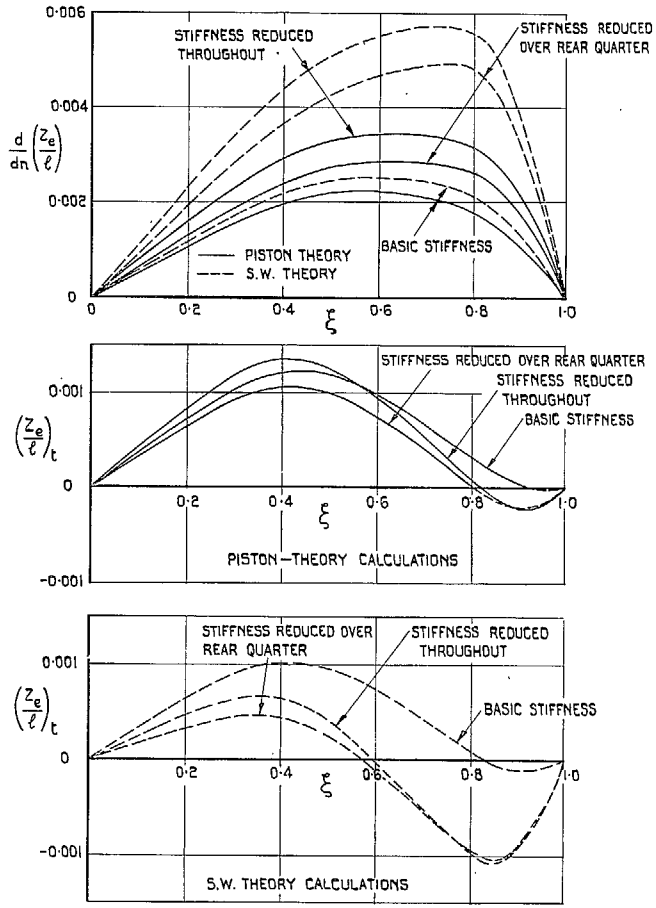

FIG. 13. Comparative ('modified derivative') estimates of deflections for various stiffness distributions at $M = 2{\cdot}2$, $Q = 637{\cdot}8$ lb/ft².

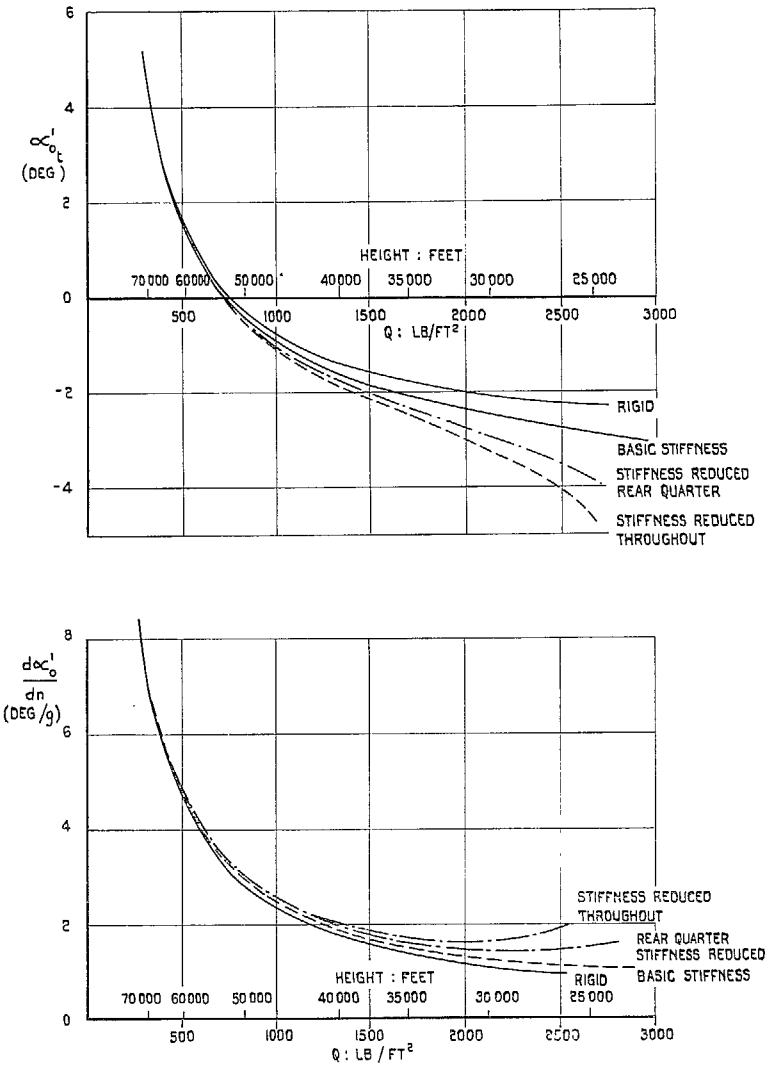

FIG. 14. Effect of stiffness on 'additional' angle of attack required in trimmed level and manoeuvring flight at $M = 2{\cdot}2$ (piston-theory calculations).

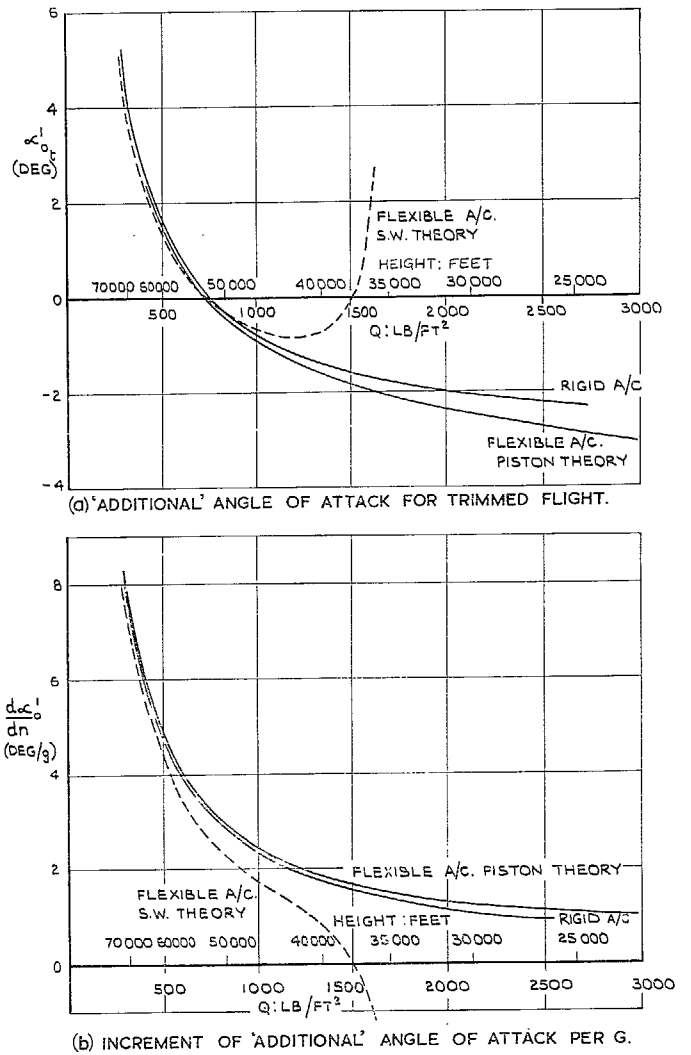

FIG. 15. Influence of aerodynamic assumptions on computed 'additional' angles of attack for trimmed level and manoeuvring flight at $M = 2{\cdot}2$ (basic stiffness distribution).

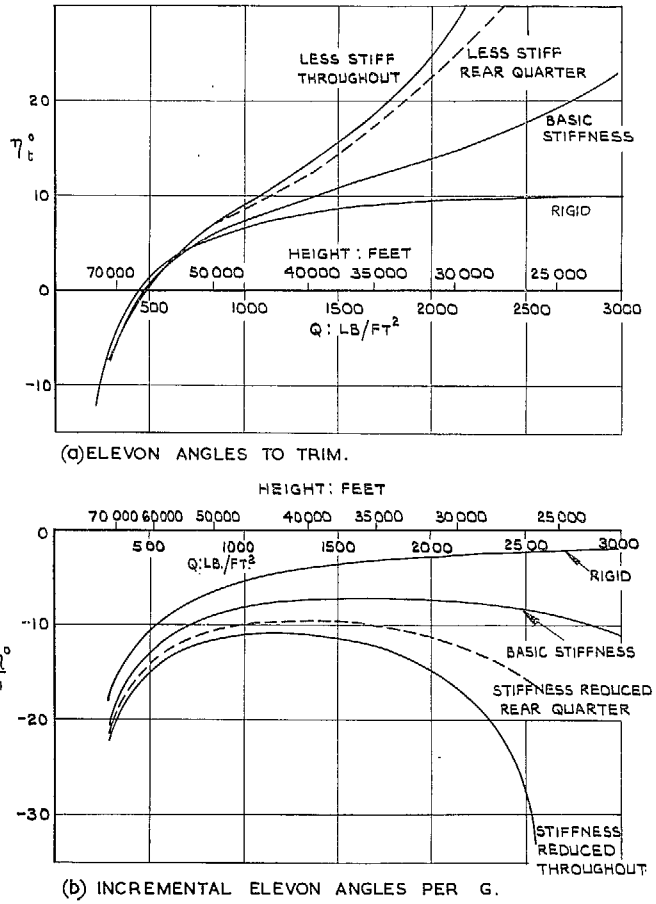

FIG. 16. Effect of stiffness on elevon angles required in trimmed level and manoeuvring flight at M = 2·2 (piston-theory calculations).

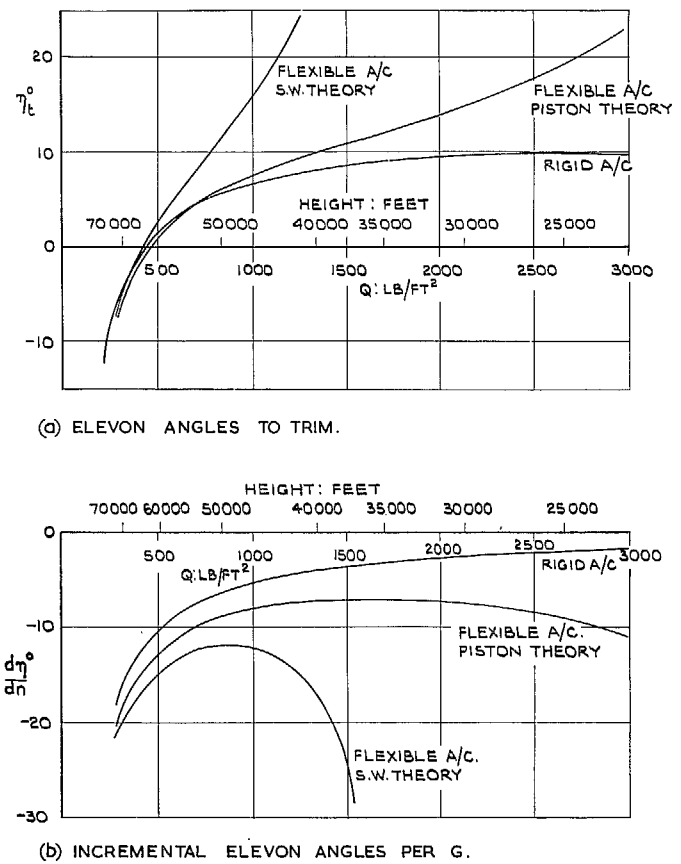

FIG. 17. Influence of aerodynamic assumptions on computed elevon angles for trimmed level and manoeuvring flight at $M = 2{\cdot}2$ (basic stiffness distribution).

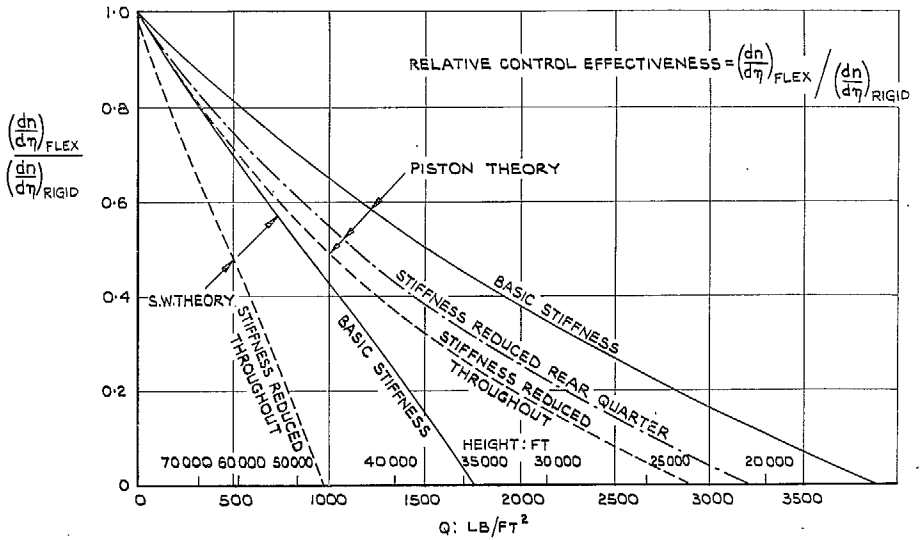

FIG. 18. Effect of stiffness on relative control effectiveness at $M = 2{\cdot}2$.

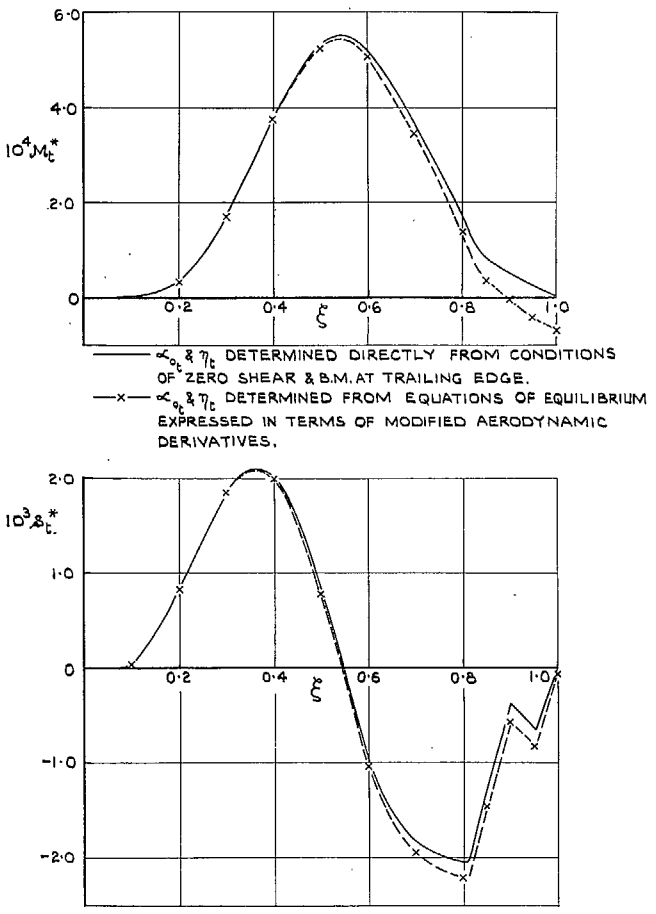

FIG. 19. Non-dimensional shear force and bending-moment distributions in trimmed flight at $M = 2{\cdot}2$, $Q = 425{\cdot}3$ lb/ft² (piston-theory calculations).

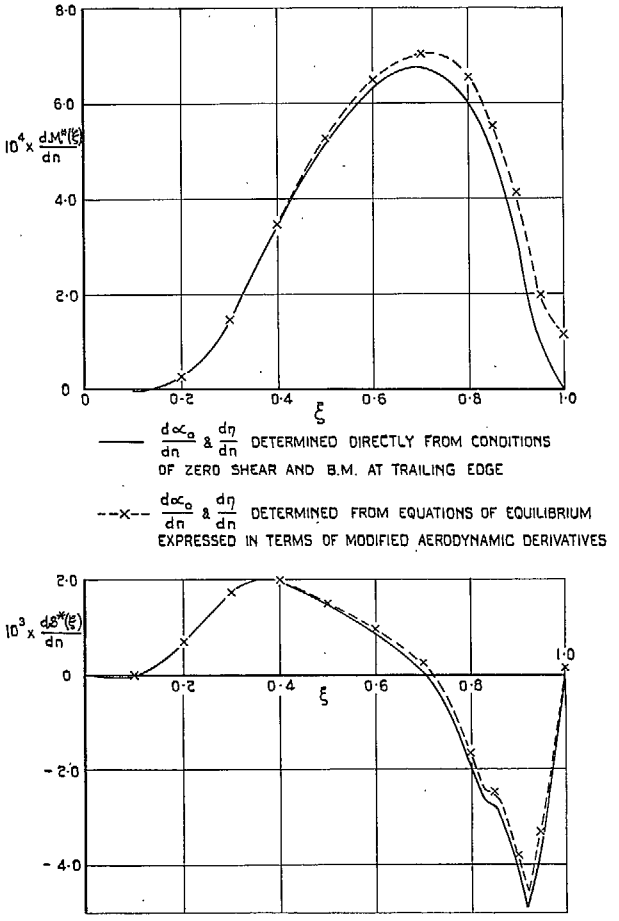

FIG. 20. Distributions of incremental shear force and bending moment per g in manoeuvring flight at $M = 2{\cdot}2$, $Q = 425{\cdot}3$ lb/ft² (piston-theory calculations).

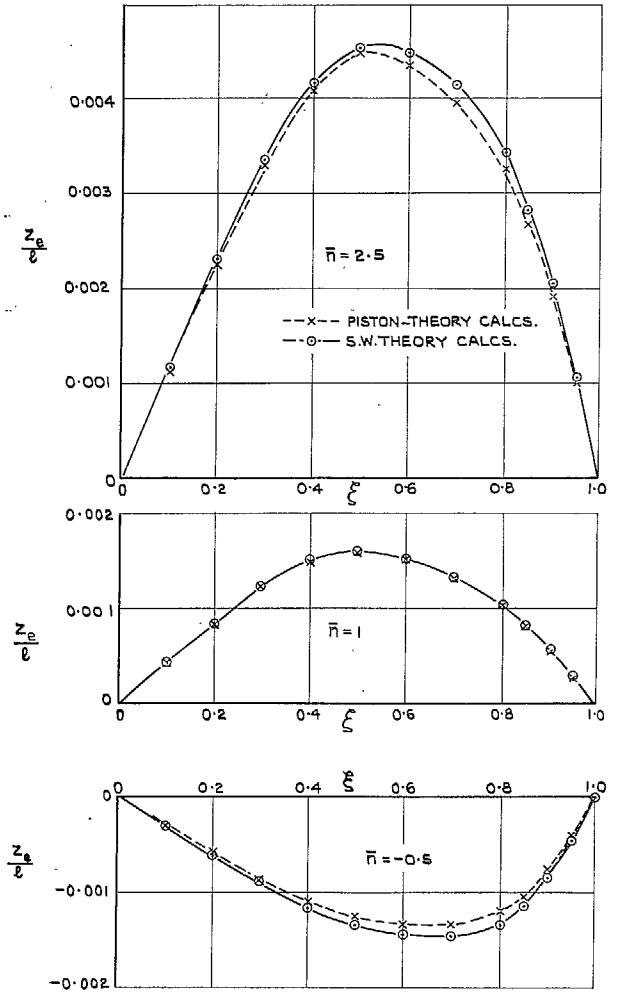

FIG. 21. Comparison of deflections as computed using slender-wing theory and piston theory for flight at load factors ($\bar{n}$) of 2·5, 1·0 and −0·5 at $M = 2·2$, $Q = 283·5$ lb/ft².

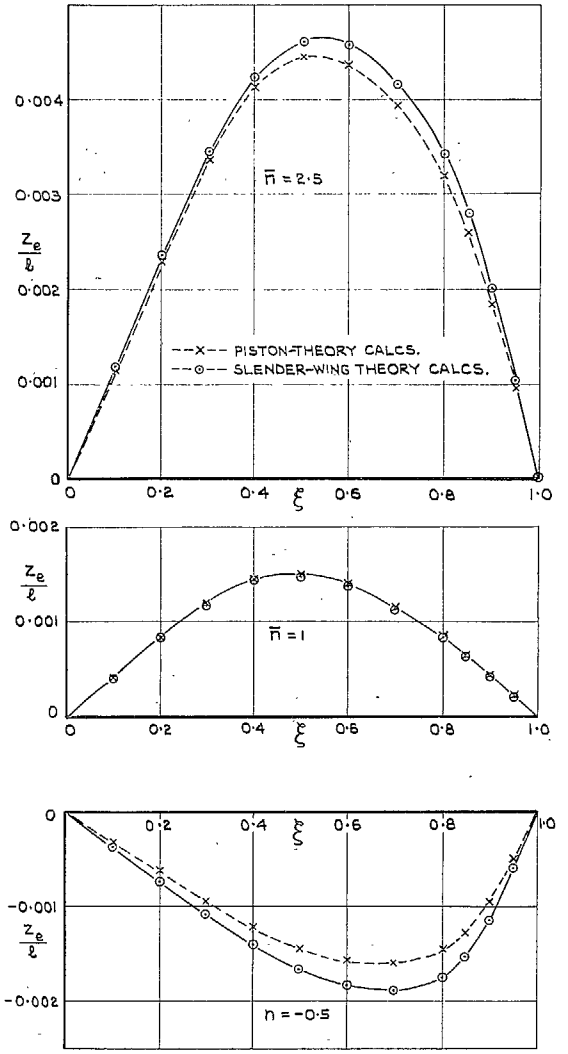

FIG. 22. Comparison of deflections as computed using slender-wing theory and piston theory for flight at load factors ($\bar{n}$) of 2·5, 1·0 and − 0·5 at $M = 2·2$, $Q = 425·3$ lb/ft².

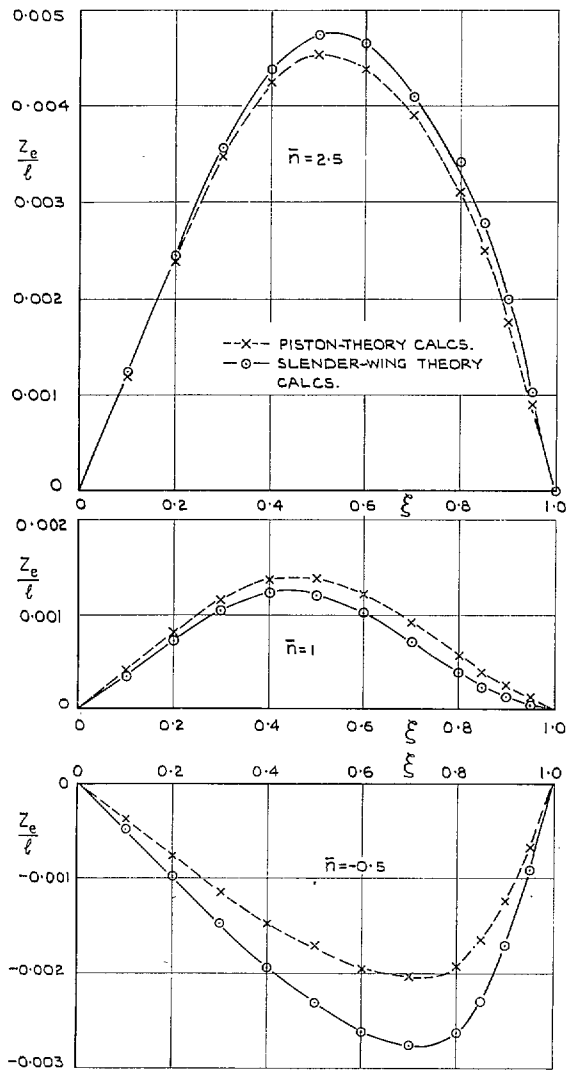

FIG. 23. Comparison of deflections as computed using slender-wing theory and piston theory for flight at load factors ($\bar{n}$) of 2·5, 1, −0·5 at $M = 2{\cdot}2$, $Q = 637{\cdot}8$ lb/ft.²

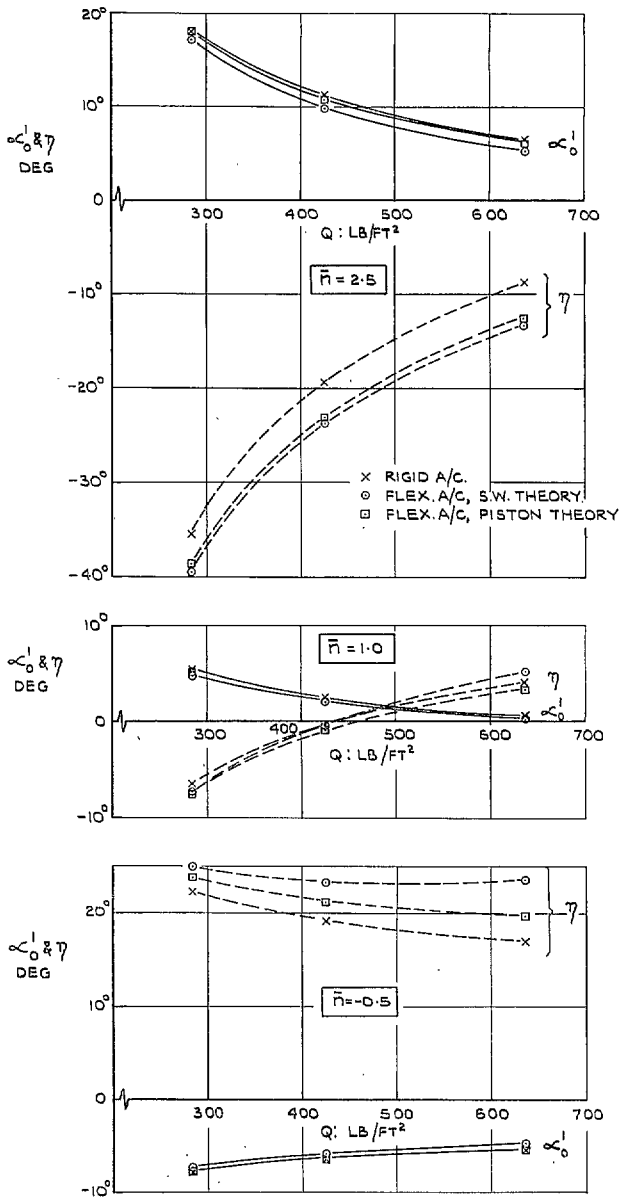

FIG. 24. Additional angles of attack and elevon deflections required in quasi-steady manoeuvre cases.

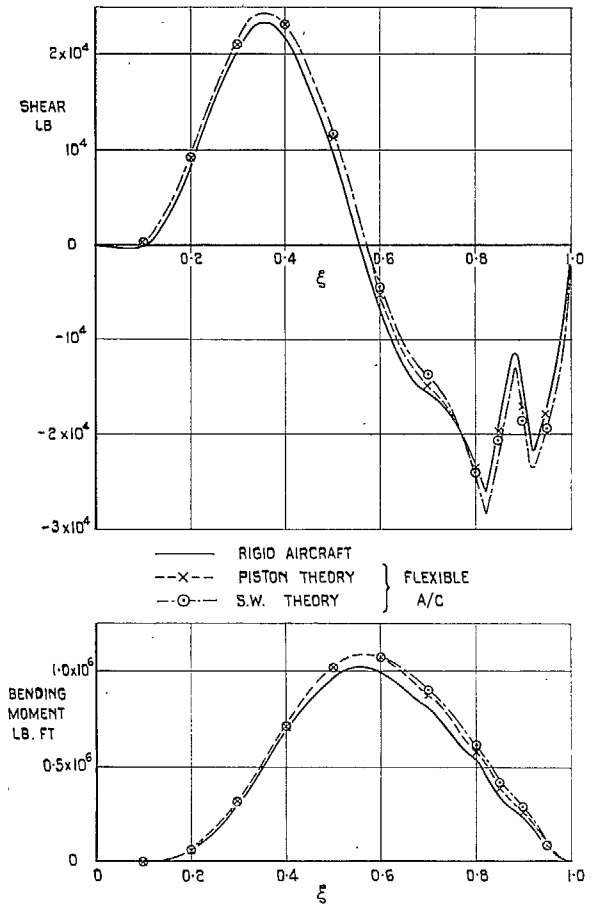

FIG. 25. Effect of flexibility on longitudinal distributions of shear force and bending moment in symmetrical flight at $M = 2{\cdot}2$, $Q = 283{\cdot}5$ lb/ft²: $\bar{n} = 1{\cdot}0$.

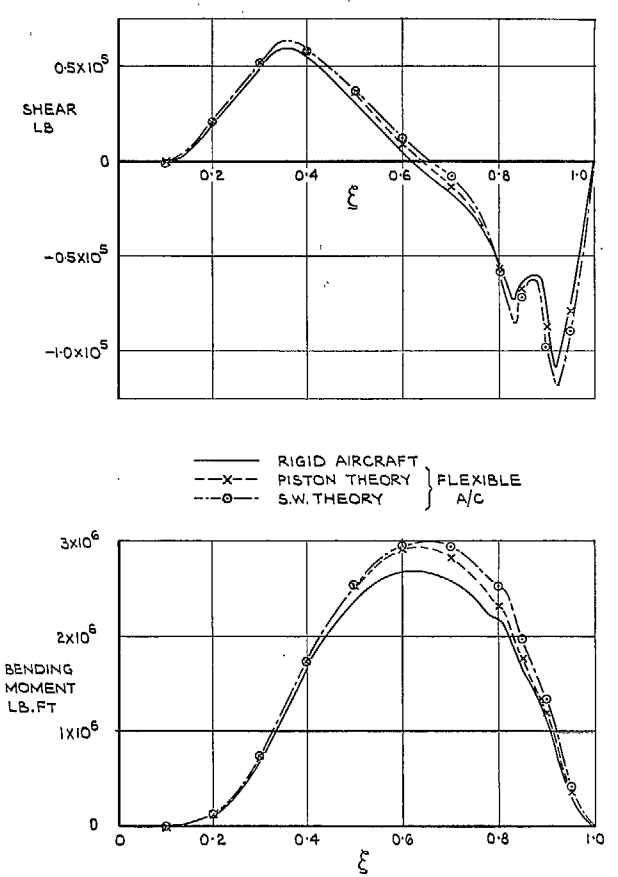

FIG. 26. Effect of flexibility on longitudinal distributions of shear force and bending moment in symmetrical flight at $M = 2{\cdot}2$, $Q = 283{\cdot}5$ lb/ft²: $\bar{n} = 2{\cdot}5$.

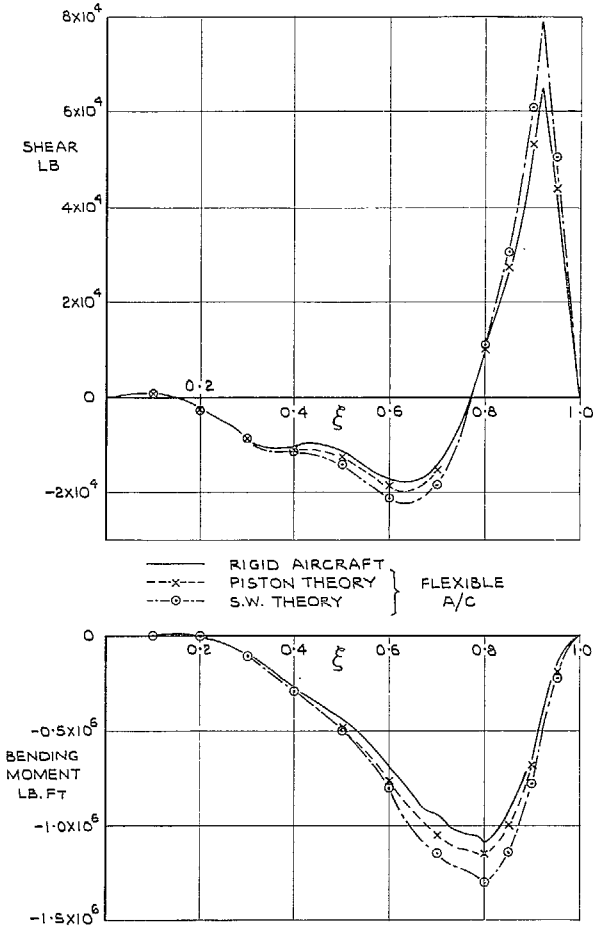

FIG. 27. Effect of flexibility on longitudinal distributions of shear force and bending moment in symmetrical flight at $M = 2{\cdot}2$, $Q = 283{\cdot}5$ lb/ft²: $\bar{n} = -0{\cdot}5$.

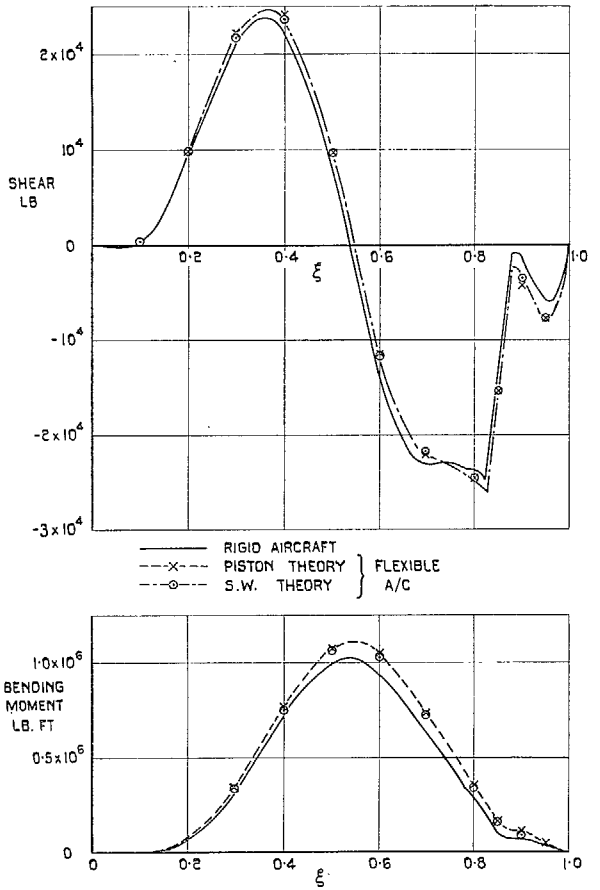

FIG. 28. Effect of flexibility on longitudinal distributions of shear force and bending moment in symmetrical flight at $M = 2{\cdot}2$, $Q = 425{\cdot}3$ lb/ft²: $\bar{n} = 1{\cdot}0$.

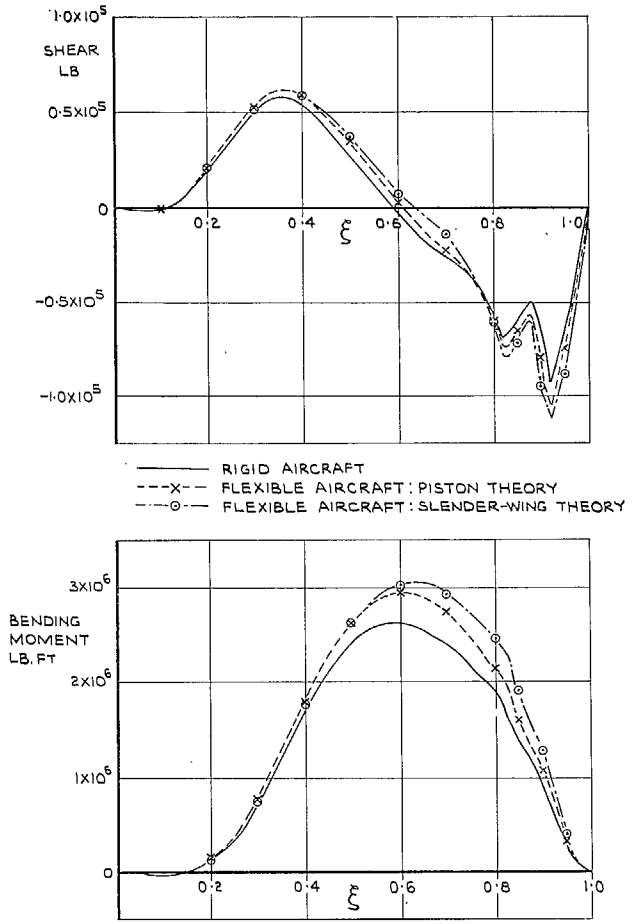

FIG. 29. Effect of flexibility on longitudinal distributions of shear force and bending moment in symmetrical flight at $M = 2{\cdot}2$, $Q = 425{\cdot}3$ lb/ft^2: $\bar{n} = 2{\cdot}5$.

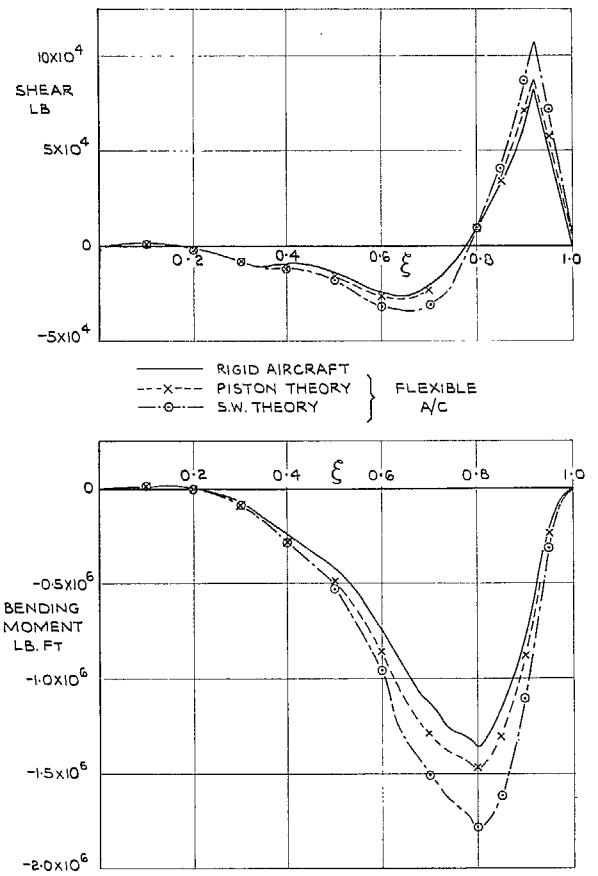

FIG. 30. Effect of flexibility on longitudinal distributions of shear force and bending moment in symmetrical flight at $M = 2{\cdot}2$, $Q = 425{\cdot}3$ lb/ft^2: $\bar{n} = -0{\cdot}5$.

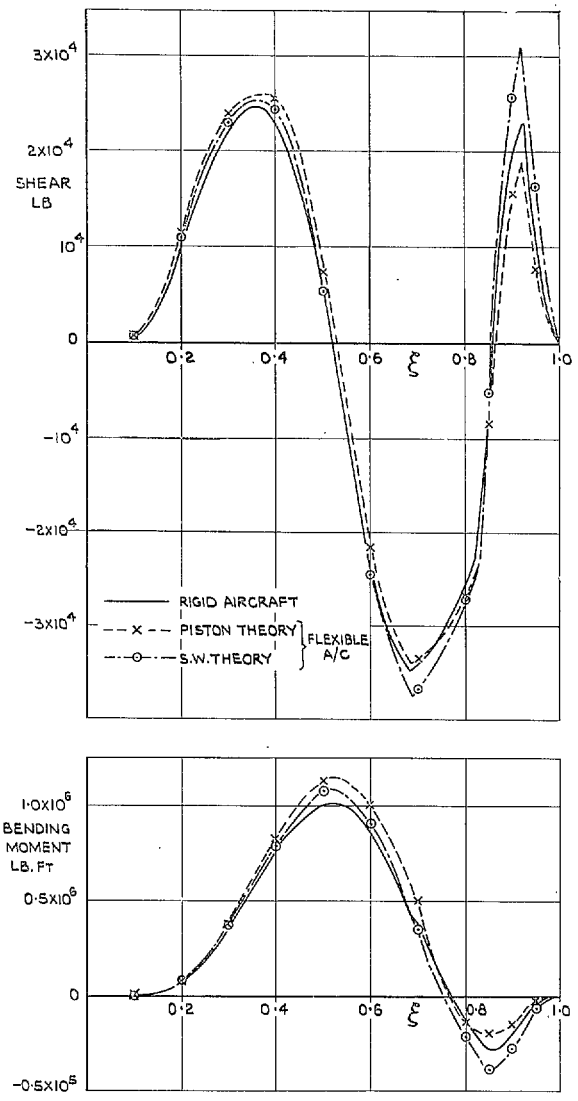

FIG. 31. Effect of flexibility on longitudinal distributions of shear force and bending moment in symmetrical flight at $M = 2{\cdot}2$, $Q = 637{\cdot}8$ lb/ft^2: $\bar{n} = 1{\cdot}0$.

(92862) Wt. 67/7689 K5 9/66 Hw.

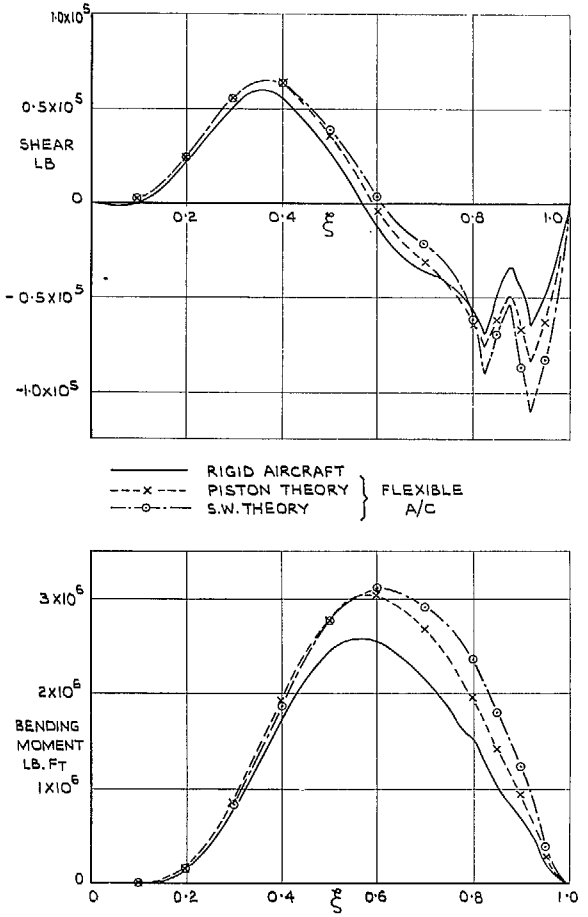

FIG. 32. Effect of flexibility on longitudinal distributions of shear force and bending moment in symmetrical flight at $M = 2{\cdot}2$, $Q = 637{\cdot}8$ lb/ft^2: $\bar{n} = 2{\cdot}5$.

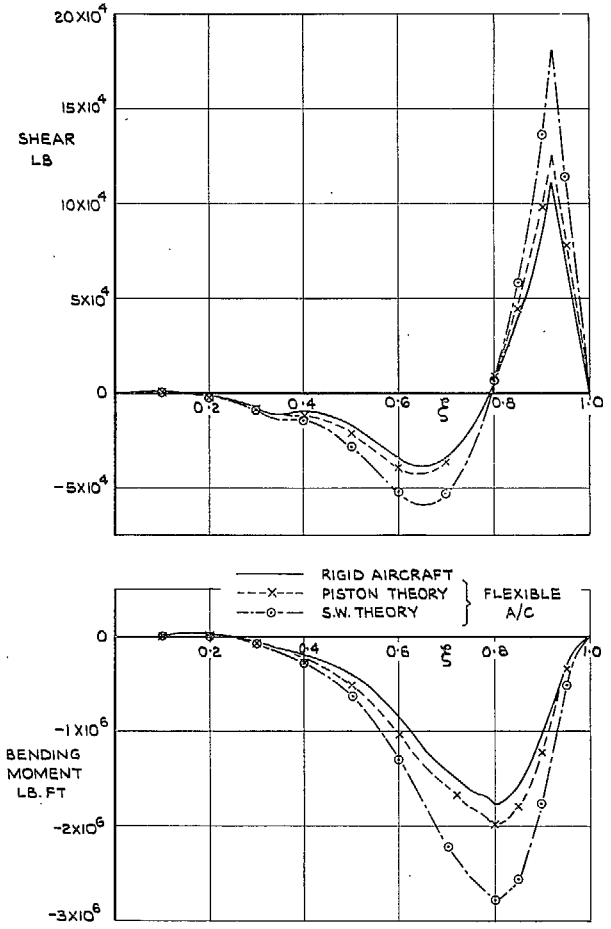

FIG. 33. Effect of flexibility on longitudinal distributions of shear force and bending moment in symmetrical flight at $M = 2{\cdot}2$, $Q = 637{\cdot}8$ lb/ft^2: $\bar{n} = -0{\cdot}5$.

Publications of the Aeronautical Research Council

ANNUAL TECHNICAL REPORTS OF THE AERONAUTICAL RESEARCH COUNCIL (BOUND VOLUMES)

1945 Vol. I. Aero and Hydrodynamics, Aerofoils. £6 10s. (£6 13s. 6d.)
Vol. II. Aircraft, Airscrews, Controls. £6 10s. (£6 13s. 6d.)
Vol. III. Flutter and Vibration, Instruments, Miscellaneous, Parachutes, Plates and Panels, Propulsion. £6 10s. (£6 13s. 6d.)
Vol. IV. Stability, Structures, Wind Tunnels, Wind Tunnel Technique. £6 10s. (£6 13s. 3d.)

1946 Vol. I. Accidents, Aerodynamics, Aerofoils and Hydrofoils. £8 8s. (£8 11s. 9d.)
Vol. II. Airscrews, Cabin Cooling, Chemical Hazards, Controls, Flames, Flutter, Helicopters, Instruments and Instrumentation, Interference, Jets, Miscellaneous, Parachutes. £8 8s. (£8 11s. 3d.)
Vol. III. Performance, Propulsion, Seaplanes, Stability, Structures, Wind Tunnels. £8 8s. (£8 11s. 6d.)

1947 Vol. I. Aerodynamics, Aerofoils, Aircraft. £8 8s. (£8 11s. 9d.)
Vol. II. Airscrews and Rotors, Controls, Flutter, Materials, Miscellaneous, Parachutes, Propulsion, Seaplanes, Stability, Structures, Take-off and Landing. £8 8s. (£8 11s. 9d.)

1948 Vol. I. Aerodynamics, Aerofoils, Aircraft, Airscrews, Controls, Flutter and Vibration, Helicopters, Instruments, Propulsion, Seaplane, Stability, Structures, Wind Tunnels. £6 10s. (£6 13s. 3d.)
Vol. II. Aerodynamics, Aerofoils, Aircraft, Airscrews, Controls, Flutter and Vibration, Helicopters, Instruments, Propulsion, Seaplane, Stability, Structures, Wind Tunnels. £5 10s. (£5 13s. 3d.)

1949 Vol. I. Aerodynamics, Aerofoils. £5 10s. (£5 13s. 3d.)
Vol. II. Aircraft, Controls, Flutter and Vibration, Helicopters, Instruments, Materials, Seaplanes, Structures, Wind Tunnels. £5 10s. (£5 13s.)

1950 Vol. I. Aerodynamics, Aerofoils, Aircraft. £5 12s. 6d. (£5 16s.)
Vol. II. Apparatus, Flutter and Vibration, Meteorology, Panels, Performance, Rotorcraft, Seaplanes. £4 (£4 3s.)
Vol. III. Stability and Control, Structures, Thermodynamics, Visual Aids, Wind Tunnels. £4 (£4 2s. 9d.)

1951 Vol. I. Aerodynamics, Aerofoils. £6 10s. (£6 13s. 3d.)
Vol. II. Compressors and Turbines, Flutter, Instruments, Mathematics, Ropes, Rotorcraft, Stability and Control, Structures, Wind Tunnels. £5 10s. (£5 13s. 3d.)

1952 Vol. I. Aerodynamics, Aerofoils. £8 8s. (£8 11s. 3d.)
Vol. II. Aircraft, Bodies, Compressors, Controls, Equipment, Flutter and Oscillation, Rotorcraft, Seaplanes, Structures. £5 10s. (£5 13s.)

1953 Vol. I. Aerodynamics, Aerofoils and Wings, Aircraft, Compressors and Turbines, Controls. £6 (£6 3s. 3d.)
Vol. II. Flutter and Oscillation, Gusts, Helicopters, Performance, Seaplanes, Stability, Structures, Thermodynamics, Turbulence. £5 5s. (£5 8s. 3d.)

1954 Aero and Hydrodynamics, Aerofoils, Arrester gear, Compressors and Turbines, Flutter, Materials, Performance, Rotorcraft, Stability and Control, Structures. £7 7s. (£7 10s. 6d.)

Special Volumes

Vol. I. Aero and Hydrodynamics, Aerofoils, Controls, Flutter, Kites, Parachutes, Performance, Propulsion, Stability. £6 6s. (£6 9s.)
Vol. II. Aero and Hydrodynamics, Aerofoils, Airscrews, Controls, Flutter, Materials, Miscellaneous, Parachutes, Propulsion, Stability, Structures. £7 7s. (£7 10s.)
Vol. III. Aero and Hydrodynamics, Aerofoils, Airscrews, Controls, Flutter, Kites, Miscellaneous, Parachutes, Propulsion, Seaplanes, Stability, Structures, Test Equipment. £9 9s. (£9 12s. 9d.)

Reviews of the Aeronautical Research Council

1949–54 5s. (5s. 5d.)

Index to all Reports and Memoranda published in the Annual Technical Reports

1909–1947 R. & M. 2600 (out of print)

Indexes to the Reports and Memoranda of the Aeronautical Research Council

Between Nos. 2451–2549: R. & M. No. 2550 2s. 6d. (2s. 9d.); Between Nos. 2651–2749: R. & M. No. 2750 2s. 6d. (2s. 9d.); Between Nos. 2751–2849: R. & M. No. 2850 2s. 6d. (2s. 9d.); Between Nos. 2851–2949: R. & M. No. 2950 3s. (3s. 3d.); Between Nos. 2951–3049: R. & M. No. 3050 3s. 6d. (3s. 9d.); Between Nos. 3051–3149: R. & M. No. 3150 3s. 6d. (3s. 9d.); Between Nos. 3151–3249: R. & M. No. 3250 3s. 6d. (3s. 9d.); Between Nos. 3251–3349: R. & M. No. 3350 3s. 6d. (3s. 10d.)

Prices in brackets include postage

Government publications can be purchased over the counter or by post from the Government Bookshops in London, Edinburgh, Cardiff, Belfast, Manchester, Birmingham and Bristol, or through any bookseller

Printed and published by
HER MAJESTY'S STATIONERY OFFICE

To be purchased from
49 High Holborn, London WC1
423 Oxford Street, London W1
13A Castle Street, Edinburgh 2
109 St. Mary Street, Cardiff
Brazennose Street, Manchester 2
50 Fairfax Street, Bristol 1
35 Smallbrook, Ringway, Birmingham 5
80 Chichester Street, Belfast 1
or through any bookseller

Printed in England

S.O. Code No. 23-3426